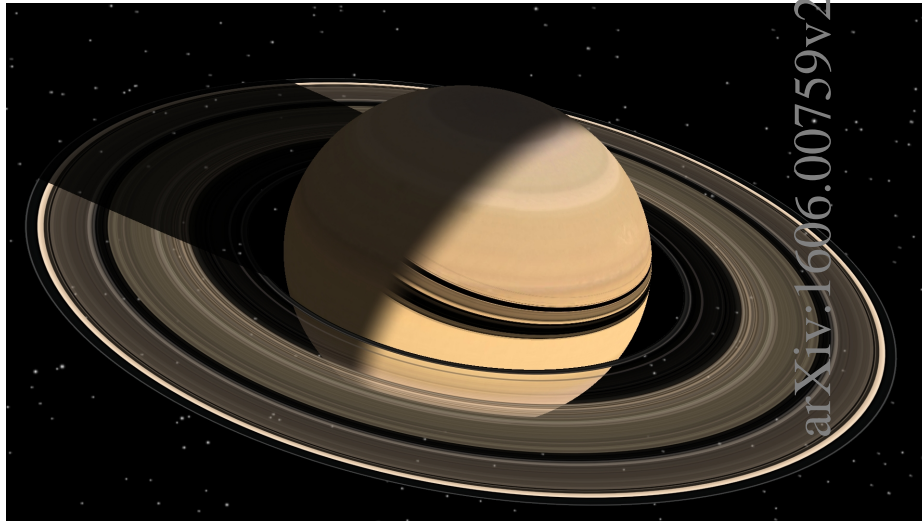


arXiv:1606.00759v2 [astro-ph:EP] 15 Mar 2017

Planetary Ring Dynamics

The Streamline Formalism

1. *From Boltzmann Equation to Celestial Mechanics*



Pierre-Yves Longaretti

IPAG, CNRS & UGA

pierre-yves.longaretti@univ-grenoble-alpes.fr



Contents

Foreword	iii
1 Introduction	1
2 Basic concepts and orders of magnitude	2
2.1 Angular momentum axis	3
2.2 Collisional quasi-equilibrium	4
2.2.1 Optical depth, collision frequency, and ring thickness	5
2.2.2 Ring viscosity	6
2.2.3 Velocity dispersion quasi-equilibrium	7
2.2.4 Limitations and extensions of the previous model	8
2.3 Angular momentum transport and the origin of the rings radial structures	9
3 The Boltzmann equation and its moments	10
3.1 The moments of the Boltzmann equation	11
3.2 The moment equations in ring systems	12
4 Ring kinematics: streamlines	18
4.1 Fluid test particle motion	18
4.2 Epicyclic versus elliptic elements	23
4.3 Ring streamlines and kinematics	24
4.3.1 Eccentric rings	26
4.3.2 Density waves	26
4.3.3 Eccentric modes	30
4.3.4 Summary	32
4.4 Ring surface density	35
5 Ring pressure tensor	37
5.1 Dilute systems	38
5.1.1 Collision frequency, effective particle size, and effective optical depth	38
5.1.2 Quasi-equilibrium of perturbed and unperturbed ring systems	41
5.2 Dense systems	46
5.2.1 Macroscopic equations	47
5.2.2 Microscopic equations	49
5.2.3 The pressure tensor components	50
5.3 Energy dissipation, and viscous flux of angular momentum	52
5.3.1 Energy dissipation in planetary rings	52
5.3.2 Viscous flux of angular momentum	54
5.4 Summary and parametrization of the pressure tensor	56
6 Ring dynamics: perturbation equations and conserved quantities	57
6.1 Disk self-gravity	58
6.2 Satellite perturbations	60
6.3 Pressure tensor	61

6.4	Mass, energy, and angular momentum budget of ring systems: . . .	62
7	Applications to ring dynamics	66
7.1	The self-gravity model for elliptic rings	67
7.2	Density waves at Lindblad resonances with external satellites . . .	71
7.2.1	Dispersion relation	73
7.2.2	Forced amplitude and wave damping	78
7.2.3	Satellite torque and angular momentum transport	81
8	Conclusion	85
	Acknowledgements	87
	Appendix	88
A	Free density waves	88
B	Forced density wave	89
B.1	Conclusions in a nutshell	89
B.2	Setting up the problem	90
B.3	Evaluation on C_+ and C_-	92
B.4	Evaluation on I_+ and I_-	93
	References	97

Photo credits:

Cover: NASA

Backpage:

- Collection of early drawings of Saturn by various observers, from Huyghens' *Systema Saturnium* (1659).
- Guido Bonatti, from his *De Astronomia Tractatus X Universum quod ad iudiciariam rationem nativitatum* (Basel, 1550)

Foreword

The present notes constitute a somewhat corrected and mildly extended — through the addition of an appendix — version of a set of lecture notes devoted to planetary ring dynamics and initially published in the *Goutelas* series of volumes (Longaretti, 1992). They were designed to form an overall but rather complete pedagogical introduction to their subject matter, i.e. to cover the material needed for a detailed understanding of the theoretical results published by Borderies, Goldreich and Tremaine — but also Shu and coworkers to a smaller extent — in a variety of research papers in the late 70s and in the 80s. However, some sections are more detailed than others.

These notes have never been widely distributed, and are almost impossible to find now. But although they are more than 20 years old, I believe or at least hope they might still be useful to a number of people in the field. The upcoming book (*Planetary Ring Systems*), edited by Matt Tiscareno and Carl Murray and to be published later on this year at Cambridge University Press has been an incentive to post them on the Astrophysics Preprint Archive. In particular these notes are occasionally referenced in my own chapter of this book (*Theory of Narrow Rings and Sharp Edges*). If you wish to refer to these notes, please quote the initial publication above along with their *arXiv* number for accessibility.

Needless to say, these notes ignore recent advances in the understanding of ring macro- and microphysics, such as the existence of propellers, the more recent focus on viscous overstabilities, the existence and potential rôle of self-gravitational wakes, the now large albeit indirect body of evidence against the DEBs model of ring particles which was fashionable back in the 1980s, and of course the wealth of new observational constraints and theoretical challenges brought to light by the *Cassini* mission.

A number of these shortcomings are addressed in my chapter of the new “ring book”. The interested reader will find in there both a complete although less detailed exposition than the present one of the streamline formalism and a thorough discussion of all the physics that has not found its way in the present notes, most notably the physics of narrow rings and sharp edges and associated modes, as indicated by the chapter’s title. The literature review will be complete up to the time of publication. If permitted by the copyright agreement, this chapter will also be posted on *arXiv* as part 2 of these notes. The two main topics covered in detail in the present notes and that have not been revisited in my ring book chapter are the ring microphysics theory and the theory of linear and nonlinear density waves.

Last point: please feel free to send me any feedback on these notes, if only to point out the unavoidable remaining mistakes.

Pierre-Yves Longaretti, June 1, 2016

1 Introduction

Ring systems are now known to exist around the four giant planets of the Solar System. However, they differ widely from one another. Jupiter's ring is very tenuous, and its constituting particles are permanently destroyed and created. Saturn's rings constitute the most extensive system: from the inside to the outside, one successively finds the D, C, B rings, the Cassini division, the A, F, G and E rings; rings D, F, G and E are rather tenuous, whereas the others are much more massive and more opaque. Uranus is surrounded by nine main rings of high optical depth, separated by dust bands. Finally, Neptune has a very peculiar system of very low optical depth rings, with some azimuthal structures known as "ring arcs".

Rings are made up of particles of various sizes and compositions, and this property allows us to divide them roughly in two broad classes: the "major" rings contain mostly "big" particles (typically meter-sized); the "ethereal" rings are made of much smaller particles (typically microns). Saturn's main rings (A to C) and the nine main rings of Uranus (ϵ , α , β , γ , δ , η , 4, 5, 6) belong to the first category. The other rings of Saturn and Uranus, as well as the rings of Jupiter and Neptune belong the second.

The two classes of rings thus defined exhibit very different dynamical behaviors, because light particles are submitted to important electromagnetic forces, which is not the case for meter-sized particles. In this lecture, we will restrict ourselves to the dynamics of the major ring systems. Of course, the distinction between the two types of rings is not absolute: ring particles have a broad size distribution, and micron-sized particles can also be found in the major rings; for example, they play an essential rôle in the well-known "spokes" phenomenon, mainly seen in Saturn's B ring. However, they dominate neither the mass nor the optical depth of these rings, and can therefore be ignored in discussions of their global dynamics.

The aim of these notes is to develop from first principles a general approach to ring dynamical phenomena, usually referred to as the "streamline formalism". This formalism was introduced by Borderies et al. (1982) and used by these authors in their subsequent papers (e.g. Borderies et al. 1983a,b, 1985 and references therein). It is a fluid approach to ring dynamics, based on the first three moments of the Boltzmann equation, and making use of perturbation techniques developed in celestial mechanics; in this sense, this is a hybrid (but powerful) method. Quite a number of fundamental theoretical results were obtained in this framework, but its main assumptions, limitations, methods and domains of application are not easily extracted from the existing literature. These notes are designed to remedy these shortcomings, by providing the reader with all the building blocks of the formalism. Therefore, the writing is designed to be as self-contained as possible, and the amount of material rather large. The reference list is purposely biased and limited, in the spirit of an introduction rather than a review. It is useful for the readers to have some practical knowledge of celestial mechanics, and some notions of fluid dynamics and physical kinetics. Some background knowledge on rings is not strictly necessary, but certainly helpful.

In the next section, basic notions and orders of magnitudes are presented. Section 3 introduces the Boltzmann equation and discusses the fundamental features of its application to ring systems. It is argued in these two sections that ring

systems can be described with the Boltzmann moment equations, up to second order; that the velocity field and the corresponding variations of the ring density are mainly imposed by the planet; and that the evolution of these two quantities takes place on a time-scale much longer than the orbital time-scale, whereas the pressure tensor (measuring the random motions) reaches steady-state on a time-scale comparable to the orbital time-scale. Therefore, ring dynamical problems can be solved in several steps: first, the general form of the ring density and velocity field must be found. Then the ring pressure tensor corresponding to this form of the velocity field and ring density can be computed, using a (semi)-Lagrangian description. Finally, the long time-scale evolution of the velocity field and ring density can be found, by using standard perturbation techniques inspired from Celestial Mechanics, as all the forces involved in the problem (the ring self-gravity, internal stress and satellite perturbations) are small compared to the gravitational attraction of the planet. This program is detailed in sections 4 through 7. The basic concepts of ring kinematics and dynamics are elaborated in section 4. In particular, a simple and general parametrization of ring shapes, motions (streamlines) and densities is introduced, which constitutes the root of the streamline formalism. Solutions for the pressure tensor are given in Section 5, for both dilute and dense systems, and some important general features of its behavior in rings are outlined. Section 6 presents the basic perturbation equations, borrowed from Celestial Mechanics, and provides a general discussion of ring mass, energy and angular momentum budgets. Some applications are described in Section 7, namely the now standard (but questioned) self-gravity model of narrow elliptic rings and the theory of density waves at Lindblad resonances. Section 8 presents a critical assessment of the scope and limitations of the formalism, as well as a quick overview of important issues in ring dynamics, and concludes these notes.

2 Basic concepts and orders of magnitude

The dynamics of the major rings, as we have defined them, is dominated by the gravitational field of their parent planet. The motion of individual ring particles is perturbed from an ellipse by interparticle collisions, the gravitational field of the other ring particles – the disk self-gravity – and the planet satellites.

Major rings all share a number of striking characteristics: they are flat and confined to the equatorial plane of their planet, they exhibit mostly axisymmetric features and the existing non-axisymmetric features show simple and regular patterns, they have complicated radial structures. . . In this section, we wish to develop some kind of heuristic understanding of the physical processes which generate these remarkable features.

The reason for the axisymmetry is easily understood. Any non-axisymmetric feature is quickly erased by the Keplerian shear supplied with a little diffusion. The existing non-axisymmetric features – like density-waves, ring arcs, or the global eccentricity of some Uranian rings and some Saturn ringlets – must have a dynamical origin (which is the reason for their regularity).

2.1 Angular momentum axis

Rings form thin circular disks because collisions dissipate energy while they conserve angular momentum. For an oblate planet, only the component of angular momentum parallel to the planet rotation axis is conserved, and the rings lie in the equatorial plane. A simple (although somewhat unrealistic) Celestial Mechanics argument can be made to illustrate this point.

Let us consider a situation in which the ring particles are initially confined to a plane different from the equatorial plane of the planet, on uninteracting, inclined circular orbits, as in Figure 1.

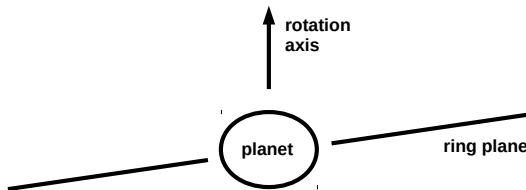


Figure 1: Sketch of an hypothetical ring initially inclined with respect to the equatorial plane of an oblate planet.

In this situation the total angular momentum of the ring is not aligned with the axis of symmetry of the planet. Due to the planet-induced differential precession of the lines of nodes, the system quickly falls into the stable situation represented on Figure 2. The total angular momentum of the disk has changed, and is now aligned with the symmetry axis of the planet. Because the system is isolated, some angular momentum has been transferred to the planet, but the orientation of its spin axis has basically not been affected, because it is much more massive than the rings.

It is interesting to give an order of magnitude estimate of the time-scale of this process, by considering the time required for two particle orbits of semimajor axes a , separated by the typical ring width d , to lose the correlation of their lines of nodes¹. This differential precession time-scale t_{pr} is then given by:

$$t_{pr} \sim \left[J_2 \Omega \left(\frac{d}{a} \right) \right]^{-1}, \quad (1)$$

where Ω is the angular frequency (mean motion) and J_2 the oblateness of the planet. It is interesting to have in mind typical orders of magnitude for the various quantities entering this formula: J_2 is of order 10^{-2} to 10^{-3} , $d \sim a$ (in Saturn's rings), $a \sim 10^5$ km, and particle rotation periods around the planet

¹In narrow rings, this process can be prevented by the action of the ring self-gravity. However, the ring viscous stress associated with the Keplerian shear probably leads to the damping of the ring inclinations, as it does for the ring eccentricities, at least if no viscous overstability occurs.

are typically of the order of a few hours. For Saturn’s rings, e.g., one obtains $t_{pr} \sim 10$ to 100 days; this figure reaches $\sim 10^4$ to 10^5 years for a 1 km wide ringlet.

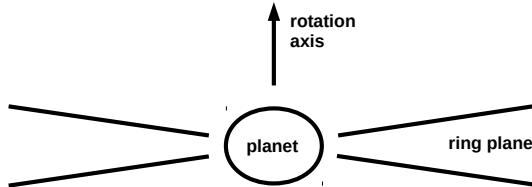


Figure 2: Situation reached from the starting point of Figure 1 under the action of differential precession.

2.2 Collisional quasi-equilibrium

Assuming that an hypothetical ring has reached the state just described, there is no net vertical motion: the vertical velocity averaged over a large number of ring particles is zero. The thickness of the ring measures the velocity dispersion of the ring particles². In reality, collisions affect this velocity dispersion and control the ring thickness, in various ways:

1. Direct collisions are inelastic. Consider two particles on a collision orbit with relative velocity v_r . During the collision, the relative velocity is reduced and one has

$$v'_r \sim \epsilon v_r, \quad (2)$$

where v'_r is the post-collision relative velocity, and ϵ is the so-called “*coefficient of restitution*”³; ϵ is a function of the relative velocity before encounter. Its functional form depends strongly on the bulk and surface properties of the colliding materials, and is unfortunately not very well constrained for planetary ring particles; however it is usually a decreasing function of v_r , so that the energy lost is larger for larger relative impact velocities, as one would intuitively expect. The important point here is of course that the velocity dispersion of the particles (which is the source of their relative collision velocities) is damped due to the inelasticity of the collisions.

2. On the other hand collisions are as usual a source of random motions: they scatter the particles. Furthermore in a sheared medium like planetary

²The velocity dispersion is in principle anisotropic. This anisotropy is ignored here.

³In fact one should define normal and tangential coefficients of restitution. The tangential coefficient is often ignored in the specialized literature, although it provides an important source of coupling between the translation and the spin degrees of freedom. However, such distinctions are not important for our order of magnitude estimates.

rings, collisions can transfer energy from the mean Keplerian motion to the random motions, thus increasing the velocity dispersion. This process appears macroscopically as the viscosity of the rings in the hydrodynamical approximation.

3. As orbital energy is transferred into random motions some of the ring material must fall on the planet. However as the total angular momentum of the ring is conserved, some other fraction of the material must go away from the planet. In fact, collisions do actually transfer the orbital motion angular momentum from the inside to the outside, while most of the mass is transferred inwards, and the ring spreads. Expressions for the rate of spreading will be given in Eq. (2.11) and for the rate of angular momentum transfer in sections 5 and 6.

The net result of all these processes is that the velocity dispersion attains an equilibrium when the rate of transfer of energy from the orbital motion equals the rate of dissipation of energy during collisions. The equilibrium can be obtained in particular through the dependence of the coefficients of restitution on the relative collision velocities (but see also section 2.2.4). In the process, rings spread. Thus, very sharp or narrow features must be confined by some sort of dynamical agent. This is why the discovery of the complex radial structure of Saturn's and Uranus' rings was so surprising.

We are going to quantify somewhat these processes, but some important notions must be introduced first.

2.2.1 Optical depth, collision frequency, and ring thickness

Under the simplistic assumption that the ring particles all have the same radius r , the optical depth τ is related to the particle number density n , the ring thickness H and the particle cross section $S \sim \pi r^2$ by:

$$\tau \sim nHS. \quad (3)$$

Note that the particle number density n is related to the ring surface density σ by $nH \sim \sigma/m$ where m is the mass of the particles.

One can also obtain an expression for the collision frequency as follows. The number of collisions N_c undergone by a given ring particle during a short time δt is $N_c \sim nSc\delta t$ where c is the velocity dispersion of the ring particles. Thus, the collision frequency ω_c (which is the inverse of the time δt during which, on average, a particle experiences only one collision), is given by:

$$\omega_c \sim nSc. \quad (4)$$

On the other hand, Figure 2 above shows that for small inclinations, the thickness H of the ring is of order ai where i is the typical inclination of ring particles at distance a ; furthermore, the typical vertical velocity of a ring particle on such an inclined orbit is typically of the order of the orbital velocity Ωa times the inclination i . Therefore, as the vertical velocity is of the order of the random velocity, one obtains:

$$c \sim \Omega ai \sim \Omega H. \quad (5)$$

By combining Eqs. (3), (2) and (5), one obtains the following relation between the collision frequency and the optical depth⁴:

$$\omega_c \sim \Omega\tau. \quad (6)$$

It is again useful to have in mind some orders of magnitude for the various quantities we have just introduced. The velocity dispersion is best estimated from the analysis of the damping of density and bending waves in Saturn's rings⁵; this yields $c \sim$ a few mm/s. This corresponds to a ring thickness of a few tens of meters at most, which is 10^7 times smaller than the typical radius of the rings; rings are *extremely* flat, and, correlatively, extremely cold⁶. As the major rings have optical depths which are typically of order unity, the collision frequency is comparable with the orbital frequency (the orbital period is about a few hours).

2.2.2 Ring viscosity

The concept of viscosity is strictly speaking dependent on the existence of a local stress-strain relation. It turns out that in rings, (and more generally for all fluids which cannot be described in the hydrodynamic limit) no such relation exists in general, but one can be found in the special (but important) case of axisymmetric flows. However, the concept of viscosity is convenient to discuss dissipation phenomena, and a heuristic derivation of the form of the viscous coefficient, due to Goldreich and Tremaine (1978b), is provided here. Microscopically, the kinematic viscosity coefficient can be expressed in terms of the collision frequency and the particles mean free path l as [see, e.g., Reif (1965)]:

$$\nu \sim \omega_c l^2. \quad (7)$$

If the optical depth τ is larger than unity, there are several collisions per rotation period. The particles follow more or less rectilinear trajectories between two collisions, and the mean free path is simply given by $l \sim c/\omega_c \sim c/\Omega\tau$. On the other hand, if the optical depth is smaller than unity, collisions occur only once in several rotation periods, and the particle paths are curved between two collisions. Note also that in this case, the mean free path and the transport coefficients should become anisotropic and one should define viscosity coefficients for all directions. However, such complications are again ignored here. Then, according to what we just said, the mean free path is of the order of the radial excursion of a particle on its elliptic motion, i.e., the ring thickness: $l \sim H \sim c/\Omega$ [see Eq. (2.5)]. Both regimes can be included in the same simple interpolation formula, which reads:

$$l \sim \frac{c}{\Omega(1 + \tau^2)^{1/2}}; \quad (8)$$

⁴A more quantitative estimate is given in Section 5. It is also discussed there that the ring vertical self-gravity increases substantially the effective vertical oscillation frequency, leading to significantly higher collision frequencies in main ring systems

⁵In the hydrodynamic approximation, the damping is controlled by the ring viscosity, which can be related to the velocity dispersion; see below.

⁶The ring Reynolds number is enormous, but they can't be turbulent, because their scale of granularity is comparable to the vertical scale; this is a major difference with other astrophysical disks.

Replacing this expression in Eq. (7) and making use of Eq. (6) yields:

$$\nu \sim \frac{c^2 \tau}{\Omega(1 + \tau^2)}; \quad (9)$$

Note that the same expression holds for the transverse viscosity of a plasma in a magnetic field, provided that the mean motion Ω is replaced by the plasma gyrofrequency.

2.2.3 Velocity dispersion quasi-equilibrium

We can now derive an approximate equation of evolution of the ring velocity dispersion. The internal energy of the ring (kinetic energy of random motions) per unit mass is c^2 . The rate of viscous transfer of energy per unit mass from the orbital motion to the random motions is $\sim \nu(ad\Omega/da)^2 \sim \nu\Omega^2$ (for a simple justification, see Landau and Lifshitz 1987, p. 50, Eq. (16.3), with the Keplerian circular velocity field, which has zero divergence). The rate of change of c^2 due to the energy loss during collisions is comparable to the change of the squares of the relative velocities of the colliding particles, i.e., to $v_r^2 - v_r'^2 \sim (1 - \epsilon^2)v_r^2 \sim (1 - \epsilon^2)c^2$ [see Eq. (2)]. The typical collision time is of order $1/\omega_c$, so that the rate of damping of c^2 is of order $\omega_c(1 - \epsilon^2)c^2$. Putting these two results together and making use of Eq. (6) leads to the desired equation of evolution of the velocity dispersion:

$$\frac{dc^2}{dt} \sim -\alpha\Omega\tau c^2(1 - \epsilon^2) + \beta\frac{\Omega c^2 \tau}{1 + \tau^2}, \quad (10)$$

where coefficients of order unity, α and β , have been introduced. This equation of evolution has two important consequences:

1. There is only one time scale involved: the orbital time-scale. Thus, the velocity dispersion reaches equilibrium on a time-scale comparable to the particle orbital period, i.e. a few hours. This is exceedingly short. When the velocity dispersion equilibrium is reached, the ring equilibrium thickness is also reached: thus the flattening of the rings takes place in a few hours. This is much shorter than the spreading time-scale t_{sp} , which is basically the time for a particle to random-walk across the ring:

$$t_{sp} \sim (R/l)^2 \omega_c^{-1}, \quad (11)$$

where R is the ring radial extent.

2. At equilibrium ($dc^2/dt = 0$), the equation of evolution yields a relation between the coefficient of restitution ϵ and the optical depth τ :

$$\epsilon^2 \sim 1 - \frac{\gamma}{1 + \tau^2}, \quad (12)$$

where γ is another coefficient of order unity ($\gamma \sim 0.5$; see section 5). Note that ϵ is an increasing function of τ , the minimum of which is obtained for $\tau = 0$; this minimum is rather high (0.6 or 0.7) and is even higher when coupling with the spin degrees of freedom is considered (citealtS84,AT86). This relation is known as the $\epsilon - \tau$ relation, and was derived by Goldreich

and Tremaine (1978b), both in the heuristic manner presented here and in a more formal way by solving Boltzmann's equation. At first glance, this relation does not seem to involve the ring velocity dispersion. Remember however that the coefficient of restitution is a function of the particles' velocity: $\epsilon = \epsilon(c)$. This determines in principle the magnitude of the velocity dispersion once the optical depth and the functional form of ϵ are known (which, let us recall, is not the case). Notice finally that the equilibrium is stable if ϵ is a decreasing function of the impact velocity; this is the case for all known materials. This result can be understood as follows. The rate of transfer of energy from the orbital energy into random motions is proportional to c^2 ; the rate of dissipation of random energy is proportional to $(1 - \epsilon^2)c^2$. If c^2 is, e.g., increased from, its equilibrium value, the collisions become more inelastic, ϵ is decreased, and the rate of loss of random motions wins over the injection from the shear: the disk is returned to equilibrium. A similar reasoning holds if c^2 is decreased rather than increased.

2.2.4 Limitations and extensions of the previous model

The preceding analysis ignores a number of complications. We are not going to present them with as many details, but just outline the problems and their solutions when they are known, and refer the reader to the specialized literature.

First, we have ignored the possibility of having perturbed flows, i.e. flows for which the mean velocity is not circular. Such flows occur for example in the vicinity of resonances with the planet satellites. This type of flow will be fully discussed from section 4 onwards.

We have implicitly assumed that the particles have the same size. It appears that the equilibrium velocity dispersion is roughly independent of the particle size, provided that the coefficient of restitution ϵ does not depend too strongly on v (see e.g. Salo and Lukkari 1984). Note also that the upper bounds to the ring thickness derived from the Voyager data argues also strongly in favor of an equilibrium velocity dispersion independent on the particle size (equipartition would lead to a ring thickness of the order several tens of kilometers whereas the Voyager data imply one or two hundred of meters at most). The single particle size model poses however one difficulty: the effective particle size, optical depth, collision frequency... are not unambiguously defined (this issue will be addressed in section 5). Note also that in most models, the particles are assumed spherical.

Gravitational binary encounters have been neglected. They also act as an effective particle scatterer. A heuristic discussion of the effect of these encounters can be found in Cuzzi et al. (1979) (see also Shu and Stewart 1985). The main effect is on small particles, which are scattered out of the ring plane by large particles, with a velocity dispersion a few times larger than the velocity dispersion of the large particles. Note that because of the thin disk geometry, the main contribution is not due to the encounters with large impact parameters, in opposition to the standard situation in galactic dynamics.

The ring particles are usually assumed indestructible. This is a crude assumption, especially that accretion and erosion processes are likely to be very important in planetary ring dynamics. The problem of the collisional evolution of the particle size distribution has been addressed by a few authors (see Weiden-

schilling et al. 1984; Longaretti 1989a), but no self-consistent model taking into account both the evolution of the size distribution and the velocity dispersion is available.

The coupling between the velocity dispersion and the spin degrees of freedom has been neglected. A heuristic discussion of these effects can be found in Shukhman 1984. Basically, a rough equipartition of energy is established between the velocity dispersion and the energy of rotation.

Finally, one can wonder what happens if the ring material does not allow the coefficient of restitution ϵ to be larger than the minimum value required for the equilibrium to exist. This is quite likely to be the case if the particles are regolith-covered, or are the loose aggregates called *Dynamical Ephemeral Bodies*, as has been suggested in the past few years (Weidenschilling et al. 1984; Longaretti 1989a)). The velocity dispersion then decreases, and the ring becomes more compact until a different regime is reached, in which the particles are no longer at mutual distances much larger than their sizes. In this case, the collisional processes are dramatically altered. For example, the viscous transfer of momentum occurs not because the particles carry the momentum on the mean free path, but because it is carried across the particle itself; this gives rise to a minimum viscosity

$$\nu \sim \Omega d^2, \quad (13)$$

where d is the typical particle size (Brahic, 1977; Shukhman, 1984; Araki and Tremaine, 1986). The properties of particle flows in such conditions have been investigated by Borderies et al. (1985).

The reader will notice that none of these complications alters the basic physical phenomena described earlier: the equilibrium velocity dispersion is established on a time-scale comparable to the orbital time-scale; in the process, energy is permanently drawn from the orbital motion into random motions, and then dissipated as heat; as orbital energy is dissipated while angular momentum is conserved, rings spread. The only important issue is to know whether the ring particle properties are compatible with a “thick” equilibrium in which the viscosity is given by Eq. (9), or lead to a “thin” equilibrium for which it is reduced to its minimum value given by Eq. (13); this last possibility seems most likely in high optical depth ring systems.

2.3 Angular momentum transport and the origin of the rings radial structures

Angular momentum transport is a key concept to the understanding of gross and fine features of planetary ring dynamics. There are two major causes of angular momentum transport in planetary rings: the ring viscous stress and the gravitational perturbations, either due to the ring itself or to some external agents, e.g. satellites.

To the lowest order of approximation, as we have just argued, the ring viscous stress transports the angular momentum from the inside to the outside⁷. However, some interesting other phenomena can occur. The viscous luminosity of angular momentum (the rate of transfer of angular momentum through

⁷This is true only of unperturbed flows. In perturbed flows, the viscous flow of angular momentum can be reversed; see section 5.

a given radius of the ring due to the viscous stress) is proportional to $\nu\sigma$ (cf section 5), so that the viscous torque on a ringlet is proportional to $d\nu\sigma/dr$. The reader can check that if $\partial\nu\sigma/\partial\sigma < 0$, fluctuations in the ring density are amplified, because the viscous torques tend to push material from regions of low optical depths to regions of high optical depths. This is the case for example for viscosities of the form of Eq. (9), if one uses $\sigma \propto \tau$. Such a phenomenon is at the origin of the viscous and thermal instabilities which have been invoked to explain the complex radial structure of planetary rings (for a review, see Stewart et al. 1984). However, it appears that this such a possibility does not occur in dense rings (see e.g. Araki and Tremaine 1986; Wisdom and Tremaine 1988)

On the other hand the gravitational interaction between rings and satellites often results in the creation of density waves, or at least in the creation of some kind of wake. This generates a net angular momentum exchange between the disk and the satellite, the angular momentum flowing again from the inside to the outside (Goldreich and Tremaine 1980; see also sections 6 and 7): if the satellite lies inside the ring, it gives angular momentum to the ring; this is the case for example with the inner “shepherd” satellite of the ϵ ring; the reverse is true in the opposite case. Thus a satellite and a ring repel one another. This phenomenon was invoked as a possible confining process to explain the outer edges of Saturn’s A and B ring, and also to explain the confinement of narrow rings (Goldreich and Tremaine, 1979a; Borderies et al., 1982, 1989). One also sees that a small satellite situated in a ring “repels” the ring material around it, by virtue of these angular momentum exchanges. The existence of a collection of kilometer-sized particles randomly distributed in the rings was therefore envisioned as a possible cause to their radial structure.

Let us stress that these mechanisms are not the only possible source of structure in the rings⁸. In the analysis of dense rings performed by Araki and Tremaine (1986), these authors argued that no viscous instability of the type described here actually occurred, but instead that some type of “phase transition” between zero shear (solid) and high shear (fluid) regimes was possible, and suggested that this could also account for the ring complex radial structure. However, angular momentum exchanges (and energy exchanges) are of fundamental importance, because they regulate the long term dynamics of the rings.

3 The Boltzmann equation and its moments

Rings are composed of countless particles. This suggests various types of approach to study their dynamics. For example, one can treat them as a collection of independent test particles. This yields some crude estimates of some basic dynamical properties, but as a given particle experiences many collisions during its life-time, it cannot give a realistic description of ring evolution. The statistical character of the effects of collisions on ring particles dynamics is in fact appropriately described by the Boltzmann equation, which applies to the evolution of the particle distribution function $f(\mathbf{r}, \mathbf{v}, m, t)$. By definition, $f d^3\mathbf{r} d^3\mathbf{v} dm$ is the number of particles of mass m at position \mathbf{r} , with velocity \mathbf{v} in the el-

⁸Density and bending waves are also well-identified sources of structure in Saturn’s A and B rings.

elementary seven-dimensional volume of phase space $d^3\mathbf{r}d^3\mathbf{v}dm$. One should in principle consider that the distribution function depends on the particle spin as well. This would however unnecessarily complicate the analysis without affecting the basic principles that we wish to expose. Therefore, the coupling with the spin degrees of freedom is ignored from now on. For the same reason, the parameters describing the particle shapes and surfaces (which are important for the collisional dynamics) are also ignored.

The Boltzmann equation reads:

$$\frac{\partial f}{\partial t} + \mathbf{v} \cdot \frac{\partial f}{\partial \mathbf{r}} + \nabla \phi \cdot \frac{\partial f}{\partial \mathbf{v}} = \left(\frac{\partial f}{\partial t} \right)_c, \quad (3.1)$$

where the right-hand side represents the effect of the particle collisions on the evolution of the distribution function f . The form of this collision term does not need to be further specified yet. The potential ϕ includes all the dynamical agents acting on the particles except the collisional forces: the planet potential ϕ_p , the potential arising from the disk self-gravity ϕ_d , and the satellite perturbations ϕ_s .

The Boltzmann equation without collisions expresses the fact that the six-dimensional flow of particles of a given mass in phase space is incompressible (the flow is confined to constant mass hypersurfaces). It has the form of a continuity equation. The collision term acts as a local source and sink term in phase space.

3.1 The moments of the Boltzmann equation

The Boltzmann equation, involving six-dimensional derivatives, is in general rather difficult to solve. This is why one usually prefers to work with its moments. It is necessary to define first various local (in physical space) average quantities: the mean density of particles N , the mean velocity \mathbf{u} , the pressure tensor⁹ p_{ij} . these quantities are defined as follows:

$$N = \int f d^3\mathbf{v}, \quad (3.2)$$

$$\mathbf{u} = \frac{1}{N} \int \mathbf{v} f d^3\mathbf{v}, \quad (3.3)$$

$$p_{ij} = \int (v_i - u_i)(v_j - u_j) f d^3\mathbf{v}, \quad (3.4)$$

where the subscripts i, j refer to a cartesian inertial reference frame. The integrals are performed over all velocity space. One sees that these mean quantities are indeed the velocity moments of the distribution function. Note that these quantities are defined per unit particle mass, except for the mean velocity; for example, to retrieve the usual number density of particles, one needs to integrate N over all masses. Also, $p_{ij} \sim Nc^2$ where c is the mean square one dimensional velocity dispersion, defined by $3Nc^2 \equiv p_{xx} + p_{yy} + p_{zz}$.

By multiplying the Boltzmann equation by $1, v_i, v_i v_j$ and integrating over the velocity space, one obtains respectively, after some manipulations:

⁹The pressure tensor is the opposite of the stress tensor, and the two expressions may indifferently be used.

$$\frac{\partial N}{\partial t} + \frac{\partial}{\partial x_i}(Nu_i) = \left(\frac{\partial N}{\partial t}\right)_c, \quad (3.5)$$

$$N \left(\frac{\partial u_i}{\partial t} + u_j \frac{\partial u_i}{\partial x_j} \right) = -N \frac{\partial \phi}{\partial x_i} - \frac{\partial p_{ij}}{\partial x_j} + \left(\frac{\partial Nu_i}{\partial t}\right)_c, \quad (3.6)$$

$$\frac{\partial p_{ij}}{\partial t} + p_{ik} \frac{\partial u_j}{\partial x_k} + p_{jk} \frac{\partial u_i}{\partial x_k} + \frac{\partial}{\partial x_k}(p_{ij}u_k) + \frac{\partial q_{ijk}}{\partial x_k} = \left(\frac{\partial p_{ij}}{\partial t}\right)_c, \quad (3.7)$$

where q_{ijk} is the tensor of the third order velocity moments of the distribution function.

Note that the equation of evolution of the moments of any order depends on the moments to the next order. Thus, one needs some external information in order to close the hierarchy of moment equations. Fortunately, the special characteristics of ring systems provide us with quite a number of simplifying assumptions which make the problem tractable.

3.2 The moment equations in ring systems

Rings constitute cold media: the mean velocity \mathbf{u} , of the order of the orbital velocity (a few km/s), is several orders of magnitude larger than the velocity dispersion c (a few mm/s). Thus, the term involving the third order moments $q_{ijk} \sim Nc^3$ can be neglected in comparison with the other terms of Eq. (3.7), except maybe the z -derivative terms, because of the small vertical scale height of the rings. From a hydrodynamical point of view, this approximation is equivalent to killing the heat conduction terms. It is justified because the equilibrium of the internal heat of the ring particle fluid (i.e., its velocity dispersion) is controlled by the input from the shear, and the loss due to the inelasticity of the collisions, as argued in the previous section, and not by heat conduction phenomena, which occur on a much longer time-scale, except possibly in the vertical direction where on the contrary they tend to make the disk isothermal¹⁰.

We have argued that the velocity dispersion is more or less size independent. Furthermore, all the forces which can generate the mean velocity are gravitational, and therefore insensitive to the particle mass. Thus, in first approximation, both \mathbf{u} and p_{ij} do not depend on the particle mass, and one can integrate Eqs. (3.5) through (3.7) on the mass parameter. Notice also that $\int m(\partial N/\partial t)_c dm = 0$, because the collisions conserve the total local mass (the size distribution evolves by creation, destruction accretion and erosion of particles, but in all these processes, the total mass is locally conserved). Therefore, multiplying Eq. (3.5) by m and integrating over mass yields:

$$\frac{\partial \rho}{\partial t} + \frac{\partial}{\partial x_i}(\rho u_i) = 0, \quad (3.8)$$

where $\rho \equiv \int mN dm$ is the local mass density. This equation has the standard form of a continuity equation. Let us also introduce here, for future use, various mass averaged quantities. The mean mass of the distribution is defined by $M = \int mN dm / \int N dm$; in first approximation, M is independent of the location

¹⁰Horizontal gradients can also lead to a non negligible heat conduction term when the flow is sufficiently perturbed from the axial symmetry, but this phenomenon is neglected throughout these lecture.

in the rings. With this definition, $\rho = Mn$, where $n = \int N dm$ is the local particle density. One can also define a mass weighted pressure tensor $p_{ij} \equiv \int m p_{ij} dm = Mp_{ij}$ and a mass weighted third order moment $q_{ijz} \equiv \int m q_{ijz} dm = Mq_{ijz}$.

Collisions are locally momentum conserving if the particle size is smaller than the mean free path (even if coupling with the spin degrees of freedom is included). If the particle size is of the same order as or larger than the mean free path, there is a non-local collisional contribution to momentum transport, across the particle size, because the particles behave as an almost incompressible medium in comparison with the rings. However, one can show that this contribution can be expressed as the divergence of a second rank tensor (see Shukhman 1984). Therefore, it can be simply taken into account by a suitably redefinition of p_{ij} , and one can assume, without loss of generality, that $(\partial N u_i / \partial t)_c = 0$. Multiplying Eq. (3.6) by m and integrating over mass yields, after division by ρ :

$$\frac{\partial u_i}{\partial t} + u_j \frac{\partial u_i}{\partial x_j} = -\frac{\partial \phi}{\partial x_i} - \frac{1}{\rho} \frac{\partial p_{ij}}{\partial x_j}, \quad (3.9)$$

which has the standard form of an equation of fluid motion. The physical meaning of the pressure tensor term in Eq. (3.9) is well-known from Fluid Mechanics. Let us ignore the term due to ϕ , and compute the rate of change of momentum per unit volume, $\partial \rho \mathbf{u} / \partial t$ from the momentum equation and the continuity equation. Integrating over some arbitrary fixed volume in space, one obtains $\partial / \partial t \iiint \rho u_i dV = - \iint (p_{ij} + \rho u_i u_j) dS_j$, where $d\mathbf{S}$ is an elementary surface vector. The right-hand side of this expression is the flux of momentum through the surface bounding the volume considered. The second term is the momentum that the fluid crossing the surface during the motion carries with it (the so-called advective term), the first term characterizes the fact that the fluid outside the volume considered exerts a force equal to $-(\mathbf{n} \cdot \mathbf{e}_i) p_{ij} \mathbf{e}_j$ on the fluid in the volume considered per unit area of the bounding surface, where \mathbf{n} is the outside normal to the surface, and $\{\mathbf{e}_i, i = x, y, z\}$ are the unit vectors of a cartesian system of coordinates. The existence of this term is natural, because p_{ij} is a measure of the correlation of the random velocities in the (i, j) directions, and is therefore similar to the $\rho u_i u_j$ term. Note also that this contribution is a consequence of the existence of random velocities, and not of collisions, although random velocities are often the result of collisions.

Let us now complete our mass integrations by noting that Eq. (3.7) is unchanged by the mass weighting process, except for the third order moment term, which reduces to $\partial q_{ijz} / \partial z$, and, possibly, for the collisional term.

For completeness, let us mention the existence of a few processes which do not conserve mass nor momentum locally. For example, micron-sized particles are permanently accreted onto large particles and formed from them. As these micron-sized particles are submitted to electromagnetic forces as well as gravitational ones, they evolve differently from the large ones. Such effects could introduce mass and momentum source and sink terms, and require a multi-fluid description. However, we have already mentioned that the ring fraction of mass included in these particles is very small, so that this contribution can be safely neglected. Also, ballistic transport processes can result in mass and momentum exchanges across large distances in the rings (for a review, see Durisen 1984). These processes are neglected in this lecture.

Finally, let us point out that the mass integration just performed is not completely innocuous. Very big particles are quite underpopulated with respect to smaller ones in rings, so that their mean separation can be very large. If one considers dynamical phenomena having characteristic scales smaller than the mean separation of the bigger particles, the mass integration is not very meaningful.

This problem is specific to ring systems and cannot be found in ordinary fluids, because the individual particles, usually molecules, all have roughly the same size, much smaller than any scale of interest for the macroscopic motions. In ring systems, the size distribution spans several orders of magnitude... There is also another major difference between ordinary fluids and rings. In ordinary fluids – i.e., in the so-called hydrodynamical approximation – the divergence of the pressure tensor in Eq. (3.9) is reduced to the sum of a pressure term and of a viscous term, and the pressure tensor evolution, Eq. (3.7), is reduced to the evolution of its diagonal trace, which represents the internal energy of the fluid. The third order moments of the form q_{ij} are expressed as heat flux terms. The system of equation is finally closed with the provision of an equation of state (see also section 5). No such manipulation is possible in rings, because the pressure tensor is not symmetric enough. This is due to the fact that the particle paths are curved between collisions, whereas in ordinary fluids, the collision time is always much shorter than the dynamical time (or equivalently that the distance travelled between two collisions is smaller than the system characteristic scales).

It is necessary for future use to recast the equations just obtained in Lagrangian form. Eqs. (3.8), (3.9) and (3.7) constitute a Eulerian description of ring systems: the various moments, n , \mathbf{u} , p_{ij} , are functions of position and of time, and describe the state of the rings at a given place and at a given moment. In the Lagrangian description, the attention is focused on a *fluid* particle, i.e., a collection of ring particles. This collection must be large enough so that its size is much larger than the typical particle size and particle mean separation, but much smaller than the typical length-scale of the phenomena under consideration. Also, the concept of fluid particle can be meaningful only if the typical time for a ring particle to random-walk out of the fluid particle is much larger than the dynamical time-scale. One sees again that the existence of a broad particle size distribution can in certain circumstances invalidate these assumptions. In order to have a complete description of the fluid, one wants to know at each time the position, density... of all its fluid particles. Let us call \mathbf{r} the position of a fluid particle, and \mathbf{r}_0 its position at some initial time t_0 . The position of the fluid particle depends necessarily on time. Also, for a given flow, the fluid particles paths do not cross at any given time, so that the path is completely specified if the initial position is known; thus the fluid particle position depends on its initial position as well:

$$\mathbf{r} = \mathbf{r}(\mathbf{r}_0, t). \quad (3.10)$$

With these definitions, the velocity of the flow at a given time and location is equal to the velocity of the fluid particle located at the same place at the same time, and tangent to the fluid particle path:

$$\left(\frac{\partial \mathbf{r}}{\partial t}\right)_{\mathbf{r}_0} = \mathbf{u}(\mathbf{r}, t) = \mathbf{u}(\mathbf{r}(\mathbf{r}_0, t), t), \quad (3.11)$$

By the same token, any fluid quantity X (scalar, vector or tensor) can be considered as a function of either \mathbf{r} and t or of the fluid particle to which it belongs, i.e. as a function of \mathbf{r}_0 and t through Eq. (3.10). This enables us to introduce the concept of substantial derivative, noted D/Dt :

$$\frac{DX}{Dt} \equiv \left(\frac{\partial X(\mathbf{r}_0, t)}{\partial t}\right)_{\mathbf{r}_0} = \frac{\partial X(\mathbf{r}, t)}{\partial t} + \mathbf{u} \cdot \frac{\partial X(\mathbf{r}, t)}{\partial \mathbf{r}}. \quad (3.12)$$

This substantial derivative, commonly used in Fluid Dynamics, expresses the change with time of a given quantity X along the flow, i.e. as it is carried by a fluid particle along its path. Note that we have implicitly assumed that all quantities are defined in a “smooth” way at the initial time t_0 ; for example, the initial velocity is assumed to vary smoothly from one fluid particle to the next (it is a continuous function of \mathbf{r}_0).

We are now in position to recast Eqs. (3.8), (3.9) and (3.7) in Lagrangian form. They read:

$$\frac{D\rho}{Dt} + \rho \frac{\partial u_i}{\partial x_i} = 0, \quad (3.13)$$

$$\frac{D^2 r_i}{Dt^2} = \frac{Du_i}{Dt} = -\frac{\partial \phi}{\partial x_i} - \frac{1}{\rho} \frac{\partial p_{ij}}{\partial x_j}, \quad (3.14)$$

$$\frac{Dp_{ij}}{Dt} + p_{ik} \frac{\partial u_j}{\partial x_k} + p_{jk} \frac{\partial u_i}{\partial x_k} + p_{ij} \frac{\partial u_k}{\partial x_k} + \frac{\partial q_{ijz}}{\partial z} = \left(\frac{\partial p_{ij}}{\partial t}\right)_c. \quad (3.15)$$

where again all derivatives with respect to x_i are evaluated at $\mathbf{x} = \mathbf{r}$ (this will be implicitly assumed in the remainder of these notes).

Further progress can be made by taking advantage of the extreme thinness of ring systems, and of the dominance of the planet attraction over the potential of the disk self-gravity, the perturbations of the satellite¹¹, and the disk pressure tensor, except for the determination of the ring vertical structure. Thus the horizontal component of the velocity, which is mainly driven by the planet, is nearly independent of the vertical coordinate in the ring plane. A somewhat different result holds for the vertical component, for the following reason. Let us consider for example a ring in circular motion in the equatorial plane of its parent planet but with non zero thickness. Typically, $H/r \sim 10^{-7}$. Thus, the variation of the vertical component of the planet force across the ring thickness is very small, comparable to the vertical component of the pressure tensor force, and even smaller than the ring self-gravity; the pressure tensor can then prevent the crossing of the fluid particle paths that the planet and the ring self-gravity would tend to impose in the vertical direction. This physical constraint is often expressed through a condition of vertical hydrostatic equilibrium both in ring dynamics and in accretion disk theory. In this case, the vertical velocity is nearly independent of the vertical coordinate; it essentially is equal to zero, except for example when inclined satellites excite coherent vertical motions of the ring

¹¹This is true even near a resonance with a satellite.

plane (this is the case for bending waves). Alternatively, when the ring particles are in a “thin” equilibrium (in the sense defined in section 2), i.e. when the ring particles have mean separations comparable to their radii, the hydrostatic condition has to be replaced with the constraint of incompressibility of the three dimensional flow (see Borderies et al. 1985 and section 5).

In any case, because of the remarkable thinness of the rings, it is useful to vertically integrate the preceding equations, and forget about the precise vertical structure. In this operation, all fluid particles with different z are replaced by an equivalent fluid particle whose vertical coordinate is equal to the mean plane height. Let us call $\mathbf{R} = (R, \Theta, \mathcal{Z})$ the position of this equivalent fluid particle; $\mathcal{Z} = \int z \rho dz / \sigma$, and the vertically integrated equation of motion Eq. (3.14) reduces to the equation of motion of this equivalent particle. For simplicity, we will assume here that the condition of vertical hydrostatic equilibrium holds¹²; similar results are obtained in the incompressible case (see section 5). The integration of the continuity equation and of the equations of fluid motion is greatly simplified by the fact that the velocity is nearly independent on the vertical coordinate in comparison with the density ρ . Therefore, in cylindrical coordinates (r, θ, z) , the vertically integrated continuity equation reads:

$$\frac{D\sigma}{Dt} + \sigma \frac{\partial u_r}{\partial r} + \frac{\sigma}{r} \frac{\partial u_\theta}{\partial \theta} = 0, \quad (3.16)$$

where $\sigma \equiv \int \rho dz$ is the surface density of the ring.

Multiplying Eq. (3.14) by ρ , integrating over z and dividing the resulting equations by σ yields:

$$\frac{D^2 R}{Dt^2} - R \left(\frac{D\Theta}{Dt} \right)^2 = -\frac{\partial \phi_0}{\partial r} - \frac{1}{\sigma} \left[\frac{1}{r} \frac{\partial (r P_{rr})}{\partial r} + \frac{1}{r} \frac{\partial P_{r\theta}}{\partial \theta} - \frac{P_{\theta\theta}}{r} \right], \quad (3.17)$$

$$\frac{1}{R} \frac{D}{Dt} \left(R^2 \frac{D\Theta}{Dt} \right) = -\frac{1}{r} \frac{\partial \phi_0}{\partial \theta} - \frac{1}{\sigma} \left[\frac{1}{r^2} \frac{\partial (r^2 P_{r\theta})}{\partial r} + \frac{1}{r} \frac{\partial P_{\theta\theta}}{\partial \theta} \right], \quad (3.18)$$

$$\frac{D^2 \mathcal{Z}}{Dt^2} = - \left(\frac{\partial \phi}{\partial z} \right)_{z=\mathcal{Z}} - \frac{1}{\sigma} \left[\frac{1}{r} \frac{\partial (r P_{rz})}{\partial r} + \frac{1}{r} \frac{\partial P_{\theta z}}{\partial \theta} \right], \quad (3.19)$$

where $P_{ij} \equiv \int p_{ij} dz$ are the vertically integrated components of the pressure tensor, and where $\phi_0 = \int \rho \phi dz / \sigma$ is the vertically averaged potential (function of \mathcal{Z}). Due to the small thickness of the ring, $\phi_0 \simeq \phi$. In Eq. (3.19) we have used the constraint of vertical hydrostatic equilibrium with respect to the mean plane, which reads $\partial p_{zz} / \partial z = -\rho [\partial \phi / \partial z - (\partial \phi / \partial z)_{z=\mathcal{Z}}]$, and $D\mathcal{Z} / Dt = \int u_z \rho dz / \sigma$, which follows from Eqs. (3.13) and (3.16) (for details, see Shu and Stewart 1985).

Finally, Eq. (3.15) yields:

¹²One could think at first glance that this assumption is not very good for perturbed flows, because the horizontal and vertical orbit perturbations seem to have the same period. However, this is not true: in the vertical direction, the self-gravity of the ring is much larger than the restoring force of the planet, which is not the case in the horizontal direction. Therefore, the vertical effective epicyclic frequency is about ten times larger than the horizontal one, and the vertical structure adjusts on a time-scale much shorter than the horizontal perturbation time-scale (see section 5).

$$\frac{DP_{ij}}{Dt} + P_{ik} \frac{\partial u_j}{\partial x_k} + P_{jk} \frac{\partial u_i}{\partial x_k} + P_{ij} \frac{\partial u_k}{\partial x_k} = \left(\frac{\partial P_{ij}}{\partial t} \right)_c. \quad (3.20)$$

where all terms involving z derivatives have been removed by the vertical integration. In Eqs. (3.17) through (3.20), all quantities depending on the spatial coordinates are evaluated at \mathbf{R} .

Note that when there are no vertical motions ($D^2Z/Dt^2 = 0$), the rings are in principle symmetric with respect to the equatorial plane, so that $P_{rz} = 0$ and $P_{\theta z} = 0$, and Eq. (3.19) is trivially satisfied.

It is useful to recast Eq. (3.20) in cylindrical coordinates. There are several ways to perform the change of variables. One can make it directly on Eq. (3.20); or directly on the Boltzmann equation itself Eq. (3.1) and compute afterwards the moment equations; or use tensor calculus, by replacing the partial derivatives in cartesian coordinates by covariant derivatives in cylindrical coordinates and compute the Christoffel symbols. The latter is probably the fastest. In any case, we give the resulting equations for P_{rr} , $P_{r\theta}$, $P_{\theta\theta}$ and P_{zz} (we will see in section 5 that the remaining equations are not needed for our purposes, but the interested reader can find them in the appendix B of Shu and Stewart (1985)):

$$\begin{aligned} \frac{DP_{rr}}{Dt} + P_{rr} \left(3 \frac{\partial u_r}{\partial r} + \frac{u_r}{r} + \frac{1}{r} \frac{\partial u_\theta}{\partial \theta} \right) + 2P_{r\theta} \left(\frac{1}{r} \frac{\partial u_r}{\partial \theta} - \frac{2}{r} u_\theta \right) \\ = \left(\frac{\partial P_{rr}}{\partial t} \right)_c, \end{aligned} \quad (3.21)$$

$$\begin{aligned} \frac{DP_{\theta\theta}}{Dt} + P_{\theta\theta} \left(\frac{\partial u_r}{\partial r} + \frac{3u_r}{r} + \frac{3}{r} \frac{\partial u_\theta}{\partial \theta} \right) + \frac{2}{r} P_{r\theta} \frac{\partial}{\partial r} (ru_\theta) \\ = \left(\frac{\partial P_{\theta\theta}}{\partial t} \right)_c, \end{aligned} \quad (3.22)$$

$$\begin{aligned} \frac{DP_{r\theta}}{Dt} + 2P_{r\theta} \left(\frac{\partial u_r}{\partial r} + \frac{u_r}{r} + \frac{1}{r} \frac{\partial u_\theta}{\partial \theta} \right) + \frac{1}{r} P_{rr} \frac{\partial}{\partial r} (ru_\theta) + P_{\theta\theta} \left(\frac{1}{r} \frac{\partial u_r}{\partial \theta} - \frac{2}{r} u_\theta \right) \\ = \left(\frac{\partial P_{r\theta}}{\partial t} \right)_c, \end{aligned} \quad (3.23)$$

$$\begin{aligned} \frac{DP_{zz}}{Dt} + P_{zz} \left(\frac{\partial u_r}{\partial r} + \frac{u_r}{r} + \frac{1}{r} \frac{\partial u_\theta}{\partial \theta} \right) + 2P_{zr} \frac{\partial}{\partial r} \left(\frac{DZ}{Dt} \right) + 2P_{\theta z} \frac{1}{r} \frac{\partial}{\partial \theta} \left(\frac{DZ}{Dt} \right) \\ = \left(\frac{\partial P_{zz}}{\partial t} \right)_c, \end{aligned} \quad (3.24)$$

Let us conclude this section with a final fundamental comment. We have already pointed out that all forces are small compared to the planet's, except in the vertical direction, but the question of the vertical structure has just been evicted by the vertical integration. This means also that the dynamical time-scale imposed by the planet is much shorter than the dynamical evolution time-scale due to the disk self-gravity, the satellite perturbations, or the pressure tensor.

Furthermore, we have also argued in section 2 that the pressure tensor reaches steady-state on a time scale comparable to the orbital time scale. This means that *the pressure tensor components reach steady-state for steady-state values of the mean velocity \mathbf{u} and surface density σ mainly imposed by the planet.* Therefore, the theory of ring dynamics can be developed according to the following scheme:

1. The motion is first solved when the planet force is the only one acting on the rings.
2. The P_{ij} are then found by solving Eq. (3.21) with steady-state \mathbf{u} and σ appropriately chosen.
3. The others forces (self-gravity, satellite perturbations and pressure tensor) are treated as perturbations. When they drives a slow evolution of the surface density and velocity field of the rings, the pressure tensor evolution is of course “enslaved” to this evolution.

This program forms the basis of the streamline formalism and is described in the next sections.

4 Ring kinematics: streamlines

Our primary objective is to find the general solution of Eqs. (3.17) and (3.18) when the potential is reduced to the planetary potential, and when the viscous stress terms are neglected. Thus, the problem at hand is analogous to the motion of a test particle around a planet, except that it applies to a fluid particle rather than to an individual particle. We refer to this problem as to the “fluid test particle motion” in the remainder of these notes. For convenience, we drop the capital letter notation for the position of the equivalent fluid particle.

Furthermore, for simplicity, we will restrict ourselves to motions confined to the equatorial plane of the planet, i.e., $z = 0$ and Eq. (3.19) does not need to be considered. This restriction eliminates the dynamics of bending waves and inclined rings from the analysis. However, bending waves do not differ very much from density waves, and inclined rings are similar in their dynamical properties to eccentric rings, so that this restriction is not essential while simplifying the exposition of the method.

Note that the total derivative (d/dt) and the substantial derivative (D/Dt) have very similar meanings: the total time derivative of Classical Mechanics (resp. the substantial derivative) refers to the motion of a given point (resp. fluid) particle under given initial conditions. It is therefore customary to write Eqs. (3.17) through (3.19) with usual total derivatives instead of substantial ones, and reserve the substantial derivative symbol to express the time variation along the fluid particle paths of quantities expressed in usual Eulerian coordinates. We will follow this custom in the remainder of these notes, but the reader should not forget that we are solving a fluid problem and not a point particle one.

4.1 Fluid test particle motion

In the conditions just outlined, the equation of motion of the fluid test particle reads:

$$\frac{d^2\mathbf{r}}{dt^2} = -\nabla\phi_p. \quad (4.1)$$

where \mathbf{r} is restricted to the equatorial plane of the planet. This equation is formally identical to the equation of motion of a point particle in the planet potential; the only difference is that \mathbf{r} is a function of the initial position as well as of time. This equation can therefore be solved with standard techniques. It is usual in Celestial Mechanics to use the elliptic solution of the two-body problem and treat the deviations of the planet from spherical symmetry as perturbations. This procedure raises however quite a number of subtle technical issues which will be briefly described in section 4.2. We will therefore depart from this well-established custom; however, the solution used here is closely related to the elliptic solution, and everyone already used to Celestial Mechanics techniques will feel at ease with it. Note that the equation of motion Eq. (4.1) does not depend on the surface density, so that it can be solved independently of the continuity equation.

The solution we will use derives from the epicyclic theory, which was initially developed for galactic dynamics. A fundamental feature of ring problems is that although the density contrast can be strongly nonlinear, the deviations from circular trajectories are always very small (see in particular section 4.4). The analysis therefore relies on the existence of purely circular solutions (the planet is axisymmetric), and looks for general solutions in the form of small deviations around one of these circular solutions, in successive approximations. Up to second order in deviation from circularity, the radius r and true longitude θ of a fluid test particle on an equatorial orbit read (Longaretti and Borderies, 1991):

$$r = r_0 \left[1 + \frac{3\eta^2}{2\kappa^2}\epsilon^2 - \epsilon \cos \xi - \frac{\eta^2}{2\kappa^2}\epsilon^2 \cos 2\xi \right], \quad (4.2)$$

$$\theta = \gamma + \frac{2\Omega}{\kappa}\epsilon \sin \xi + \frac{\Omega}{2\kappa} \left(\frac{3}{2} + \frac{\eta^2}{\kappa^2} \right) \epsilon^2 \sin 2\xi, \quad (4.3)$$

with

$$\xi = \int_0^t \kappa dt + \delta = \kappa t + \delta, \quad (4.4)$$

$$\begin{aligned} \gamma = \theta_0 + \int_0^t \Omega \left[1 + \left(\frac{3}{2} - \frac{3\eta^2}{\kappa^2} \right) \epsilon^2 \right] dt = \theta_0 \\ + \Omega \left[1 + \left(\frac{3}{2} - \frac{3\eta^2}{\kappa^2} \right) \epsilon^2 \right] t, \end{aligned} \quad (4.5)$$

$$\Omega^2 \equiv \frac{1}{r_0} \frac{d\phi_p}{dr}(r_0), \quad (4.6)$$

$$\kappa^2 \equiv \left[\frac{3}{r} \frac{d\phi_p}{dr} + \frac{d^2\phi_p}{dr^2} \right]_{r=r_0}, \quad (4.7)$$

$$\eta^2 \equiv \left[\frac{2}{r} \frac{d\phi_p}{dr} - \frac{r}{6} \frac{d^3\phi_p}{dr^3} \right]_{r=r_0}, \quad (4.8)$$

where r_0, ϵ, θ_0 , and δ are the constants of integration of the problem, and are functions of the initial position of the fluid particle \mathbf{r}_0 (do not get confused between r_0 and \mathbf{r}_0 !!): r_0 is the radius of the circular motion around which the solution is expanded (analogous to an average radius); ϵ is the relative departure from circularity (analogous to an eccentricity); in ring problems, ϵ is always a small quantity; θ_0 and δ are initial phases; Ω and κ are the usual rotation and epicyclic frequencies, i.e. the frequencies of the motion around the planet and of the radial oscillations, respectively; η is an auxiliary quantity homogeneous to a frequency; ϕ_p is the potential of the planet, including the J_k terms (the coefficients of the expansion of the planetary potential in spherical harmonics¹³). In the limit of a spherical planet, $\Omega^2 = \kappa^2 = \eta^2 = GM_p/r_0^3$, where M_p is the mass of the planet, so that in general, the three frequencies differ only by terms of order J_2 and smaller. General expressions for these frequencies in terms of the J_k s can be found in Borderies and Longaretti (1987). Expressions in terms of J_2 are given below.

These expressions constitute the epicyclic solution as it is generally derived; however, the close analogy with the elliptic solution is much more apparent if one makes use of a somewhat different set of epicyclic elements¹⁴: $a_e, \epsilon, \varpi_e, M_e \equiv \xi$, where a_e and ϖ_e are defined by:

$$a_e \equiv \frac{r_0}{1 - \epsilon^2}, \quad (4.9)$$

$$\varpi_e \equiv \gamma - \xi = \gamma - M_e. \quad (4.10)$$

The change of notation from ξ to M_e is adopted for mnemonic reasons which will soon be made obvious. Keeping terms up to second order in ϵ , the preceding formulæ become:

$$r = a_e \left[1 + \left(\frac{3\eta_a^2}{2\kappa_a^2} - 1 \right) \epsilon^2 - \epsilon \cos M_e - \frac{\eta_a^2}{2\kappa_a^2} \epsilon^2 \cos 2M_e \right], \quad (4.11)$$

$$\theta = \varpi_e + M_e + \frac{2\Omega_a}{\kappa_a} \epsilon \sin M_e + \frac{\Omega_a}{2\kappa_a} \left(\frac{3}{2} + \frac{\eta_a^2}{\kappa_a^2} \right) \epsilon^2 \sin 2M_e, \quad (4.12)$$

where now the frequencies are evaluated at a_e , so that¹⁵:

$$M_e = \int_0^t \kappa_a dt + \delta + O(J_2 \epsilon^2), \quad (4.13)$$

$$\gamma = \theta_0 + \int_0^t \Omega_a \left[1 + \left(\frac{7}{2} - \frac{3\eta_a^2}{\kappa_a^2} - \frac{\kappa_a^2}{\Omega_a^2} \right) \epsilon^2 \right] dt, \quad (4.14)$$

¹³In some cases, it is useful to include the axisymmetric contributions of the satellites and of the rings in the definition of ϕ_p .

¹⁴The usefulness of the change of variable from r_0 to a_e was pointed out by Phil Nicholson 1990 (private communication).

¹⁵Note that the terms of order $\epsilon^2 \kappa_a t$ are not explicitly given in Eq. (4.13). Such terms cannot be self-consistently computed from a second order epicyclic theory, because a third order expansion produces a nonlinear frequency correction of the same magnitude to M_e . This correction actually kills the contribution of order ϵ^2 to κ_a , so that the remaining contribution is of order $J_2 \epsilon^2$. Note also that in this case, Ω_a and κ_a differ by a term of order $J_2 \epsilon^2$. The knowledge of this contribution is important for some ring problems, but is not needed in these notes.

$$\Omega_a^2 \equiv \frac{1}{a_e} \frac{d\phi_p}{dr}(a_e), \quad (4.15)$$

$$\kappa_a^2 \equiv \left[\frac{3}{r} \frac{d\phi_p}{dr} + \frac{d^2\phi_p}{dr^2} \right]_{r=a_e}, \quad (4.16)$$

$$\eta_a^2 \equiv \left[\frac{2}{r} \frac{d\phi_p}{dr} - \frac{r}{6} \frac{d^3\phi_p}{dr^3} \right]_{r=a_e}. \quad (4.17)$$

For definiteness, let us give expressions for Φ_p , Ω_a and κ_a in terms of J_2 (η_a is not needed):

$$\begin{aligned} \Phi_p(a_e) &= \frac{GM_p}{a_e} \times \left[-1 + \frac{1}{2} \left(\frac{R_p}{a_e} \right)^2 J_2 \right], \\ \Omega_a(a_e) &= n_a \times \left[1 + \frac{3}{4} \left(\frac{R_p}{a_e} \right)^2 J_2 \right], \\ \kappa_a(a_e) &= n_a \times \left[1 - \frac{3}{4} \left(\frac{R_p}{a_e} \right)^2 J_2 \right], \end{aligned}$$

where M_p and R_p are the planet mass and radius. For future use, we have also introduced an effective elliptic mean motion defined by $n_a = (GM_p/a_e^3)^{1/2}$.

The analogy is apparent if one expands the elliptic solution to second order in eccentricity:

$$r = a \left[1 + \frac{1}{2}e^2 - e \cos M - \frac{1}{2}e^2 \cos 2M \right], \quad (4.18)$$

$$\theta = \varpi + M + 2e \sin M + \frac{5}{4}e^2 \sin 2M, \quad (4.19)$$

with standard notations for the elliptic elements. If one makes the following formal identifications:

$$a \rightarrow a_e,$$

$$e \rightarrow \epsilon,$$

$$M \rightarrow M_e,$$

$$\varpi \rightarrow \varpi_e,$$

one sees that the two types of expansions are formally nearly identical; the only difference comes from the ratios of frequencies in the epicyclic solution, which differ from unity by terms of order J_2 . In the epicyclic solution, the precession due the deviations of the planet from sphericity is of course already included: $\dot{\varpi}_e = \Omega_a - \kappa_a \sim J_2 \Omega_a$. For convenience, we will refer to the elements $(a_e, \epsilon, M_e, \varpi_e)$ as to the epicyclic semi-major axis, eccentricity, mean motion and periape angle respectively. These elements are also, of course, function of the initial position of the fluid particle. They represent the average of the epicyclic elements of the individual ring particles composing the fluid particle

under consideration. The individual particle epicyclic eccentricities are made up of two contributions: this mean part, and a random contribution which is connected to the velocity second moments (the pressure tensor) of the fluid particle.

To conclude this subsection, let us write down the perturbation equations of the epicyclic elements. Such equations are necessary as we have decided to treat all forces but the planet's as perturbations. Due to the formal analogy between the point particle equations of motion and the Lagrangian equations we have derived, the perturbation equations can be obtained with standard variation of the constants techniques. They read (Longaretti and Borderies, 1991):

$$\frac{da_e}{dt} = \frac{2}{\kappa_a} \left[R\epsilon \sin M_e + \frac{\Omega_a}{\kappa_a} S (1 + \epsilon \cos M_e) \right] + O(\epsilon^2), \quad (4.20)$$

$$\frac{d\epsilon}{dt} = \frac{1}{\kappa_a a_e} \left[R \sin M_e + 2 \frac{\Omega_a}{\kappa_a} S \cos M_e \right] + O(\epsilon), \quad (4.21)$$

$$\frac{d\varpi_e}{dt} = \Omega_a - \kappa_a + \frac{1}{\kappa_a a_e \epsilon} \left[-R \cos M_e + 2 \frac{\Omega_a}{\kappa_a} S \sin M_e \right] + O(\epsilon^0), \quad (4.22)$$

$$\begin{aligned} \frac{dM_e}{dt} = \kappa_a + \frac{1}{\kappa_a a_e \epsilon} \left[R \left(\cos M_e - 3 \frac{\eta_a^2}{\kappa_a^2} \epsilon + \frac{\eta_a^2}{\kappa_a^2} \epsilon \cos 2M_e \right) - \right. \\ \left. \frac{\Omega_a}{\kappa_a} S \left(2 \sin M_e + \left(\frac{1}{2} + \frac{\eta_a^2}{\kappa_a^2} \right) \epsilon \sin 2M_e \right) \right] + O(\epsilon), \end{aligned} \quad (4.23)$$

The $\Omega_a - \kappa_a$ term in Eq. (4.22) represents the effect of the planet oblateness on the precession of the apsides. For comparison, let us write down the equations of perturbation of the elliptic motion (see, e.g., Murray and Dermott 1999), to first order in eccentricity:

$$\frac{da}{dt} = \frac{2}{n} [Re \sin M + S (1 + e \cos M)] + O(e^2), \quad (4.24)$$

$$\frac{de}{dt} = \frac{1}{na} [R \sin M + 2S \cos M] + O(e), \quad (4.25)$$

$$\frac{d\varpi}{dt} = \frac{1}{nae} [-R \cos M + 2S \sin M] + O(e^0), \quad (4.26)$$

$$\begin{aligned} \frac{dM}{dt} = n + \frac{1}{nae} \left[R (\cos M - 3e + e \cos 2M) \right. \\ \left. - S \left(2 \sin M + \frac{3}{2} e \sin 2M \right) \right] + O(e), \end{aligned} \quad (4.27)$$

with standard notations. In both sets of equations, R and S are the radial and tangential components of the perturbing acceleration, as usual. Notice the similar roles played by n and κ_a . One sees here again that the perturbation equations for elliptic and epicyclic variables are formally nearly identical, except for the various ratios of frequencies in the epicyclic equations, which differ from unity by terms of order J_2 ($\ll 1$).

In what follows these relations are used to first order in eccentricity at most. As a consequence, $d\varphi/dt = d(\varpi_e + M_e)/dt$ is negligible compared to $d\varpi_e/dt$, and only the first free equations are needed in practice. Because R, S are small (compared to the planet’s acceleration) and $\epsilon \ll 1$, one can replace all frequency ratios with 1 in these relations; we also replace everywhere κ_a and Ω_a by the effective mean motion n_a except in $\Omega_a - \kappa_a$, to the same level of precision. In this limit, these relations become formally identical to their elliptic counterpart, except for the notable fact that a_e and ϵ differ from the osculating elliptic ones by terms of order J_2 . This simplification is usually made from now on.

The comparison of the expressions of the specific energy and angular momentum in terms of the elliptic and epicyclic elements is also useful. In elliptic variables, the specific energy and angular momentum are related to the semimajor axis and the eccentricity by the well-known formulæ:

$$E = -\frac{GM_p}{2a}, \quad (4.28)$$

$$H = \sqrt{GM_p a(1 - e^2)} = na^2 \left(1 - \frac{e^2}{2}\right) + O(e^4), \quad (4.29)$$

whereas in epicyclic variables, we have:

$$E = \phi_p(a_e) + \frac{\Omega_a^2 a_e^2}{2} + O(\epsilon^4), \quad (4.30)$$

$$H = \Omega_a a_e^2 \left[1 - \frac{1}{2} \left(\frac{\kappa_a}{\Omega_a}\right)^2 \epsilon^2\right] + O(\epsilon^4). \quad (4.31)$$

It is easily seen that Eqs. (4.28) and (4.29) are recovered in the case of a spherical planet. Note that r_0 (resp. a_e) is the radius of the circular orbit having the same angular momentum (resp. the same energy to order ϵ^4) as the non-circular epicyclic orbit of Eqs. (4.2) and (4.3) [resp. (4.11) and (4.12)].

4.2 Epicyclic versus elliptic elements

Although elliptic elements are much more widely known and almost exclusively used in Celestial Mechanics in general and in the “ring community” in particular, epicyclic elements are much more adapted to the observational and theoretical descriptions of planetary rings for the three following reasons:

1. First, the fluid particle trajectories in a circular ring are described by the simple equation $r = \text{constant} = a_e$ in the streamline formalism (see section 4.3). However, it is well-known that although the ring fluid particles follow a circular trajectory, their elliptic osculating eccentricity e_0 is non zero; $e_0 = 3/2J_2(R/r)^2$ to leading order in the gravitational coefficients of the planet potential. Furthermore, the eccentricities which are typically considered in some ring problems, e.g. *the mean eccentricities* which are involved in the description of density waves in Saturn’s rings, *can be orders of magnitudes smaller than the osculating eccentricities*, which are then of order e_0 (Longaretti and Borderies, 1986). Similarly, the osculating semimajor axis $a_0 \simeq r[1 + 3/2J_2(R/r)^2]$ is substantially different in absolute

value from its “mean” value r , although not in relative value. Second, for non-circular motions, the osculating elements exhibit short-period variations due to the harmonic coefficients of the planet, whereas the elements used in the streamline formalism, as well as in data fits, are supposed to be time-independent, or, to the very least, to vary only on much longer time scales than the orbital period. This time variation cannot be ignored: it is at the origin of this sometimes very large discrepancy between the osculating and observed elements.

2. Epicyclic elements are “more constant” than elliptic elements: the non-sphericity of the planet is readily taken into account in the epicyclic formulæ whereas, as already pointed out, it leads to short-period variations of the elliptic elements. Furthermore, the non-sphericity of the planet is the most important source of short-period variations. The main effects of the shepherd satellites, and of the ring self-gravity and pressure tensor (which perturb both elliptic and epicyclic elements) occur on much longer time-scales (their short-period contributions are negligible). The argument developed in this paragraph can be rephrased and summarized in a different way: *the mean (short-period averaged) and the osculating elliptic elements of a ring particle can be substantially different, whereas its mean (short-period averaged) and osculating epicyclic elements are always identical or nearly identical.*
3. No approximation with respect to the harmonic coefficients of the planet is involved, which is not the case for elliptic elements. On the other hand, elliptic formulæ are valid to all orders in eccentricity, but in practice, expansions in eccentricity (and inclination) are always required, and the exactitude of the elliptic formulæ turns out to be no great advantage, because epicyclic formulæ can easily be obtained to the order needed for a good description of the data.

Up to now the equations which have been used both in data fits and in dynamical analyses are the equations of the elliptic motion, although they were applied to elements which were assumed to be constant at least on the short time-scale, and known to be quite different from the elliptic osculating elements in some circumstances. It is therefore legitimate to wonder why this procedure was valid, especially at the light of the comments above. However, we have shown [Eqs. (4.11) to (4.27)] that the elliptic elements are formally nearly identical to a suitably defined set of epicyclic element. This argument combined with the three points exposed above shows that (i) the elements obtained from the observations are indeed the epicyclic elements $a_e, \epsilon, M_e, \varpi_e$ and (ii) the application of elliptic formulæ and equations to these epicyclic elements generally constitutes an acceptable approximation.

4.3 Ring streamlines and kinematics

In fluid dynamics, the streamlines are the lines of the velocity field of the fluid. In the streamline formalism, the word is sometimes used in a different way. Most of the times, it designates the actual streamlines of the flow, at least in some suitably defined rotating frame. For example, this is the case for density waves

and eccentric rings, but the $m = 0$ mode of the γ ring of Uranus is a notable exception. In all cases, the streamlines provide a description of ring shapes: more precisely, they designate the curve that an infinitely thin ring would define in space. Therefore, to conform with past usage, we will use the word “streamline” to designate both ring velocity field lines and ring shapes, keeping in mind that when the two concepts do not overlap, the word refers to the latter, in opposition to the more common usage.

It is customary when treating a fluid dynamics problem to look for solutions with a specific space and time dependence. For example, in the analysis of fluid stability in the linear approximation, one often looks for oscillating solutions with phases of the form $kx - \omega t$ for a one-dimensional problem, s being the space variable. The same approach is assumed in ring problems, with two notable subtleties attached:

1. The celestial mechanics perturbation technique adopted in the streamline formalism implies to define not only the streamline shapes, but also the defining quantities of each individual particle in a given streamline. As the unperturbed background is not at rest but is constituted by circular motions around the planet, this makes the *a priori* specification of the shape of the motion somewhat more involved than usual.
2. One looks for *nonlinear* solutions in general, but with a specific form of nonlinearity that makes them analytically tractable to a larger extent. In disk systems in general, one can identify two types of nonlinearity: large radial extension, and large density variations. The two are not necessarily coupled, and it turns out that, in rings, deviations from circularity are always quite small, but the associated density contrast can be quite large. This will be discussed in section 4.4

Let us start with the trivial case: a circular ring, in which the fluid particles are in circular motion¹⁶. The fluid particles’ positions reduce to:

$$r = a_e, \tag{4.32}$$

$$\theta = \varphi \equiv \varpi_e + M_e. \tag{4.33}$$

where φ is the epicyclic mean longitude. One sees also that at any given time, to any given fluid particle with initial position \mathbf{r}_0 corresponds a unique set (a_e, φ) . This suggests that these quantities can be chosen as (semi-)Lagrangian labels instead of the initial position \mathbf{r}_0 if needed. This is also obviously true for the more general eccentric solution, and in the rest of these notes, it is considered when needed that the epicyclic elements ϵ , ϖ_e and M_e are functions of a_e and φ considered as Lagrangian labels (naturally, ϖ_e and M_e are functions of time as well in the fluid test particle solution). Of course, a_e and φ are independent Lagrangian variables: the change of variable from \mathbf{r}_0 to (a_e, φ) is nowhere singular at any given time. Note that in non steady-state flows, the change of variable from \mathbf{r}_0 to (a_e, φ) may be time dependent.

¹⁶We have argued in section 2 that, because interparticle collisions are dissipative, orbital energy is permanently lost, so that no fluid particle can be exactly in circular motion, but let us ignore this complication for the time being, as we have not yet included the effect of the viscous stress in our analysis. In any case, this is a small effect, occurring on the longest of all the time-scales of interest in ring dynamics.

4.3.1 Eccentric rings

Let us now consider some more general cases. Usually, in Eulerian fluid dynamics, one is interested in special solutions of the Navier-Stokes equations. The situation is similar here, because it is observationally found that rings can be well described by some special form of the general solution we have just written down. For example, the shape of the elliptic Uranian rings is known from the analysis of stellar occultation data (for a review, see Elliot and Nicholson 1984). Their mean eccentricity is typically of the order of 10^{-3} to 10^{-4} ; they also present a difference of eccentricity between the inner and outer edges, of the order of 10^{-4} to 10^{-5} (French et al., 1986, 1988). The analysis of the data strongly suggests that the ring fluid particles having the same (epicyclic) semimajor-axis also have the same (epicyclic) eccentricity and the same (epicyclic) periapse angle. This means that the ring shape, which in this case coincide with the ring fluid particle streamlines – is parametrized as follows, to first order in eccentricity [combine Eqs. (4.11) and (4.12)], as in Figure 3 below:

$$r(a_e, \phi) = a_e [1 - \epsilon(a_e) \cos(\theta - \varpi_e(a_e))]. \quad (4.34)$$

In this type of solution, the epicyclic elements ϵ and ϖ_e do not depend on the Lagrangian coordinate φ . Note that if such a dependence existed, it would generate an increased shear, and therefore, in usual situations, be quickly erased by viscous forces, unless it were maintained by some dynamical agent. This is also true for eccentric rings, which tend to generally tend to become circular under the action of the ring viscous stress. Thus, the eccentricities of elliptic rings need generally speaking to be maintained by some external agents (for example the shepherd satellites), unless the viscous stress has such an unusual form that viscous instabilities can take place and generate them (see section 7.1).

Note also that the dependence of the precession rate on the fluid particle semimajor axis implies that the inner edge streamline of elliptic rings tends to precess faster than the outer one under the action of the planet. In the absence of other forces, the alignment of the inner and outer apsides would be very quickly destroyed, streamlines would cross and the ring would become circular. Therefore, this differential precession must be balanced by some dynamical agent, e.g. the ring self-gravity (Goldreich and Tremaine 1979a,b; see section 7.1).

4.3.2 Density waves

It is also instructive to consider the case of density waves. Such waves are excited by the satellites near resonance locations, and propagate away from the resonance. They are sustained by the self-gravity of the disk, arise from the coherent radial excursions of the ring fluid particles, and look stationary in a particular rotating frame. The eccentricities involved are typically of order 10^{-3} to 10^{-5} . The form of the fluid particle paths has been known for a long time in galactic dynamics from the work of Lindblad on spiral galaxies. The usual parametrization is most conveniently understood from the following elementary analysis, reproduced from Goldreich and Tremaine (1982).

Let us consider the forced linear response of a test particle in circular orbit around an oblate planet, perturbed by a satellite. Expressing the radius and

longitude of the test particle as $r = r_0 + r_1$ with $r_1 \ll r_0$ and $\theta = \theta_0 + \Omega t + \theta_1$, where r_0 is the radius of the circular orbit and Ω is the orbital frequency, given by Eq. (4.6), the linearized equations of motion for r_1 and θ_1 read:

$$\frac{d^2 r_1}{dt^2} + r_0 \left(\frac{d\Omega^2}{dr} \right)_{r_0} r_1 - 2r_0 \Omega_0 \frac{d\theta_1}{dt} = - \left(\frac{\partial \phi_s}{\partial r} \right)_{r_0}, \quad (4.35)$$

$$r_0^2 \frac{d^2 \theta_1}{dt^2} + 2r_0 \Omega_0 \frac{dr_1}{dt} = - \left(\frac{\partial \phi_s}{\partial \theta} \right)_{r_0}, \quad (4.36)$$

where ϕ_s is the satellite potential. The satellite is supposed to orbit in the equatorial plane of the planet. Let us call a_s its (epicyclic) semimajor axis, e_s its eccentricity, and ϖ_s its periape angle; κ_s is the epicyclic frequency evaluated at a_s . At any given time, the satellite potential is of course periodic in azimuth. Furthermore, in a frame rotating at $\dot{\varpi}_s$, the satellite orbit is closed of period $2\pi/\kappa_s$. Thus, the satellite potential can be expanded in a double Fourier series, one in time, and one in azimuth; this yields¹⁷:

$$\phi_s(r, \theta, t) = \sum_{m=0}^{\infty} \sum_{k=-\infty}^{\infty} \Phi_{mk}(r/a_s) \cos [m(\theta - \dot{\varpi}_s t) - (m+k)\kappa_s t]. \quad (4.37)$$

The Fourier coefficients Φ_{mk} are expressed in terms of Laplace coefficients (Murray and Dermott 1999; a particularly synthetic and convenient derivation can be found in the appendix A of Shu 1984):

$$b_{1/2}^m(\alpha) = \frac{2}{\pi} \int_0^\pi \frac{\cos mu \, du}{(1 - 2\alpha \cos u + \alpha^2)^{1/2}}. \quad (4.38)$$

The coefficients Φ_{mk} are of order $e_s^{|k|}$, so that only the Fourier coefficients with small k are important in practice, because usually $e_s \ll 1$. Let us define $\alpha = r/a_s$, and call M_s the mass of the satellite. The terms of order $|k| \leq 1$ read:

$$\Phi_{m0} = - \frac{GM_s}{a_s} \frac{b_{1/2}^m(\alpha) - \delta_{m1}\alpha}{1 + \delta_{m0}}, \quad (4.39)$$

$$\Phi_{m,\pm 1} = - \frac{GM_s e_s}{a_s} \frac{\left[\frac{1}{2} (1 \pm 2m + \alpha \frac{d}{d\alpha}) b_{1/2}^m(\alpha) - \alpha \delta_{m1} (1 \pm 1) \right]}{1 + \delta_{m0}}, \quad (4.40)$$

where δ_{ij} is the Kronecker delta symbol (the contribution of the indirect term is included).

For a single Fourier component, the solution of the linearized equations of motion reads:

$$r_1 = \left\{ \frac{\cos[m(\Omega - \Omega_p)t + m\theta_0]}{m^2(\Omega - \Omega_p)^2 - \kappa^2} \left(\frac{d\Phi_{mk}}{dr} + \frac{2m\Omega}{m(\Omega - \Omega_p)r} \Phi_{mk} \right) \right\}_{r_0}, \quad (4.41)$$

¹⁷The phase of the satellite has been taken equal to 0 at $t = 0$ (the origin of time $t = 0$ is chosen when the satellite is at periape); also, corotation resonances with $a = a_s$ are excluded from the expansion of Eq. (4.37): $r < a_s$ is assumed.

$$\theta_1 = - \left\{ \frac{\sin[m(\Omega - \Omega_p)t + m\theta_0]}{m^2(\Omega - \Omega_p)^2 - \kappa^2} \left(\frac{2\Omega}{m(\Omega - \Omega_p)r} \frac{d\Phi_{mk}}{dr} + \left[\frac{4\Omega^2 - \kappa^2}{m^2(\Omega - \Omega_p)^2} + 1 \right] \frac{m\Phi_{mk}}{r^2} \right) \right\}_{r_0}, \quad (4.42)$$

where $\Omega_p = \Omega_s + k/m$ κ_s is the so-called pattern speed: it is the angular speed of the frame in which the (m, k) potential component is stationary. The linear response is singular either when $\Omega_p = \Omega_0$ (corotation resonance) or when $\kappa_0 = \pm m(\Omega_0 - \Omega_p)$ (Lindblad resonance). The corotation resonances that lie within a ring arise because the satellite orbit is eccentric, and have $|k| \geq 1$; the $k = 0$ corotation resonance (the strongest) occurs at the satellite radius. The inner Lindblad resonance occurs inside the corotation resonance, and corresponds to the positive sign; the other one is the outer Lindblad resonance, and lies outside. If the multipole moments of the planet potential are neglected, the Lindblad (resp. corotation) resonance condition reduces to $\Omega_0/\Omega_s = (m + k)/(m \mp 1)$ (resp. $\Omega_0/\Omega_s = m + k/m$). This ratio is often used to label a resonance. For example, the $k = 0$, $m = 2$ inner Lindblad resonance is called a 2 : 1 resonance (the outer edge of the Saturn's B ring corresponds to such a resonance with the satellite Mimas).

The resonance condition implicitly defines the resonance radius r_R , which is the only radius for which the condition is satisfied. Near a resonance, the radial perturbation r_1 can be expressed as a function of θ and of the distance to the resonance $\Delta r = r_0 - r_R$. For a corotation resonance, we have:

$$r_1 \simeq \frac{A_{mk}^c}{\Delta r} \cos m(\theta - \Omega_p t), \quad (4.43)$$

with

$$A_{mk}^c = \left(\frac{4\Phi_{mk}}{3\Omega^2} \right)_{r_R}, \quad (4.44)$$

whereas for a Lindblad resonance, one obtains:

$$r_1 \simeq \frac{A_{mk}^L}{\Delta r} \cos m(\theta - \Omega_p t), \quad (4.45)$$

$$A_{mk}^L = \left[\frac{1}{3\Omega^2(1 \mp m)} \left(r \frac{d\Phi_{mk}}{dr} \pm 2m\Phi_{mk} \right) \right]_{r_R}, \quad (4.46)$$

Note that this solution describes the circulating orbits at corotation resonances, and the librating orbits at Lindblad resonances. Density waves at corotation resonances will not be discussed in this lecture, and from now on, only Lindblad resonances are considered. Notice also that the amplitudes $A_{mk}^L/\Delta r \sim r^2 M_s/M_p(r - r_R)$, and that in a region of width $\Delta r \sim r(M_s/M_p)^{1/2}$, these test

particle orbits intersect. Therefore, collective effects are expected to be important in this region. Note finally that the relative sign of r_1 and θ_1 is preserved at OLR with respect to ILR upon the substitution of $m(\Omega - \Omega_p) = \pm\kappa$ (preserving the usual direction of epicyclic motions at both resonances).

Although this test particle solution is somewhat unrealistic¹⁸, it indicates that ring streamlines can be chosen, to first order in eccentricity, as sinusoidal functions of the basic angle $m(\theta - \Omega_p t)$ when one considers a density wave driven by the (m, k) component of the satellite potential. This choice reflects the fact that the ring fluid particles behave like a forced oscillator, responding with the time and angular dependence of the forcing. Notice also that all particles with the same semimajor axis have the same eccentricity and periape angle in this simple test particle solution. Similarly, density waves are special solutions for which the eccentricities of the fluid particles are function of the semimajor axis only. For density waves at Lindblad resonances, we are therefore motivated to assume that the streamlines are parametrized by (see Figure 3):

$$r(a_e, \phi) = a_e \{1 - \epsilon \cos[m(\theta - \Omega_p t) + m\Delta]\}, \quad (4.47)$$

where $\epsilon \ll 1$ everywhere in the wave region¹⁹. Finding solutions of this type will demonstrate *a posteriori* that our assumption is correct²⁰.

Combining Eqs. (4.11) and (4.12) necessarily yields $r = a_e[1 - \epsilon \cos(\varphi - \varpi_e)]$ to lowest order in eccentricity. This is compatible with Eq. (4.47) only if $m(\varphi - \Omega_p t) + m\Delta = \varphi - \varpi_e$, i.e., if

$$m(\Omega_a - \Omega_p) = \Omega_a - \dot{\varpi}_e, \quad (4.48)$$

$$\varpi_0 = \varphi_0(1 - m) - m\Delta, \quad (4.49)$$

where ϖ_0 and φ_0 are the periape angle and mean longitude of the fluid particle at $t = 0$. Note that in Eq. (4.48) $\dot{\varpi}_e$ includes the precession rates due to the perturbations; the contribution of the perturbations to $d\varphi/dt$ is negligible in front their contribution to $\dot{\varpi}_e$, to leading order in ϵ [see Eqs. (4.12), (4.22) and (4.23)]. The second relation expresses the condition that the initial periape angles and initial azimuths of particles having the same semi-major axis must satisfy in order for these particles to belong both to the streamline Eq. (4.47) and to their epicyclic orbit around the planet (it generalizes the equivalent condition for elliptic rings, which is that all fluid particles with the same semimajor axis have the same periape angle). Eq. (4.48) expresses the Lindblad resonance condition, and is required if the ring fluid particles are to belong to the streamline and to their natural epicyclic orbits at all times, and not only the initial one. These requirements follow from the fact that all forces are small in comparison with the planet attraction, so that the streamlines of the the flow cannot differ very much from the natural fluid particle orbits.

¹⁸In any case, this solution breaks down too close to the resonance where the condition $r_1 \ll r_0$ is no longer satisfied.

¹⁹Collective effects prevent the divergence seen in the test particle solution at the resonance (see section 7). Notice also that, although $\epsilon \ll 1$, the density contrast can be highly nonlinear (see section 4.4) so that Eq. (4.47) describes both linear and nonlinear density waves.

²⁰A formal justification of Eq. (4.47) is also provided from first principles by Shu (1984) in an *ab initio* analysis of nonlinear density waves.

The phase angle Δ has been added for the following reason. Note that the trajectories of the fluid particles having epicyclic semimajor axes equal to the resonance radius and eccentricity ϵ , which are elliptic in an inertial reference frame, appear as the m -lobe shape of Eq. (4.47) when viewed in a frame rotating at Ω_p . This is a purely geometric and kinematic effect; Eq. (4.49) then states that the trajectories of all such particles will be identical in the rotating frame. However, for fluid test particles, this is true only at the resonance, and density waves cannot exist, as the precession rate $\dot{\varpi}_e$ is imposed by the planet only: for example, just outside the resonance [i.e., for fluid test particles of semimajor axis $a > a_R$, where a_R is the semimajor axis at resonance, defined by $\kappa_{a_R} = m(\Omega_{a_R} - \Omega_p)$], $m(\Omega_a - \Omega_p) \neq \kappa_a$, and the streamlines appear to have an angular velocity $\kappa_a - m(\Omega_a - \Omega_p)$ with respect to the streamline at the resonance, quickly leading to streamline crossing and to the destruction of any density wave pattern, as the one shown on Figure 4. Thus, fluid test particles cannot support free density wave. But the ring self-gravity can produce a contribution to the precession rate $\dot{\varpi}_{sg}$ which actually cancels this secular drift, so that the resonance condition is satisfied throughout the wave region. As the ring gravity is nevertheless a very small force, it can only reach the right magnitude when the phase shift between adjacent streamlines is large enough, i.e., when the WKBJ, or tight-winding condition

$$ma_e \left| \frac{d\Delta}{da_e} \right| \gg 1, \quad (4.50)$$

is satisfied. This is why density waves are so tightly-wound in rings²¹. In spiral galaxies, as the self-gravity of the disk dominates the gravity from the central bulge, the spiral arms appear much more open. We will return to the discussion of density waves and justify these assertions later on in section 7, after having introduced the dynamical tools of the streamline formalism.

4.3.3 Eccentric modes

As a last example, let us consider the case of the γ and δ rings of Uranus, whose streamlines are not described by the simple elliptic shape Eq. (4.34).

Actually, the δ ring is well-fitted by Eq. (4.47), with $m = 2$, and with Δ almost constant across the ring. This last characteristic allows us to introduce the notion of *mode*: a mode is a global sinusoidal oscillation of a ring, with streamlines given by Eq. (4.47) where ϵ and Δ depend on a_e , and where Δ , as we just said, is more or less constant across the ring; a mode is characterized by its number of lobes m and its pattern speed Ω_p . Elliptic rings enter this definition, with $m = 1$ and $m\Delta - m\Omega_p t = -\varpi_e$; note that in this case, Eq. (4.49) implies as required that the periapse angle depends only on semimajor axis, and not on θ_0 . Note also that spiral density waves are excluded from this definition (but not standing waves). In these notes only single mode motions are considered. The generalisation to multimode motions is somewhat discussed in Longaretti (1989b).

²¹Waves in rings are forced density waves. However, the coupling of the wave with the forcing potential occurs at the resonance on a small fraction of the wave zone, and the wave propagates essentially as a free wave on most of its radial extent.

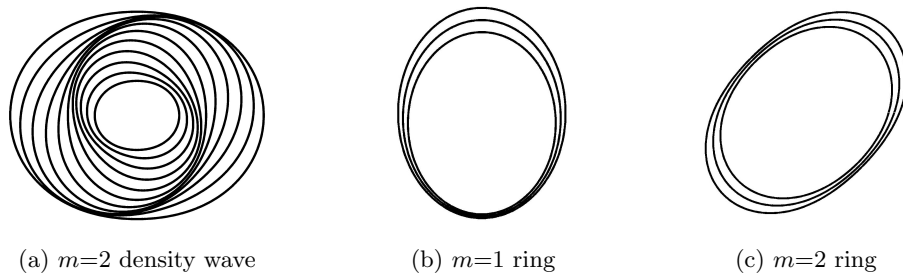


Figure 3: Examples of eccentric fluid motion in rings.

Because all forces are much smaller than the planet's, and because the radial extent of the rings in which these modes are found is very small, the contributions of the perturbations to the frequencies and precession rates are much smaller than the planet's, and the pattern speed of the modes obeys the condition:

$$m(\Omega_a - \Omega_p) - (\Omega_a - \dot{\omega}_{plan}) \ll \Omega_a - \dot{\omega}_{plan}. \quad (4.51)$$

Note that for density waves, the precession rate is not limited in theory, because the winding can, in principle, be as high as needed. However, the winding is nevertheless meaningful only as long as the wavelength is larger than the typical particle size, and in any case, the wave is damped before this limit is reached, so that in practice Eq. (4.51) applies to density waves as well. The streamlines of an $m = 2$ density wave, and of $m = 1, 2$ ringlets are displayed on Figure 3 for comparison.

Let us now consider the case of the $m = 0$ mode of the γ ring. To understand the basic kinematic properties of this mode, let us consider an infinitely thin ringlet whose fluid particles orbit on eccentric trajectories, with the same semimajor axis a_e and the same eccentricity ϵ . The periapse angles are evenly distributed, and the phases of the ring particles on their orbits are initially all identical, so that at any given time, all the fluid particles are at the same radial distance from the planet. This situation is schematically depicted on Figure 4 where the positions of the fluid particles are represented by dots; the particles belong both to their epicyclic orbit and to the circular ring; particles never collide. Note that this situation is substantially different from the case of the other modes. In Figure 3 for example, ring fluid particles are present all along any given eccentric orbit (the fluid particle orbits and streamlines are identical in the rotating frame). Here, the orbits are essentially empty and the fluid particles are confined to a special point along the orbit. At any given time, the ring appears circular. Its radius oscillates sinusoidally at the orbital frequency: $r = a_e(1 - \epsilon \cos \zeta)$ where $d\zeta/dt = \kappa_a$. As the number of lobes m of the other modes refer to their azimuthal structure (it is the azimuthal wavenumber), this type of motions actually corresponds to the case $m = 0$ in Eulerian analyses, i.e., a purely radial motion.

Turning back to the case of a real ring (not infinitely thin), one sees that the ring streamlines can be chosen as:

$$r = a_e [1 - \epsilon(a_e) \cos(\Omega_p t + \Delta(a_e))]. \quad (4.52)$$

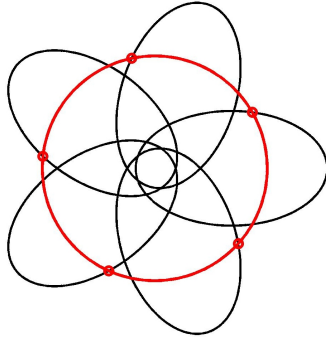


Figure 4: Sketch of an infinitely narrow $m = 0$ mode. All fluid particles belong to the same circle oscillating radially, while occupying a given but identical azimuthal location along their individual orbits. This mode is kinematically different from $m \neq 0$ modes, for which orbits and streamlines are identical in the rotating frame.

Here again because all perturbing forces are such weak forces, Eq. (4.52) is compatible with $r = a_e[1 - \cos(\theta - \varpi_e)]$ only if $\Omega_p - (\Omega_a - \dot{\varpi}_{plan}) \ll \Omega_a - \dot{\varpi}_{plan}$. However, we shall see that the perturbing forces, although very weak, are nevertheless essential, because they can counteract the action of the Keplerian and precession shear, and therefore allow the mode to exist.

4.3.4 Summary

Let us summarize and complete the results obtained so far on ring kinematics. The results are discussed assuming $m \neq 0$, but can be transposed to the $m = 0$ case by replacing $-m\Omega_p$ by Ω_p and $m\Delta$ by Δ in the following equations [compare Eqs. (4.47) and (4.52)]. Unperturbed ring fluid particles travel on epicyclic orbits, which read²²:

$$r = a_e[1 - \epsilon \cos M_e], \quad (4.53)$$

$$\theta = \varpi_e + M_e + 2 \frac{\Omega_a}{\kappa_a} \epsilon \sin M_e, \quad (4.54)$$

where $(a_e, \epsilon, \varpi_e, M_e)$ are the “constants” of the motion, and are functions of the fluid particle initial position (ϖ_e and M_e depend on time as well). They can equivalently be considered as functions of a_e and θ_0 (the fluid particle initial phase), or of a_e and $\varphi \equiv M_e + \varpi_e$; M_e is given by Eq. (4.13), $\varpi_e = \varpi_0 + \int_0^t (\Omega_a - \kappa_a) dt$, and Ω_a and κ_a are defined in Eqs. (4.15) and (4.16). This fluid test particle solution is perturbed by the ring self-gravity, the ring viscous stress, and the satellites. These perturbations induce a time dependence of the “constants” of the motion which is expressed by Eqs. (4.20) through (4.23). Differentiating Eqs. (4.53) and (4.54) with respect to time yields the velocity field of the unperturbed motion:

²²From now on, we keep terms up to first order in eccentricity only, as second order terms are generally not accessible from the data.

$$u_r = \frac{dr}{dt} = a_e \epsilon \kappa_a \sin M_e, \quad (4.55)$$

$$u_\theta = r \frac{d\theta}{dt} = a_e \Omega_a [1 + \epsilon \cos M_e]. \quad (4.56)$$

As usual Eqs. (4.51) through (4.56) apply to the perturbed fluid particle motion as well: they give its osculating position and velocity.

On the other hand, the collective motion of ring fluid particles is *assumed* to constitute an m -lobe mode in a frame rotating with an angular velocity noted Ω_p :

$$r(a_e, \varphi, t) = a_e \{1 - \epsilon(a_e, t) \cos(m(\varphi - \Omega_p t) + m\Delta(a_e, t))\}. \quad (4.57)$$

In these relations, (a_e, φ) represent the circular motion the fluid particle would have in the absence of perturbation, and are used as (semi-)Lagrangian labels. This choice is clearly motivated by observations, and the dynamical equations self-consistently specify the conditions of existence of such motions. Quite often, the m -lobe shape is stationary and ϵ and Δ are independent of t ; a time-dependence occurs, e.g., due to viscous overstabilities or in the relaxation phase to stationary in which case the time dependence is transient.

Eqs. (4.57) and (4.53) can be satisfied simultaneously only if

$$M_e = m(\varphi - \Omega_p t) + m\Delta, \quad (4.58)$$

i.e., if the following relations are satisfied

$$\frac{dm\Delta}{dt} = -m(\Omega_a - \Omega_p) + \Omega_a - \dot{\varpi}_e, \quad (4.59)$$

$$\varpi_0 = \varphi_0(1 - m) - m\Delta_0, \quad (4.60)$$

where ϖ_0, θ_0 are the periapse angle and azimuth of the fluid particle at $t = 0$ and Δ_0 the phase at the same time [remember that the contribution of the perturbations to $d\varphi/dt$ is negligible; see the discussion after Eq. (4.49)]. Note that for stationary patterns, equation (4.59) implies that

$$\begin{aligned} \dot{\varpi}_{pert.} &= -m(\Omega_a - \Omega_p) + (\Omega_a - \dot{\varpi}_{plan.}) \\ &\simeq \left[\frac{3}{2}(m-1) + \frac{21}{4} \left(1 + \frac{m-1}{2} \right) \left(\frac{R_p}{a_R} \right)^2 J_2 \right] \times \left(\frac{GM_P}{a_R^3} \right) \left(\frac{a - a_R}{a_R} \right) \end{aligned} \quad (4.61)$$

where a_R is the resonance radius, and where $\dot{\varpi}_{pert.}$ and $\dot{\varpi}_{plan.}$ are the contributions of the perturbing forces and of the planet to the precession rate, respectively.

We have up to now encountered two basic time-scales:

1. The short or orbital time-scale.
2. The intermediate or “synodic” time-scale arising from the secular drift of test particle streamlines with respect to one another in the vicinity of the “resonance” radius a_R implicitly defined by the relation $m(\Omega - \Omega_p) = \kappa$. This time scale is of order $[\Omega_a \delta a / a]^{-1}$ (or $[J_2 \Omega_a \delta a / a]^{-1}$ if $m = 1$) where δa is the width of the perturbed region; also, as argued in the paragraph around Eq. (4.51), $\delta a / a \ll 1$.

One sees that the perturbing accelerations must produce a secular variation of the line of the apses on the intermediate time-scale. Because the perturbing forces are weak forces, $\dot{\omega}_{pert} \ll \Omega_a - \dot{\omega}_{plan}$. (or equivalently $a_e - a_R \ll a_R$), and the motion is mainly imposed by the planet. This precession rate is in general provided by the ring self-gravity. Note also that for an elliptic ring ($m = 1$), the required contribution of the perturbations to the precession rate is down by a factor J_2 . Therefore the $m = 1$ mode is easier to maintain than other modes, and elliptic rings more common; this is a natural result, because ellipses are the natural form of oscillations of the fluid particles around the planet. In spiral galaxies, as the central bulge does not dominate the gravity, the most common mode of oscillation corresponds to $m = 2$, as can be expected for objects with a flat rotation curve. Thus, two-arms spiral galaxies tend to be more common.

Let us conclude this section with a final comment. Generally, unperturbed rings appear circular, and are described by $r = a_e$; the motion of ring fluid particles reduces to $r = a_e, \theta = \varphi$. When the ring is perturbed, it is useful to express the perturbed position (r, θ) of a fluid particle in terms of the unperturbed position (a_e, φ) it would have in the absence of perturbation. This is easily performed from Eqs. (4.53), (4.54) and (4.58), and yields:

$$r = a_e [1 - \epsilon \cos(m(\varphi - \Omega_p t) + m\Delta)], \quad (4.62)$$

$$\theta = \varphi + 2 \left(\frac{\Omega_a}{\kappa_a} \right) \epsilon \sin[m(\varphi - \Omega_p t) + m\Delta]. \quad (4.63)$$

Note that these equations define at any given time a Eulerian change of variables from (r, θ) to (a_e, φ) . This property will be sometimes used in the remainder of these notes. Note also that differentiation of Eqs. (4.62) and (4.63) yields the following expressions for the velocity field:

$$u_r = m a_e \epsilon (\Omega_a - \Omega_p) \sin[m(\varphi - \Omega_p t) + m\Delta], \quad (4.64)$$

$$u_\theta = a_e \Omega_a \left[1 + \epsilon \left(2 \frac{m(\Omega_a - \Omega_p)}{\kappa_a} - 1 \right) \cos(m(\varphi - \Omega_p t) + m\Delta) \right]. \quad (4.65)$$

The “kinematic” set, Eqs. (4.62), (4.63), (4.64) and (4.65) differs from the “osculating” set, Eqs. (4.53), (4.54), (4.55) and (4.56) by terms of order $\epsilon \delta a_e / a_e (\ll \epsilon)$, where δa_e is the distance to the resonance radius, implying that the osculating elements differ from the (correct) kinematic ones by terms of the same order²³. This difference is accounted for by the short period terms of

²³Note that the epicyclic frequency appearing in these equations is defined by Eq. (4.7) and does not include the effect of the perturbations on the periaapse angle.

the osculating elements. However, such terms are usually negligible, and the difference between the two types of elements does not have to be specified.

In the derivation of these equations, as well as in the remainder of these notes, we have assumed that a_e , ϵ , and Δ are time independent. However, most results, if not all, are still valid if these quantities are time-dependent, provided that they vary on time-scales much longer than the orbital period, as is the case in section 7.1.

4.4 Ring surface density

Having solved the equation of motion, we wish now to consider the equation of mass conservation [Eq. (3.16)]. In fact, we are not going to solve directly this differential equation, but instead present a general and well-known Lagrangian solution directly from the constraint of mass conservation between the perturbed (elliptic) and unperturbed (circular) states of a ring. The following argument should be more properly developed in integral form, but we will just present it in differential form, as this does not affect the result.

Let us consider an elementary mass element δM , defined as the mass between the two streamlines of semimajor axis a_e and $a_e + da_e$, and the two unperturbed azimuths φ and $\varphi + d\varphi$:

$$\delta M = \sigma_0(a_e)a_e da_e d\varphi, \quad (4.66)$$

where, by definition, σ_0 is the surface density in the unperturbed state. It is a function of a_e only, as any nonaxisymmetric feature should be quickly erased by the Keplerian shear and by diffusion²⁴. Let us now perturb this flow, which becomes elliptic. We assume, as argued in the previous sections, that the fluid particle positions are given most generally by Eqs. (4.62) and (4.63) so that the ring streamlines form m -lobe shapes in a frame rotating at Ω_p . The mass element is now given by:

$$\delta M = \sigma(r, \theta) r dr d\theta, \quad (4.67)$$

where σ is the surface density of the fluid particle in (r, θ) . Let us introduce the Jacobian J of the change of variable from the unperturbed flow to the perturbed flow:

$$J = \left| \frac{r}{a} \frac{\partial(r, \theta)}{\partial(a_e, \varphi)} \right|, \quad (4.68)$$

so that $r dr d\theta = J a da d\varphi$. We can express the perturbed surface density in terms of the unperturbed one and of this Jacobian, using the fact that the fluid element of mass is the same in the two states:

$$\sigma = \frac{\sigma_0}{J}. \quad (4.69)$$

²⁴Ring arcs are not discussed in these notes.

In order to evaluate the Jacobian, we need to evaluate partial derivatives of the (actual) perturbed position with respect to the (fictitious) unperturbed position. Let us start with $\partial r/\partial a_e$. As ϵ and $m\Delta$ are function of a_e only, one obtains:

$$\frac{\partial r}{\partial a_e} = 1 - q \cos[m(\varphi - \Omega_p t) + m\Delta + \gamma], \quad (4.70)$$

where q and γ are defined by:

$$q \cos \gamma = \frac{da_e \epsilon}{da_e}, \quad (4.71)$$

$$q \sin \gamma = ma_e \epsilon \frac{d\Delta}{da_e}. \quad (4.72)$$

We have just introduced another fundamental parameter: q . In general, although $\epsilon \ll 1$, q can be of order unity. Streamlines cross if $|q| > 1$. This follows from the fact that the distance between two streamlines, to lowest order in eccentricity, is given by $\Delta r = \partial r/\partial a_e \Delta a_e$ where Δr and Δa_e are the differences in radii and semimajor axes of the two streamlines; this shows also that the distance between two adjacent streamlines varies with azimuth, and so does the width of an elliptic ring, as observed for all the elliptic Uranian rings. Usually, the pressure tensor (if nothing else) will diverge as $q \rightarrow 1$ or before, preventing streamline crossing.

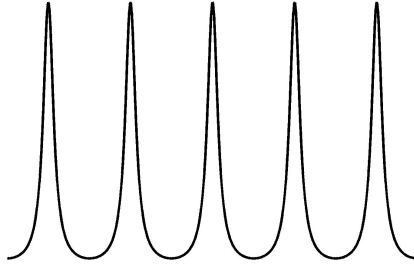


Figure 5: Schematic representation of the perturbed ring surface density as a function of azimuth for $q = 0.9$.

It is easy to check that $\partial\theta/\partial a_e \sim O(q)$, $\partial r/\partial\varphi \sim O(\epsilon)$, and $\partial\theta/\partial\varphi \sim 1 + O(\epsilon)$, so that to lowest order in ϵ , the Jacobian reads:

$$J = \frac{\partial r}{\partial a_e} = 1 - q \cos[m(\varphi - \Omega_p t) + m\Delta + \gamma], \quad (4.73)$$

The corresponding variation of the surface density with azimuth is schematically represented on Figure 5.

One sees that the surface density azimuthal variations are characterized by narrow peaks and broad troughs. An elliptic ring is narrower and denser in the vicinity of its periapse than at its apoapse. This trough-peak behavior is

also seen in the optical depths profiles of density waves in Saturn's rings. It is an unavoidable consequence of the basic kinematics discussed in the previous subsections.

A major kinematic difference between elliptic rings and density waves is that in elliptic rings, the values of $q \gg \epsilon$ arise because of the gradient of eccentricity across the ring, while the phase Δ remains constant or nearly constant. In density waves, the situation is exactly reversed: the eccentricity is nearly constant in the wave region, while the phase Δ varies very quickly with increasing semi-major axis [see the tight-winding condition Eq. (4.50)]. For elliptic rings, $\gamma \simeq 0$, whereas for density waves, $\gamma \simeq \pi/2$.

The surface density can reach very high contrasts, although the eccentricity remains very small: this type of nonlinearity is not connected to large deviations from the circular motion, but rather from the differences of deviations between neighboring streamlines. Thus we have the possibility of developing nonlinear theories while still linearizing the motion with respect to ϵ (but of course not with respect to q), which is always a small parameter in ring problems.

We have solved the continuity equation, in the sense that we have found the surface density of any ring fluid particle, in terms of three unknown functions: σ_0, q, γ . The reader can check that the *nonlinear* Eq. (3.16) is satisfied for any choice of these three functions, to lowest order in eccentricity. It is impossible to go further on purely kinematical grounds: the magnitude and form of these functions (except maybe σ_0) is determined by the perturbations.

5 Ring pressure tensor

The number of papers on the solution to the Boltzmann second-order moment equations in unperturbed flows is rather numerous. Some of them have already been quoted in section 2. But there are only three studies to date giving solutions for the second-order moments in perturbed flows. Borderies et al. (1983b) solve the Boltzmann second-order moment equations with a collision term of the Boltzmann form, modified to take the inelasticity of the collisions into account, assuming identical indestructible spherical particles characterized by a normal coefficient of restitution (there is no coupling with the spin degrees of freedom). This work is an extension of the paper by Goldreich and Tremaine (1978b). Shu and Stewart (1985) and Shu et al. (1985a) use instead a Krook collision term, also modified to account for the inelasticity of the collisions. These first two analyses are very similar in spirit and scope, but are however mostly restricted to dilute systems (i.e. systems in which the particle size is much smaller than the particle mean separations). On the other hand, Borderies et al. (1985) present a heuristic analysis of the pressure tensor behavior in dense systems (where the particle size is much bigger than the interparticle distances), which is not based on the Boltzmann second-order moment equations, but on a hydrodynamical approach. This analysis is expected to apply to high optical depth rings. Taken together, these papers give an interesting insight into the pressure tensor behavior under two opposite sets of physical conditions, which more or less span the conditions relevant to ring systems. Both dilute and dense systems will be discussed here.

5.1 Dilute systems

The approach based on the Krook model has a number of advantages: first, as the Krook model is simpler than the Boltzmann collision term, the analysis is somewhat simplified. Also, various generalizations like the inclusion of gravitational encounters are more easily performed. Furthermore, the Krook model can be looked at as a model equation for more complicated collisional operators when its parameters are appropriately chosen. Therefore, only the Krook model will be described here. The material of this section is taken from Shu and Stewart (1985), and from Shu et al. (1985a), unless otherwise specified.

In this model the collision term of the Boltzmann equation is expressed as

$$\left(\frac{\partial f}{\partial t}\right)_c = \nu_c(f_I - f), \quad (5.1)$$

where ν_c is the mean collision frequency of the system under consideration, and f_I is a Maxwellian distribution with the same local number density ρ and mean velocity \mathbf{u} as f :

$$f_I = \frac{\rho/M}{(2\pi c_I^2)^{3/2}} \exp\left(-\frac{(\mathbf{v} - \mathbf{u})^2}{2c_I^2}\right), \quad (5.2)$$

where M is the mean mass of the distribution [see the discussion after Eq. (3.12)]. To allow for the effects of inelastic collisions, we let c_I differ from c . Assuming that a collision reduces the magnitude of the component of the relative velocity along the lines of the centers of the two colliding particles by a factor²⁵ $\epsilon_r < 1$, while it preserves the two components of the tangential velocity, allows us to require

$$3c_I^2 = (2 + \epsilon_r^2)c^2, \quad (5.3)$$

where the coefficient of restitution ϵ_r has been averaged over all encounters, and can be regarded as a function of c .

The Krook collision term has the following physical meaning. As we follow the (individual) particles in orbit around the planet, per unit volume of phase space, inelastic collisions remove particles at a rate $\nu_c f$ and restore them with a Maxwellian distribution at a rate $\nu_c f_I$, i.e. isotropically around the mean velocity \mathbf{u} . This model does not examine in any detail the microphysics of the collisions. It just expresses the fact that, independently of the mechanics of individual collisions, collisional processes always tend to make the distribution isotropic, and more specifically Maxwellian, in a time-scale comparable to the collisional time-scale.

5.1.1 Collision frequency, effective particle size, and effective optical depth

The collision frequency can be estimated with the following arguments, mostly reproduced from the appendix A of Shu and Stewart 1985. Let us first compute

²⁵An index r has been added to the coefficient of restitution to prevent confusion with the epicyclic eccentricity.

the collision frequency for a collection of particles of identical masses m and sizes R , assuming that the distribution function is a maxwellian of velocity dispersion c :

$$f = \frac{\rho/m}{(2\pi c^2)^{3/2}} \exp\left(-\frac{\mathbf{w}^2}{2c^2}\right), \quad (5.4)$$

where $\mathbf{w} = \mathbf{v} - \mathbf{u}$ is the velocity with respect to the local mean velocity \mathbf{u} , and the vertical distribution of the mass density ρ is assumed isothermal:

$$\rho = \frac{\sigma\mu_0}{(2\pi c^2)^{1/2}} \exp\left(-\frac{\mu_0^2 z^2}{2c^2}\right), \quad (5.5)$$

with σ equal to the surface mass density. This distribution of density expresses the vertical hydrostatic equilibrium of the ring, i.e. the equilibrium between the planet and disk self-gravity forces on one side, and the pressure on the other. Therefore, the vertical epicyclic frequency $\mu_0 \equiv (\partial^2\phi/\partial z^2)_{z=0}$ entering Eq. (5.5) must include the contribution of the disk self-gravity, which can be much larger than the restoring force of the planet in the vertical direction, as will be seen in section 5.2.

Computing the rate at which a particle with random velocity \mathbf{w}_1 is hit by particles of all velocities \mathbf{w}_2 , and averaging over the distribution of \mathbf{w}_1 yields the local averaged collision frequency as:

$$\langle\nu_c\rangle = 4\pi R^2 \frac{\rho}{m} \int \int \frac{d^3w_1 d^3w_2}{(2\pi c^2)^3} |\mathbf{w}_1 - \mathbf{w}_2| \exp\left(-\frac{\mathbf{w}_1^2 + \mathbf{w}_2^2}{2c^2}\right). \quad (5.6)$$

The integrals are most easily computed by performing the change of variable from $(\mathbf{w}_1, \mathbf{w}_2)$ to $\{\mathbf{W} = \mathbf{w}_1 - \mathbf{w}_2, \mathbf{U} = (\mathbf{w}_1 + \mathbf{w}_2)/2\}$, which yields

$$\langle\nu_c\rangle = \frac{16\rho c R^2}{\pi^{1/2} m}. \quad (5.7)$$

We can now compute the vertically averaged collision frequency:

$$\langle\langle\nu_c\rangle\rangle \equiv \frac{1}{\sigma} \int \langle\nu_c\rangle \rho dz = \frac{8}{\pi} \mu_0 \tau, \quad (5.8)$$

where we have introduced the normal optical depth $\tau = \sigma\pi R^2/m$.

We can now generalize this expression to a general distribution of particle sizes. Let $N(R)dR$ be the number of particles per unit disk area having radii between R and $R + dR$. The surface density is related to the particle size distribution by

$$\sigma = \int_{R_1}^{R_2} mN(R)dR, \quad (5.9)$$

with $m = 4\pi\rho_p R^3$, for particles of bulk density ρ_p . The two quantities R_1 and R_2 are the two cutoff radii of the distribution. Typically in Saturn's rings, the distribution $N(R) \propto R^{-3}$, and $R_1 \sim 1$ cm and $R_2 \sim 5$ m.

Following Shu and Stewart (1985), we wish to define an effective binary collision frequency which possesses the following properties: (1) is symmetric with respect to the interchange of the members of the colliding pair, (2) is proportional to the geometric cross section $\pi(R + R')^2$, (3) is weighted by the reduced mass $mm'/(m + m')$ of the colliding pair, and (4) is equivalent to the preceding expression for a δ -function distribution of particle sizes. All these requirements seem natural, but might nevertheless need some comments. We have pointed out that the mean velocity and the pressure tensor are independent of the particle size which allows us to write the mass-dependent distribution function $f(m, \mathbf{r}, \mathbf{v})$ as $n(m)f_0(\mathbf{r}, \mathbf{v})$. Also, Eq. (5.1) should more properly be written $(\partial f(m)/\partial t)_c = \int dm' \alpha(m, m') \nu_c(m, m') n(m) (f_{0I} - f_0)$, where $\nu_c(m, m')$ is the frequency of collision of a particle of mass m with particles of mass m' ²⁶. This would indicate first that the collisional change for particles of one mass depends on the collisions with particles of all other masses, and second that not all pair of masses have the same efficiency in relaxing the distribution of a given mass to a Maxwellian, as indicated by the factor α . Indeed, in a collision between two particles of mass m and m' , the conservation of momentum requires that the change of momentum of each particle is $\mu O(c)$ where μ is the reduced mass of the colliding pair. Therefore, the change of velocity of the particle of mass m is $\mu/m O(c)$, and one can take $\alpha \propto \mu/m$. Now, remember that we have multiplied the Boltzmann moment equations by the mass and integrated over mass, which shows that the integrated collision term is proportional to $\int dm m \int dm' n(m) \mu(m, m') \nu_c(m, m') \alpha(m, m')$, and that the collision frequency must indeed be weighted by the reduced mass of the colliding pairs. Furthermore, Eq. (5.6) can be generalized to give the collision frequency of a particle of mass m with particles of mass m' , resulting in the change of the factor $4\pi R^2 \rho/m$ into $\pi(R + R')^2 n(m')$. This series of argument would give the effective collision frequency exactly, if it weren't for the efficiency factor α which is only determined to within a multiplicative constant. We can therefore only conclude that the effective collision frequency $\nu_c \propto \int \int dm dm' n(m) n(m') \pi(R + R')^2 mm'/(m + m')$. The coefficient of proportionality is constrained by the last requirement.

Finally, after getting rid of the vertical dependence of the $n(m)n(m')$ factor by a vertical integration, we can write down the desired collision frequency by inspection as

$$\nu_c = \frac{4\mu_0}{\pi\sigma} \int \int \pi(R + R')^2 \left(\frac{mm'}{m + m'} \right) N(R)N(R') dR dR', \quad (5.10)$$

where we have dropped the double-average notation. For definiteness, let us take $N(R) = CR^{-3}$. If we assume that $R_2 \gg R_1$, then $C = 3\sigma/4\pi\rho_p R_2$ from Eq. (5.9), and the double integral can be computed:

$$\nu_c = \frac{6\mu_0\sigma}{\sqrt{3}\rho_p R_2}. \quad (5.11)$$

We can put this result under a form similar to (5.8) by defining an effective optical depth and an effective particle size. We obtain

²⁶Note that at this point, ν_c is not symmetric with respect to the interchange of m and m' : if there are many more particles of mass m' than of mass m , any particle of mass m will collide much more often with a particle of mass m' than the reverse.

$$\nu_c = \frac{8}{\pi} \mu_0 \tau_e, \quad (5.12)$$

with

$$\tau_e = \frac{\sigma \pi R_e^2}{m_e} = \frac{3\sigma}{4\rho_p R_e}, \quad (5.13)$$

$$R_e = \frac{\sqrt{3}R_2}{\pi}. \quad (5.14)$$

Note that this effective optical depth differs from the actual optical depth obtained for $N(R) \propto R^{-3}$. In fact,

$$\tau = \int \pi R^2 N(R) dR = \frac{3\sigma}{4\rho_p R_2} \ln(R_2/R_1), \quad (5.15)$$

which is larger than τ_e by a factor $\sqrt{3}/\pi \ln(R_2/R_1)$; this factor amounts to 3 or 4 if $R_1 \sim 1$ cm and $R_2 \sim 500$ cm; τ_e is the quantity which should enter Eqs. (2.9), (2.10) and (2.12), and particular attention should be paid to this point when comparing theoretical results with observations.

Let us conclude this section with a few general comments. First, note that with the provision of Eqs. (5.3) and (5.12), the Krook model is completely specified: we have expressed its two parameters c_I and ν_c in terms of the other variables of the problem. The reader should however notice that instead of looking at the Krook model as to a physical model in its own right, one could as well consider Eq. (5.1) as a model equation for more complicated collision terms by keeping some freedom in the choice of c_I and ν_c . For example, Shu and Stewart (1985) show that the Boltzmann collision term for smooth identical spheres can be reproduced by adopting $c_I^2 = [(1 + \epsilon_r)/(3 - \epsilon_r)]c^2$ and $\nu_c = (4\mu_0/3\pi)(3 - \epsilon_r)(1 + \epsilon_r)\tau_e$ instead of Eqs. (5.3) and (5.12). Finally, let us note that corrective factors can be added to Eq. (5.12) to account for the effects of the anisotropy of the distribution and of the possible close-packing of the ring particles²⁷. However, Shu et al. (1985a) show that the anisotropy correction does not produce important modifications. The effect of the close-packing correction has not been analyzed in the literature. We will therefore not include it here. We merely note that Eq. (5.12) applies only to dilute systems, i.e. systems in which the filling factor is much smaller than unity.

5.1.2 Quasi-equilibrium of perturbed and unperturbed ring systems

We can pursue the program outlined at the end of section 3: we can now look for the steady-state solution of the pressure tensor equations with the velocity field of Eqs. (4.64) and (4.65), and the ring surface density of Eqs. (4.69) and (4.73).

²⁷If the particles are close-packed, i.e. if their radii are not small in comparison with their mean distances, the particles have to travel much less than their relative distance before a collision takes place, resulting in an increase of the collision frequency. This effect will be further discussed in section 5.2.

Let us first recast Eqs. (3.21) through (3.24) in an appropriate form. First, notice that to lowest order in ϵ , $\partial/\partial r = (1/J)\partial/\partial a$, and $d/dt \equiv \partial/\partial t + \Omega\partial/\partial\theta + u_r\partial/\partial r = \Omega\partial/\partial M'$ in steady-state where $M' = M + \gamma = m(\varphi - \Omega_p t) + m\Delta + \gamma$ [Eq. (4.58) has been used]. Notice that the steady-state condition $d/dt = \Omega\partial/\partial M'$ can be obtained either in an inertial frame or in a frame rotating with angular speed Ω_p . In such a rotating frame, the pressure tensor is time-independent because \mathbf{u} and σ are time-independent. The steady-state condition expresses the fact that the pressure tensor depends on time only through M' . Any other time dependence disappears in a time-scale $\sim \Omega^{-1}$, in accordance with the heuristic argument developed in section 2. Then, keeping only the leading terms in ϵ , one obtains:

$$\frac{dP_{rr}}{dM'} + \frac{3q}{J} \sin M' P_{rr} - 4P_{r\theta} = \frac{1}{\Omega} \left(\frac{\partial P_{rr}}{\partial t} \right)_c, \quad (5.16)$$

$$\frac{dP_{r\theta}}{dM'} + \frac{P_{rr}}{2J} + \frac{2q}{J} \sin M' P_{r\theta} - 2P_{\theta\theta} = \frac{1}{\Omega} \left(\frac{\partial P_{r\theta}}{\partial t} \right)_c, \quad (5.17)$$

$$\frac{dP_{\theta\theta}}{dM'} + \frac{P_{r\theta}}{J} + \frac{q}{J} \sin M' P_{\theta\theta} = \frac{1}{\Omega} \left(\frac{\partial P_{\theta\theta}}{\partial t} \right)_c, \quad (5.18)$$

$$\frac{dP_{zz}}{dM'} + \frac{q}{J} \sin M' P_{zz} = \frac{1}{\Omega} \left(\frac{\partial P_{zz}}{\partial t} \right)_c. \quad (5.19)$$

These equations show that the pressure tensor components depend on azimuth only through the angle M' . From Eq. (5.1), one obtains the right-hand sides of the preceding equations as

$$\frac{1}{\Omega} \left(\frac{\partial P_{ij}}{\partial t} \right)_c = \frac{\nu_c}{\Omega} (\sigma c_I^2 \delta_{ij} - P_{ij}), \quad (5.20)$$

where ν_c is defined by Eqs. (5.12) through (5.14), and c_I by Eq. (5.3). In performing the vertical integration, we have used the fact that c is independent of z (see the discussion at the beginning of section 3.2). Note also that by definition of the velocity dispersion

$$3\sigma c^2 = P_{rr} + P_{\theta\theta} + P_{zz}. \quad (5.21)$$

If the relation $\epsilon_r(c)$ were known, Eqs (5.16) through (5.21) supplemented by Eqs. (5.3) and (5.12) through (5.14) would yield a closed set of equations for $P_{rr}, P_{r\theta}, P_{\theta\theta}$, and P_{zz} (notice that these quantities uncouple from the other pressure tensor components). However, as this relation is not very well constrained, one usually prefers to keep the absolute scale of the pressure tensor as a free parameter, and solve rather for the relative magnitude of the pressure tensor components and for the relation $\epsilon_r(\tau_e)$ that the equilibrium requires. In doing so, the dependence of ν_c on azimuth is usually taken into account, but ϵ_r is usually taken to be constant with azimuth, as well as c^2 and c_I^2 (ν_c depends on azimuth because it is proportional to σ).

In order to illustrate these points, let us first look at the solution for unperturbed flows. In this case, the velocity field and the surface density are purely

axisymmetric, so that $q = 0$, and the pressure tensor is independent of azimuth, as well as the collision frequency. Therefore, Eqs. (5.16) through (5.19) reduce to

$$P_{rr} = \sigma_0 c_I^2 \left[1 + \frac{6\Omega^2}{\nu_c^2 + 4\Omega^2} \right], \quad (5.22)$$

$$P_{r\theta} = \sigma_0 c_I^2 \frac{\nu_c}{2\Omega} \frac{3\Omega^2}{\nu_c^2 + 4\Omega^2}, \quad (5.23)$$

$$P_{\theta\theta} = \sigma_0 c_I^2 \left[1 - \frac{3\Omega^2}{2(\nu_c^2 + 4\Omega^2)} \right], \quad (5.24)$$

$$P_{zz} = \sigma_0 c_I^2. \quad (5.25)$$

In these equations, the pressure tensor is scaled to $\sigma_0 c_I^2$, which we take as a free parameter. Combining Eqs. (5.3) and (5.21) with the “solution” we have just written down yields after some algebraic manipulations the required relation between the coefficient of restitution and the effective optical depth

$$\epsilon_r^2 = 1 - \frac{9/11}{1 + (128/11\pi^2)\tau_e^2}. \quad (5.26)$$

The reader will notice that this relation is in good agreement with Eq. (2.12), which we had derived with heuristic arguments. Again, equating this $\epsilon_r(\tau_e)$ relation to some $\epsilon_r(c)$ relation would give $c(\tau_e)$, and therefore would determine the magnitude of the pressure tensor in Eqs. (5.22) through (5.25). Furthermore, summing Eqs. (5.16), (5.18) and (5.19) yields the equation of equilibrium of the velocity dispersion, which reads

$$4\Omega \frac{P_{r\theta}}{\sigma_0} = \nu_c (1 - \epsilon_r^2) c^2. \quad (5.27)$$

In the hydrodynamical approximation (see section 5.2, or Landau and Lifshitz (1987), chapter 2), $P_{r\theta}/\sigma_0 \sim \nu\Omega$ for the Keplerian velocity field; also, Eq. (5.12) shows that $\nu_c \sim \Omega\tau_e$, so that Eq. (5.27) is in agreement with Eq. (2.10). We have already pointed out in section 2 that this equation expresses the equilibrium between the excitation due to the input from the shear of the mean motion, and the damping due to the inelasticity of the collisions.

This completes our discussion of unperturbed flows. In what concerns perturbed flows, no analytic solution of Eqs. (5.16) through (5.19) is available²⁸. The set has been solved numerically, either by integrating the differential equations from $M' = 0$ to 2π , subject to the constraint that the functions are periodic in M' (Borderies et al., 1983b), or the pressure tensor components are expanded in Fourier series, and the various coefficients computed (Shu et al., 1985a). The pressure tensor components are computed as functions of q , $\tau_{e0} \equiv J\tau_e = 3\sigma_0/4\rho_p R_e$ and M' (the weak dependence of Ω and μ_0 on a_e is ignored).

The preceding $\epsilon_r(\tau_e)$ of unperturbed flows generalizes to an $\epsilon_r(\tau_{e0}, q)$ relation, as is depicted on Figure 6 (adapted from Shu et al. 1985a): the curves show

²⁸Analytic expressions do exist in the limit of small q , but won't be given here. The interested reader is referred to the paper by Shu et al. (1985a) for their derivation.

the variation of ϵ_r with q , parametrized by the values of τ_{e0} . These curves exhibit a very important feature: if the unperturbed optical depth τ_{e0} is smaller than a critical value (here of order 0.2 or 0.3, but its exact value is sensitive to the details of the collisional model), the coefficient of restitution *must* become zero for a finite value of $q = q_m$, here of order 0.7. On the other hand, if τ_{e0} is larger than this critical value, q is not limited²⁹, and $\tau_{e0} \rightarrow 1$ as $q \rightarrow 1$. This result has the following physical interpretation. Let us consider a ring perturbed by some outside agent (a satellite near a resonance, for example), and let us increase slowly the strength of this perturbation so that the rate of perturbation of the flow, measured by q , tends to increase. To dissipate the energy input of the perturbation, ϵ_r must adjust according to the requirements of Figure 6. For small mean effective optical depths, the collision frequency is also small, and ϵ_r goes to zero to make maximum use of the rare collisional events. As a consequence the velocity dispersion increases without bound (because the coefficient of restitution is a decreasing function of the impact velocity), and the viscous damping increases [Eq. (2.9)], preventing further growth of the rate of perturbation of the flow q . On the other hand, in regions of high τ_{e0} , the collision frequency is always high enough to keep the dispersion velocity low. Therefore, in high optical depth regions, for a given strength of the outside perturbation, the viscous damping is much smaller than it would be in small optical depth regions. Shu et al. (1985a) mainly attribute to this effect the difference in damping length-scales of density waves in Saturn's A (low optical depth) and B (high optical depth) rings.

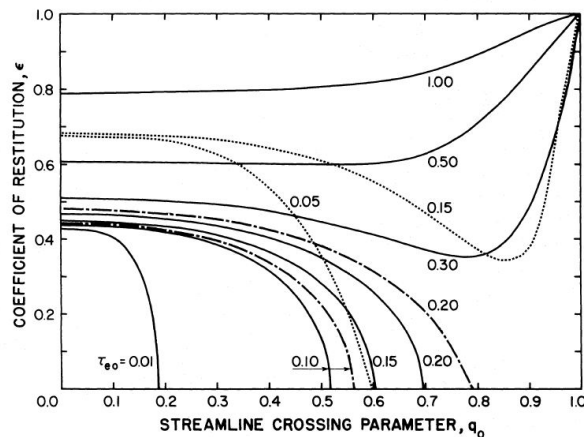


Figure 6: The relation between the particle coefficient of restitution and the rate of perturbation of the ring for several values of the effective optical depth; the three different types of lines (solid, dashed, dotted) correspond to three different forms of the Krook model (from Shu et al. (1985a)).

Let us now consider the behavior of the pressure tensor components themselves. Actually, we will see in section 6 that the pressure tensor does not affect the mean flow directly, but only through three quantities, t_1 , t_2 and $a_{r\theta}$, defined

²⁹Except by $q < 1$. This constraint arises because as $q \rightarrow 1$, the streamlines tend to cross, and therefore the pressure tensor, if nothing else, tends to diverge to prevent this crossing.

by³⁰:

$$t_1 = s_{rr} + 2c_{r\theta}, \quad (5.28)$$

$$t_2 = 2s_{r\theta} - c_{rr}, \quad (5.29)$$

$$c_{ij} + is_{ij} = \langle \exp(iM') P_{ij}(M') \rangle, \quad (5.30)$$

$$a_{ij} = \langle P_{ij}(M') \rangle, \quad (5.31)$$

where the bracket notation stands for the azimuthal average, so that, for any quantity X ,

$$\langle X \rangle \equiv \frac{1}{2\pi} \int_0^{2\pi} X dM'. \quad (5.32)$$

Note that $\langle \sigma \rangle = \sigma_0 / (1 - q^2)^{1/2}$. The quantities just defined depend only on q and τ_{e0} , or equivalently on q and $\langle \tau_e \rangle = \tau_{e0} / (1 - q^2)^{1/2}$. In dilute systems, the pressure tensor is of the order of σc^2 , so that it is useful to define

$$v^2 = \frac{\langle \sigma c^2 \rangle}{\langle \sigma \rangle}, \quad (5.33)$$

and, following Borderies et al. (1983a), to introduce dimensionless quantities of order unity Q_{ij} such that

$$P_{ij} = \langle \sigma \rangle v^2 Q_{ij}(q, \langle \tau_e \rangle, M'). \quad (5.34)$$

Due to the definitions of v^2 and c^2 , the variables Q_{ij} must satisfy the normalisation constraint $\langle Q_{rr} + Q_{\theta\theta} + Q_{zz} \rangle = 3$. The value of v^2 is essentially a free parameter in the absence of constraint on the form of the $\epsilon_r(c)$ relation, although one knows from various observations that $v^2 \sim c^2 \sim$ a few mm/s (see section 2). Similarly, one can define \mathcal{C}_{ij} , \mathcal{S}_{ij} , \mathcal{T}_i , and \mathcal{A}_{ij} such that

$$\langle \sigma \rangle v^2 \mathcal{C}_{ij} = c_{ij}, \quad (5.35)$$

$$\langle \sigma \rangle v^2 \mathcal{S}_{ij} = s_{ij}, \quad (5.36)$$

$$\langle \sigma \rangle v^2 \mathcal{A}_{ij} = a_{ij}, \quad (5.37)$$

$$\langle \sigma \rangle v^2 \mathcal{T}_i = t_i. \quad (5.38)$$

The behavior of \mathcal{C}_{ij} and \mathcal{S}_{ij} as functions of q and for $\langle \tau_e \rangle = 0.5$ is represented on Figure 7, taken from³¹ Borderies et al. (1983a).

The behavior for other values of $\langle \tau_e \rangle$ is quite similar. It is only important to remark that for dilute systems, both t_1 and t_2 are negative. The discussion of the effect of these coefficients on the mean motion is deferred to section 6 and 7. The discussion of the behavior of $a_{r\theta}$ is deferred to section 5.3.

³⁰The present definitions differs by a factor σ_0 from the equivalent definitions of Borderies et al. (1986).

³¹These curves were computed with a collision term of the Boltzmann form instead of the Krook form, but this does not affect much the results, at least for the purpose of these notes.

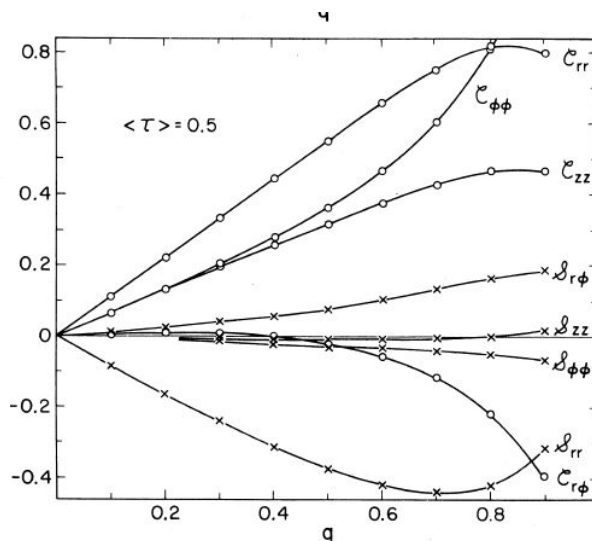


Figure 7: The behavior of the viscous coefficients defined in the text as a function of the perturbation rate of the ring q , for an effective optical depth of 0.5 (from Borderies et al. (1983a)).

5.2 Dense systems

Another important consequence of the relation displayed on Figure 6 is that for moderately opaque rings (let's say, $\tau \gtrsim 1$), the equilibrium can be obtained only for rather elastic materials (ϵ_r is always close to unity). Reversely, if the ring particle material is not elastic enough (which is quite likely, because in any case ring particles are most probably covered with some more or less fluffy layer of regolith), the equilibrium described in Figure 6 cannot be sustained, implying that the filling factor cannot be small and that the ring must collapse to a close-packed configuration (see the heuristic discussion of section 2.2.4). This argument ignores various complicating physical effects: first, gravitational encounters tend to increase the effective value of ϵ_r , because they are completely elastic; second, the coupling with spin degrees of freedom tends to decrease this effective value, since energy is lost by tangential friction; finally, irregular particle surfaces also tends to reduce ϵ_r . However, these effects could most certainly not suppress the possibility of reaching a close-packed configuration, which is likely to be relevant for Saturn's B ring as well as for the major Uranian rings, which have mean optical depths as high as 3 or 4.

In this section, we will therefore model the rings as a collection of particles with typical size $\sim d$. The typical separation distance of ring particle surfaces will be $\sim s$, with $s \ll d$. Considering that the particles have random velocity $\sim c$, the collision frequency is $\omega_c \sim c/s$, i.e. larger than the collision frequency that the dilute approximation would yield by a factor d/s . In such physical conditions, two important conditions can be drawn. First, the collision frequency being greatly enhanced, the system can most certainly be described in the framework of the hydrodynamical approximation³². But as ring particles do not resemble

³²The hydrodynamical approximation can be derived from Boltzmann equation, see, e.g., Shu

the molecules of a fluid in many respects, some attention must be paid to the computation of the pressure and the viscosity of the system. Second, as $d \gg s$, the medium is nearly incompressible, and one can assume that the divergence of the three-dimensional flow is zero. The computation of the pressure tensor in these physical conditions is the subject of this subsection. Unless otherwise specified, the material is extracted from the paper by Borderies et al. (1985).

5.2.1 Macroscopic equations

The macroscopic equations we will use are the continuity and the Navier-Stokes equation, i.e. Eqs. (3.8) and (3.9), with the pressure tensor reducing to

$$p_{ij} = p\delta_{ij} - 2\eta u_{ij}, \quad (5.39)$$

where p is the pressure, η the coefficient of dynamic viscosity and u_{ij} is the strain tensor:

$$2u_{ij} = \frac{\partial u_i}{\partial x_j} + \frac{\partial u_j}{\partial x_i}. \quad (5.40)$$

The tensor $\sigma_{ij} = 2\eta u_{ij}$ is known as the (viscous-)stress tensor and p_{ij} as the internal stress tensor in hydrodynamics. The validity of the hydrodynamical approximation relies on the existence of an isotropic pressure force, and on a linear stress-strain relation. These conditions are usually satisfied when the collision time is much smaller than the dynamical times involved in the problem.

As the medium under consideration is incompressible, ρ is constant (in space as well as in time), and the continuity equation reduces to

$$\nabla \cdot \mathbf{u} = 0. \quad (5.41)$$

From our discussion of section 3, we know that the pressure forces play essentially no rôle in determining the horizontal motion, so that the incompressibility condition Eq. (5.41) can be combined with Eqs. (4.64) and (4.65) to yield the vertical velocity:

$$u_z = -z \frac{\Omega q}{J} \sin M'. \quad (5.42)$$

In this equation, we have used $m(\Omega - \Omega_p) \simeq \kappa \simeq \Omega$. The surface and volumetric ring density are related by

$$\sigma = 2\rho h, \quad (5.43)$$

where h is the ring thickness. From $\sigma = \sigma_0/J$, one has $h = h_0/J$, where h_0 is the unperturbed ring thickness.

and Stewart 1985. However, it can also be derived directly from first physical principles, with no implicit or explicit reference to any specific form of the collision term, and therefore its range of application does not exactly overlap that of the Boltzmann moment equations.

One can plug the velocity field in the vertical component of the momentum equation, with $\phi = \phi_{plan.} + \phi_{sg}$, which then reads:

$$z \frac{\Omega^2 q}{J^2} (q \sin^2 M' + q - \cos M') = -F_2 \Omega^2 z - \frac{1}{\rho} \frac{\partial p}{\partial z} - 2 \frac{\partial \eta}{\partial z} \frac{\Omega q}{J} \sin M', \quad (5.44)$$

where one has approximated the planet by a central mass (neglected the gravitational harmonic coefficients), kept the first order term in the the z expansion of the resulting force, and used Gauss theorem to compute the contribution of the self-gravity force (the horizontal variation of thickness occurs on a scale much larger than the ring thickness). Thus, F_2 is defined by

$$F_2 = 1 + \frac{4\pi G \rho}{\Omega^2}. \quad (5.45)$$

Note that F_2 can be of order ten or larger in planetary rings (for ice particles, and a ring filling factor ~ 0.5), so that the vertical component of the ring self-gravity is much larger than the planet force in this direction, and the effect of the self-gravity on the vertical structure cannot be ignored. The vertical component of the momentum equation shows that p and η have to be quadratic in z . Furthermore, they must vanish at the top and bottom of the rings, so that we can write:

$$p = p_0 \left(1 - \frac{z^2}{h^2} \right), \quad (5.46)$$

$$\eta = \eta_0 \left(1 - \frac{z^2}{h^2} \right), \quad (5.47)$$

and recast Eq. (5.44) as

$$\frac{\Omega^2 q}{J^2} (q \sin^2 M' + q - \cos M') + F_2 \Omega^2 = \frac{2p_0}{\rho h^2} + \frac{4\eta_0}{\rho h^2} \frac{\Omega q}{J} \sin M'. \quad (5.48)$$

For certain combinations of parameters, this equation might require p_0 to be negative, at least in some locations in the ring. In these conditions, the ring material “splashes” in the vertical direction, so that our assumption of incompressibility fails. We will assume here that such conditions do not occur (formal requirements can be derived; see Borderies et al. 1985).

Finally, the rate of transfer of macroscopic energy into random motions per unit volume is (see section 5.3)

$$\left(\frac{\partial \mathcal{E}}{\partial t} \right)_{trans} = 2\eta W^2, \quad (5.49)$$

where W is the shear, i.e.,

$$\begin{aligned}
W^2 &= u_{ij}u_{ij} \\
&= \frac{\Omega^2}{8J^2} (16q^2 - 15 + 24J).
\end{aligned} \tag{5.50}$$

This completes the required set of macroscopic equation.

5.2.2 Microscopic equations

To proceed further, we need some microscopic equations for the pressure, the dynamic viscosity and the rate of collisional dissipation of energy. These quantities will be computed keeping in mind the simple physical model described at the introduction of section 5.2, following the derivation by Haff (1983).

To compute the pressure, any ring particle is imagined to vibrate with average velocity c in a cell of typical size d , and to exert some pressure p on the surrounding particles. In a collision, the typical momentum transfer is of the order of mc . The pressure being the momentum transfer per unit time and unit surface, one obtains therefore

$$p \sim \omega_c \frac{mc}{d^2} = g_1 \frac{\rho dc^2}{s}, \tag{5.51}$$

where g_1 is a dimensionless constant of order unity, and $\rho \sim m/d^3$.

The coefficient of dynamic viscosity is computed in the following way. Assume that the ring particle fluid is submitted to some shear flow, in which for definiteness the velocity u is assumed to lie in the x direction and the gradient of u in the y direction. Two adjacent “layers” of ring particles will on the average move with velocities differing by an amount $\Delta u \sim (du/dy) d$. When collisions occur between particles belonging to the two layers, the average transfer of x -momentum in the y direction is $m\Delta u$. Therefore, the shear stress, being the rate of transfer of momentum per unit time and across a unit surface [see the discussion after Eq. (3.9)] is

$$\sigma \sim \omega_c \frac{m\Delta u}{d^2}. \tag{5.52}$$

As by definition $\sigma = \eta du/dy$, one finally obtains

$$\eta = g_2 \frac{\rho d^2 c}{s}, \tag{5.53}$$

where g_2 is another factor of order unity.

Finally, the rate of dissipation of kinetic energy of random motions per unit volume is (see the discussion at the beginning of section 2.2.3)

$$-\left(\frac{\partial \mathcal{U}}{\partial t}\right)_c \sim (1 - \epsilon_r^2) \omega_c \rho c^2 = g_3 \frac{\rho c^3}{s}, \tag{5.54}$$

where g_3 is the last dimensionless constant of order unity of the problem.

We have now gathered all the pieces of the puzzle, and we can turn our attention to the computation of the pressure tensor components.

5.2.3 The pressure tensor components

Our first task is to find two relations between p_0 and η_0 , in order to obtain expressions for these two quantities. One such relation is obviously Eq. (5.48). The other one is obtained in the following way. First, equating the rate of transfer of energy from the orbital motion to random motions, Eq. (5.49) with the rate of dissipation of energy in collisions, Eq. (5.54), yields the following constraint (which will be further discussed in section 5.3):

$$2\eta W^2 = g_3 \frac{\rho c^2}{s}. \quad (5.55)$$

Combining this relation with the expression of p^2/η , computed from Eqs. (5.51) and (5.53) gives us the required relation between p_0 and η_0 , which reads

$$\eta_0 = F_1 \frac{p_0}{W}, \quad (5.56)$$

where $F_1 = (g_2 g_3 / 2g_1^2)^{1/2}$ is a dimensionless factor of order unity.

We can finally compute p_0 and η_0 from this relation and Eq. (5.48). This yields

$$p_0 = \rho h_0^2 \Omega^2 \frac{A_1 A_2}{2J^2 A_3}, \quad (5.57)$$

$$\eta_0 = \rho h_0^2 \Omega^2 2^{1/2} F_1 \frac{A_1}{J A_3}, \quad (5.58)$$

where we have defined

$$A_1 = F_2 + \frac{q}{J^2} (q \sin^2 M' + q - \cos M'), \quad (5.59)$$

$$A_2 = (16q^2 - 15 + 24J)^{1/2}, \quad (5.60)$$

$$A_3 = A_2 + 2^{5/2} F_1 q \sin M'. \quad (5.61)$$

Note that in order of magnitude $W^2 \sim \Omega^2$ so that Eqs. (5.55) and (5.53) imply $c \sim \Omega d$. Furthermore, Eqs. (5.58) and (5.53) imply $d^3 \sim h_0^2 s$, so that the condition $s \ll d$ requires $h_0^2 \gg d^2$, i.e., the rings must be many particle thick.

We are now in position to compute the vertically integrated pressure tensor components P_{ij} . First, the vertical integration of Eq. (5.39) yields

$$P_{ij} = \frac{4}{3} h (p_0 \delta_{ij} - 2\eta_0 u_{ij}), \quad (5.62)$$

except for P_{rz} and $P_{\theta z}$ which vanish. Introducing

$$A_4 = A_2 - 2^{5/2} F_1 q \sin M', \quad (5.63)$$

$$A_5 = \frac{2A_1}{3J^3}, \quad (5.64)$$

one finally obtains the nonvanishing pressure tensor component to lowest order in h/a as

$$P_{rr} = \rho h_0^3 \Omega^2 \frac{A_4 A_5}{A_3}, \quad (5.65)$$

$$P_{r\theta} = -\rho h_0^3 \Omega^2 \frac{2^{1/2} F_1 A_5 (1 - 4J)}{A_3}, \quad (5.66)$$

$$P_{\theta\theta} = \frac{4}{3} h p_0, \quad (5.67)$$

$$P_{zz} = \rho h_0^3 \Omega^2 A_5, \quad (5.68)$$

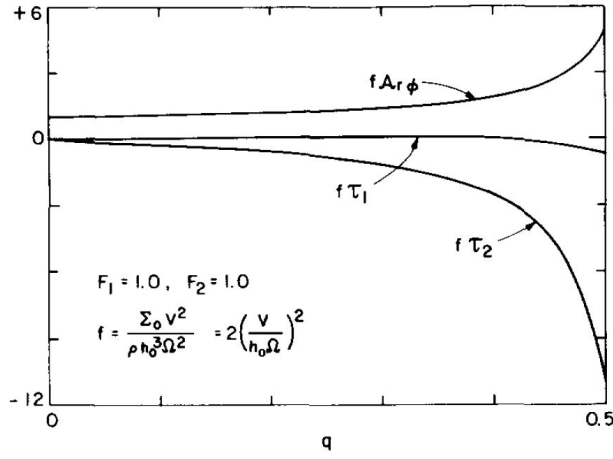


Figure 8: The behavior of the azimuthally averaged viscous coefficients as a function of the rate of perturbation of the ring streamlines q (from Borderies et al. 1985).

Notice that for dense systems, the natural scaling of the vertically integrated pressure tensor components is no longer $\langle \sigma \rangle v^2$, but $\rho h_0^3 \Omega^2$. Therefore, the three fundamental coefficients $t_1, t_2, a_{r\theta}$ defined in Eqs. (5.28) through (5.31) are most conveniently written in dimensionless form as

$$t_i = \rho h_0^3 \Omega^2 f \mathcal{T}_i, \quad (5.69)$$

$$a_{r\theta} = \rho h_0^3 \Omega^2 f \mathcal{A}_{r\theta}, \quad (5.70)$$

where, consistently with Eqs. (5.35) through (5.38),

$$f = \frac{\sigma_0 v^2}{(1 - q^2)^{1/2} \rho h_0^3 \Omega^2}, \quad (5.71)$$

The behavior of the three dimensionless quantities $f\mathcal{T}_1$, $f\mathcal{T}_2$ and $f\mathcal{A}_{r,\theta}$ for $F_1 = F_2 = 1$ is displayed on Figure 8, taken from Borderies et al. (1985). The graph is represented for values of $q < 0.5$, because otherwise p_0 becomes negative for some values of M' . Notice that \mathcal{T}_2 is negative as in the dilute approximation, but that \mathcal{T}_1 is positive for q smaller than some critical value (although this cannot be seen on the graph, due to the poor resolution), in opposition to the dilute case. The implications of these results for the dynamics will be discussed in section 5.3 and sections 6 and 7.

5.3 Energy dissipation, and viscous flux of angular momentum

Energy and angular momentum budgets are important for the long term dynamics of the rings. We will here have a look into two fundamental features of energy and angular momentum exchanges, differing a more complete discussion to section 6.

5.3.1 Energy dissipation in planetary rings

The purpose of this section is to compute the rate of dissipation of energy due to the inelasticity of the collisions, and to show that this energy is drawn from the orbital motion.

The orbital energy per unit mass is by definition

$$E = \left(\frac{1}{2} \mathbf{u}^2 + \phi_p \right). \quad (5.72)$$

From the equation of continuity (3.13) and the equation of motion (3.14), one obtains the equation of evolution of E as

$$\rho \frac{DE}{Dt} = - \frac{\partial p_{ij} u_i}{\partial x_j} + p_{ij} \frac{\partial u_i}{\partial x_j}. \quad (5.73)$$

In this equation, we have ignored the work of the ring self-gravity and of the satellite perturbations, as they have no effect on the argument. The two terms on the right-hand side are the rate of work of the internal stress of the ring during the motion.

On the other hand, the internal kinetic energy per unit ring mass is

$$U = \frac{1}{2\rho} p_{ii}. \quad (5.74)$$

From Eq. (3.15), one can derive the equation of evolution of U

$$\rho \frac{DU}{Dt} = - p_{ij} \frac{\partial u_i}{\partial x_j} + \frac{1}{2} \left(\frac{\partial p_{ii}}{\partial t} \right)_c, \quad (5.75)$$

where, consistently with the approximations made earlier, we have neglected the heat flux terms. The first term on the right-hand side is the contribution of the internal stress (in quasi-static transformations, it results in the well-known $p dV$ work of thermodynamics), and the last term is the rate of loss of energy due to

collisions (if collisions are elastic, this term equals to zero, by conservation of kinetic energy). This last term is obviously negative. Comparing Eq. (5.73) and (5.75) shows that the last term of the right-hand side of Eq. (5.73) represents the rate of transfer of macroscopic energy into random motions.

For dense systems, we can put Eq. (5.75) in a different form. From the definitions of the stress and strain tensors Eqs. (5.39) and (5.40), one obtains

$$\rho \frac{DU}{Dt} = 2\eta(u_{ij})^2 + \frac{1}{2} \left(\frac{\partial p_{ii}}{\partial t} \right)_c, \quad (5.76)$$

Eq. (5.55) is identical to Eq. (5.76) except for DU/Dt , which has been set equal to zero, because some of the (crude) approximations which we have made earlier are not compatible with this term (in particular, its vertical dependence), and because it represents no essential piece of physics, as it averages to zero [see also the discussion after Eq. (5.79)].

Now, remember that the streamlines of the flow form closed curves in a frame rotating at Ω_p (see section 4) so that we can actually integrate Eqs. (5.75) and (5.73) over an arbitrary volume bounded by streamlines³³. Notice that these volume integrals are in fact integrals over a given mass element of the ring. Note also that the steady state condition implies $DU/Dt = -(\partial U/\partial \theta)\Omega/m$, so that DU/Dt does not contribute to the integral. Thus, one obtains:

$$\int dV \rho \frac{DE}{Dt} = \int dV p_{ij} \frac{\partial u_i}{\partial x_j} - \int dV \frac{\partial p_{ij} u_i}{\partial x_j}, \quad (5.77)$$

$$\int dV p_{ij} \frac{\partial u_i}{\partial x_j} - \int dV \frac{1}{2} \left(\frac{\partial p_{ii}}{\partial t} \right)_c = 0. \quad (5.78)$$

These two equations demonstrate the advertised result, i.e. that the average energy lost per unit mass during collisions is drawn from the energy of the orbital motion. Therefore, on the average, the ring material tends to fall on the planet.

We can compute the vertically integrated average rate of loss of energy of the ring material bounded by two streamlines of radii a_1 and a_2 , by using Eqs. (5.16) through (5.19), which yield

$$\begin{aligned} & \int r dr \int d\theta \frac{1}{2} \left[\frac{\partial}{\partial t} (P_{rr} + P_{\theta\theta} + P_{zz}) \right]_c \\ &= \frac{1}{2} \int_0^{2\pi} dM' \int_{a_1}^{a_2} da Ja \left[\Omega \frac{\partial}{\partial M'} (P_{rr} + P_{\theta\theta} + P_{zz}) \right. \\ & \quad \left. + \frac{\Omega q \sin M'}{J} (3P_{rr} + P_{\theta\theta} + P_{zz}) + \Omega P_{r\theta} \left(\frac{1}{J} - 4 \right) \right] \\ &= \pi \int_{a_1}^{a_2} da a \Omega (2qt_1 - 3a_{r\theta}). \end{aligned} \quad (5.79)$$

This result is also valid for dense systems, although Eqs. (5.16) through (5.19) were derived under the assumption that $u_z = 0$. This is most easily seen from

³³This volume rotates with angular speed Ω_p in an inertial frame, but this has no effect on the argument.

Eq. (5.78) by noting that in the dense system approximation, $P_{rz} = 0$ and $P_{\theta z} = 0$, so that the only possible difference in the first term of this equation between the dilute and the dense approximations comes from the contribution of $p_{zz}\partial u_z/\partial z$, which vanishes upon vertical integration [see, e.g., Eq. (B.12c) of Shu and Stewart (1985)]. Note that as a consequence, Eq. (5.55) is compatible with Eq. (5.79).

We will show in section 6 that the rate of viscous loss of orbital energy is also given by Eq. (5.79), as can be expected from the previous argument. This equation has an interesting consequence, which will be used in section 5.4: it implies that

$$2qt_1 < 3a_{r\theta}, \quad (5.80)$$

because the collision terms are negative (the dissipation of energy in collision reduces the internal kinetic energy) and because the choice of the boundaries a_1 and a_2 is arbitrary.

5.3.2 Viscous flux of angular momentum

We have argued in section 2 that the ring internal stress results in angular momentum transport. Let us call F_H^{vis} the vertically integrated rate of transport of angular momentum across a unit length of streamline (in short, the viscous flux of angular momentum). The components of the pressure tensor being the components of the internal force of the ring fluid per unit surface [see the discussion after Eq. (3.9)], the vertically integrated torque exerted per unit length of streamline due to the material inside it is $aP_{r\theta}$, to lowest order in eccentricity. Therefore,

$$F_H^{vis} = aP_{r\theta}, \quad (5.81)$$

Defining the viscous angular momentum luminosity, L_H^{vis} , as the integral of the flux around the streamline, one has

$$L_H^{vis} = 2\pi a^2 a_{r\theta}. \quad (5.82)$$

It is instructive to derive general expressions for fluids with constant kinematic viscosity $\nu = \eta/\rho$. From Eqs. (5.39) and (5.40), one obtains

$$F_H^{vis} = 2\nu\sigma_0\Omega a \left(\frac{1}{J} - \frac{1}{4J^2} \right), \quad (5.83)$$

$$L_H^{vis} = \pi\nu\sigma_0\Omega a^2 \frac{3 - 4q^2}{(1 - q^2)^{3/2}}, \quad (5.84)$$

In the limit of axisymmetric flows ($q = 0$), the viscous luminosity of angular momentum reduces to

$$L_H^{vis} = 3\pi\sigma\nu\Omega a^2, \quad (5.85)$$

This result, derived by Lynden-Bell and Pringle (1974) in the context of the theory of accretion disks, was used in section 2.3 in the discussion of axisymmetric viscous instabilities. Eq. (5.85) shows that angular momentum flows outwards in axisymmetric flows.

Eqs. (5.83) and (5.84) show that two values of q are particularly significant. First, for $q < q_1 = 3/4$, $F_H^{vis} > 0$ for all azimuthal locations, whereas for $q > q_1$, $F_H^{vis} < 0$ for some interval of azimuth. This inward flux of angular momentum arises because the angular velocity increases outwards in this longitude interval. For $q > q_2 = \sqrt{3}/2$, the luminosity itself becomes negative: the perturbation of the flow is high enough to make the angular momentum flow inwards, in opposition to the unperturbed case.

One can wonder if this feature is a consequence of our assumption of constant kinematic viscosity. This is not the case. Borderies et al. (1983b) in their analysis of dilute systems show that the angular momentum flux and luminosity, which are both positive for axisymmetric flows, both change sign in sufficiently perturbed regions. For example, the corresponding value of q_2 is represented as a function of $\langle \tau_e \rangle$ on Figure 9.

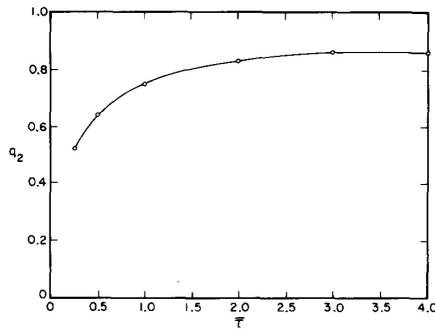


Figure 9: The value of q for which the angular momentum luminosity reverses direction as a function of the azimuthally averaged effective optical depth (from Borderies et al. 1983b).

The same feature is also true of dense systems, although this cannot be seen on Figure 8. For example, for the particular choice³⁴ of $F_1 = 0.55$ and $F_2 = 7$, Borderies et al. (1986) quote $q_2 = 0.79$.

In conclusion, it appears that the reversals of the angular momentum flux and luminosity for sufficiently perturbed flows is a general feature, the existence of which does not depend on the details of the microphysics controlling the pressure tensor. This is fortunate, as angular momentum luminosity reversal plays a central rôle in the ring confinement by satellites (the so-called “shepherding mechanism”; see Borderies et al. 1984, 1989).

³⁴These values are more appropriate for dense rings than the one chosen in Figure 8. The value of F_1 is suggested by the analysis of dense systems by Araki and Tremaine (1986) (N. Borderies, private communication) and the value of F_2 is the smallest one found in Saturn’s rings.

5.4 Summary and parametrization of the pressure tensor

This whole section was mainly devoted to the derivation of the pressure tensor under various sets of physical conditions which are likely to be relevant to planetary rings. The pressure tensor influences the mean motion only through the three coefficients t_1 , t_2 and $a_{r\theta}$ defined in Eqs. (5.28) through (5.31). The analyses presented in this section show that there exists a number of general features characterizing these three quantities, as pointed out by Borderies et al. (1986).

1. Streamlines cross at $q = 1$, so that the pressure tensor is likely to diverge as $q \rightarrow 1$, or even for smaller values of q , as shown on Figure 6 and in the related discussion.
2. t_1 and t_2 vanish as $q \rightarrow 0$, because the flow, and therefore the pressure tensor components, become axisymmetric in this limit. Hence, it is reasonable to assume that $t_{1,2} \propto q$ for small q , as this dependence is characteristic of both the dilute and dense models. Notice that t_1 is negative in the dilute approximation, whereas it is positive for small values of q in the dense model; t_2 is negative in both models.
3. We have shown that the energy dissipation due to inelastic collisions implies $2qt_1 < 3a_{r\theta}$. This is a general result, which does not depend on the choice of the collisional model [see Eq. (5.80)].
4. We have just seen that $a_{r\theta}$ is in general positive for small q , so that angular momentum flows outwards. However, as $q \rightarrow 1$, the direction of the angular momentum flow is reversed, so that there is some value $q = q_a(\sigma_0)$ for which $a_{r\theta} = 0$ and the transition between the two regimes occur. For dense systems, q_2 is independent of σ_0 .

From these general considerations, Borderies et al. (1986) were motivated to devise simple empirical formulæ for the three coefficients $a_{r\theta}$, t_1 , t_2 , of the form

$$a_{r\theta} = B_a \sigma_0^b \frac{q_a - q}{(q_c - q)^c}, \quad (5.86)$$

$$t_1 = B_1 \sigma_0^b q \frac{q_1 - q}{(q_c - q)^c}, \quad (5.87)$$

$$t_2 = B_2 \sigma_0^b q \frac{q_2 - q}{(q_c - q)^c}. \quad (5.88)$$

In these equations, B_a , B_1 and B_2 are positive quantities, $0 < q_a < 1$, $q_1 < q_a$ is either positive or negative, and q_2 is negative. In the model for dense systems, $b = 3$, $q_c = 1$ and the rapid divergence of the viscous coefficients is well represented by $c \simeq 3$. In principle, q_a , q_1 , q_2 and q_c are functions of σ_0 , except for dense systems. Orders of magnitude for B_a , B_1 and B_2 can be obtained from the comparison of these relations with Eqs. (5.37) and (5.38) on one hand, and (5.69) and (5.70) on the other.

6 Ring dynamics: perturbation equations and conserved quantities

We have already listed the perturbations acting on a ring: the ring self-gravity, the gravitational action of satellites, the disk pressure tensor. For the satellite perturbations, we will restrict ourselves to one Fourier component in the expansion of Eq. (4.37), in order to investigate in some detail the dynamics of a density wave near an isolated Lindblad resonance. A complete discussion of disk-satellite interactions (e.g. of the effect of such interactions on the eccentricity evolution of narrow elliptic rings, or of the shepherding of a ring by a satellite), would take us too far afield and is outside the scope of these notes.

A number of derivations are more easily performed when the rings are represented as a discrete collection of streamlines. This point of view is adopted in what follows. The continuum description will be recovered by taking the appropriate limits when needed. Conversely, one can go from the continuum limit to the discrete form of the equations.

It is well known in Celestial Mechanics that perturbing accelerations generate both periodic and secular (or long period) terms. The periodic effects have usually a small amplitude in ring dynamics and can safely be neglected. Also, the long term dynamics is easier to capture in simulations once the short-term effects are averaged out. We will therefore average the perturbation equations in what follows. There are some added subtlety in this procedure for the fluid equations with respect test particles:

1. The perturbation equations are not used as is commonly done in Celestial Mechanics, by inserting an unperturbed solution in the right-hand side and deducing the magnitude of the perturbation. Instead, the perturbed motion is also inserted in the right-hand side, so that these equations provide self-consistency conditions for the existence of the assumed form of the perturbed motion. Because of this, $M_e = m(\varphi - \Omega_p t) + m\Delta$ is in fact always enforced. This implies that M_e is not an independent phase, but a quantity depending on a, φ and t .
2. The equations are phase-averaged. Any form of averaging can be freely chosen — this a matter of convenience, not a theoretical requirement — and it turns out that this choice is more adequate than the usual time-averaging procedure, in particular because $M_e = M_e(a, \varphi, t)$. In the process, short-periodic terms of order $\epsilon g_{pert.}/g_{plan.}$ are averaged out ($g_{pert.}$ and $g_{plan.}$ stand for the accelerations due to the perturbing forces and the planet's, respectively). This is required for the self-consistency of the assumed form of perturbed motions and this self-consistency is ensured by the smallness of the short periodic term. In this sense, the perturbation equations are indeed handled perturbatively, albeit again in a slightly not usual way.

In what follows, the subscript e of a_e , M_e and ϖ_e is dropped for convenience. However, it should be kept in mind that the elements involved in the discussion are epicyclic elements and not elliptic ones.

For definiteness, streamlines and associated quantities are labeled with their index i ; $1 \leq i \leq N_s$, where N_s is the total number of streamlines. Streamlines

width is noted δa when needed. Streamlines semi-major axis are defined as the mid-position in the streamlines, and all quantities are evaluated there, except the stress tensor which should be evaluated at the streamline boundary; however this would introduce a staggered double-mesh and this refinement is avoided in these notes.

6.1 Disk self-gravity

Let us consider two streamlines (indexed as streamline 1 and streamline 2) with m lobes and orbital elements $a_1, \epsilon_1, \Delta_1$ and $a_2, \epsilon_2, \Delta_2$ respectively. We suppose $a_1 < a_2$ for definiteness. We are going to compute the gravitational perturbation of streamline 2 on streamline 1. In fact it is sufficient to compute the gravitational perturbation on a fluid particle of streamline 1, because this perturbation is identical for all fluid particles, once averaged over the orbital time-scale. For $\Delta a_{ij} \equiv a_i - a_j$ small enough (that is, much smaller than the curvature radius of the streamlines, i.e. $\Delta a_{ij} \ll a$) one can locally identify the streamline with a straight line and find the perturbing acceleration with the help of Gauss's theorem.

Let us call λ_2 the linear mass density of streamline 2. The gravitational acceleration \mathbf{g}_{sg} on a fluid particle is given by (Borderies et al., 1983c)

$$\mathbf{g}_{sg} = \frac{2G\lambda_2}{\Delta_c} \mathbf{u}, \quad (6.1)$$

where \mathbf{u} is the unit vector perpendicular to streamline 2 and directed outwards (from streamline 1 to streamline 2), and Δ_c the distance of the fluid particle to streamline 2 along \mathbf{u} . Let us introduce the angle β between the radial direction and \mathbf{u} , so that $\Delta_c = |r_1 - r_2| \cos \beta$. The radial and tangential components of the perturbing acceleration read:

$$R_{sg} = -\frac{2G\lambda_2}{\Delta r_{12}}, \quad (6.2)$$

$$S_{sg} = -\frac{2G\lambda_2}{\Delta r_{12} \cos \beta} \sin \beta, \quad (6.3)$$

where $\Delta r_{ij} \equiv r_i - r_j$. Elementary geometric considerations lead to the following expressions for $\sin \alpha$ and $\cos \alpha$:

$$\cos \beta = \frac{r_2 d\theta/d\varphi}{\sqrt{(r_2 d\theta/d\varphi)^2 + (dr_2/d\varphi)^2}} = 1 + \mathcal{O}(\epsilon_2^2), \quad (6.4)$$

$$\sin \beta = -\frac{dr_2/d\varphi}{\sqrt{(r_2 d\theta/d\varphi)^2 + (dr_2/d\varphi)^2}} = -\frac{1}{a_2} \frac{dr_2}{d\varphi} + \mathcal{O}(\epsilon_2^2). \quad (6.5)$$

The last equalities are evaluated from Eq. (4.57).

Finally, the components of the perturbing acceleration at position (r, θ) and at time t read:

$$R_{sg} = -\frac{GM_2}{\pi a_2 (r - r_2)}, \quad (6.7)$$

$$S_{sg} = \frac{GM_2 m \epsilon_2 \sin(m(\theta - \Omega_p t) + m\Delta_2)}{\pi a_2 (r - r_2)}, \quad (6.8)$$

where the linear mass density has been expressed in terms of the total mass of the streamline³⁵ $M_2 = 2\pi a_2 \lambda_2$ and where r_2 is a function of θ through Eq. (4.57); we have used the fact that $\varphi = \theta$ to lowest order in ϵ . The streamline mass is connected to the ring surface density by $M_2 = 2\pi a_2 \delta a \sigma_0$ where δa is the distance between two neighboring unperturbed streamlines. Eq. (6.7) corrects an unimportant error in the corresponding equation of Borderies et al. (1985).

A simple trigonometric manipulation shows that $\Delta r_{12} = J_{12} \Delta a_{12}$ where

$$J_{12} = 1 - q_{12} \cos[m(\theta - \Omega_p t) + m\Delta_1 + \gamma_{12}], \quad (6.9)$$

and

$$q_{12} \exp(i\gamma_{12}) = \frac{a_1 \epsilon_1 - a_2 \epsilon_2 \exp[im(\Delta_2 - \Delta_1)]}{\Delta a_{12}}. \quad (6.10)$$

Note that $q_{12} = q_{21}$, but $\gamma_{12} \neq \gamma_{21}$. As $\Delta a_{12} \rightarrow 0$, $J_{12} \rightarrow J$, $q_{12} \rightarrow q$ and $\gamma_{12} \rightarrow \gamma$. With the same definitions, one also has:

$$a_2 \epsilon_2 \sin[m(\theta - \Omega_p t) + m\Delta_2] = a_1 \epsilon_1 \sin[m(\theta - \Omega_p t) + m\Delta_1] - \Delta a_{12} q_{12} \sin[m(\theta - \Omega_p t) + m\Delta_1 + \gamma_{12}] \quad (6.11)$$

We can now compute the perturbations of a_1 , ϵ_1 and ϖ_1 by inserting Eqs. (6.6) through (6.11) into Eqs. (4.20) through (4.22), and averaging over φ_1 , with the additional constraint that $M_1 = m(\varphi - \Omega_p t) + m\Delta_1$ and $\theta = \varphi$. Furthermore, we take $a_1 = a_2 = a$ except in the difference Δa_{12} (remember $\Delta a_{12} \ll a$ in ring problems), and keep the results to lowest nonvanishing order in ϵ . Finally, we take $\Omega_a = \kappa_a = (GM_p/a^3)^{1/2}$ in the perturbation equation (this leads to negligible fractional errors of order J_2), except in the difference³⁶ $\Omega_a - \kappa_a$. The resulting averaged equations read:

$$\left(\frac{da_1}{dt}\right)_{sg} = -\frac{2(m-1)n_a}{\pi} \frac{M_2}{M_p} \frac{a}{\Delta a_{12}} a \epsilon_1 H(q_{12}^2) q_{12} \sin \gamma_{12}, \quad (6.12)$$

$$\left(\frac{d\epsilon_1}{dt}\right)_{sg} = \frac{n_a}{\pi} \frac{M_2}{M_p} \frac{a}{\Delta a_{12}} H(q_{12}^2) q_{12} \sin \gamma_{12}, \quad (6.13)$$

$$\left(\frac{d\varpi_1}{dt}\right)_{sg} = \frac{n_a}{\pi} \frac{M_2}{M_p} \frac{a}{\epsilon_1 \Delta a_{12}} H(q_{12}^2) q_{12} \cos \gamma_{12}, \quad (6.14)$$

where $H(q^2)$ is defined by (the last equality is taken from Gradshteyn and Ryzhik 1980):

³⁵One might wonder if the possible dependence of the linear mass density with azimuth contributes to these results, to the order in ϵ aimed at. However, this is not the case. In any case, such contributions would not affect the results of Eq. (6.12) to (6.14).

³⁶These approximations are made in the computations of all perturbations in the rest of the paper.

$$H(q^2) \equiv \frac{1}{2\pi q} \int_{-\pi}^{\pi} \frac{\cos u}{1 - q \cos u} du = \frac{1 - (1 - q^2)^{1/2}}{q^2(1 - q^2)^{1/2}}. \quad (6.15)$$

These equations are of course also valid in the case $m = 0$. The only restriction comes from the constraint $\Delta a_{12} \ll a$, so that they cannot be used to compute the axisymmetric contribution of the self-gravity of wide rings (like Saturn's rings). However, this contribution can be included, if needed, in the computation of Ω_a and κ_a , so that this limitation is not essential.

6.2 Satellite perturbations

We are now going to compute the averaged perturbation generated by one Fourier component of the satellite potential Eq. (4.37). The perturbing potential of the satellite at location r, θ and time t reduces to:

$$\phi_s = \Phi_{mk}(r/a_s) \cos m(\theta - \Omega_p t). \quad (6.16)$$

The derivatives of this potential give the components of the perturbing acceleration, which can be evaluated along a ring streamline of elements a, ϵ, Δ , and expanded to first order in ϵ with the help of Eqs. (4.62) and (4.63). After these manipulations, one obtains:

$$R_s = - \frac{d\Phi_{mk}}{da} (\cos M \cos m\Delta + \sin M \sin m\Delta), \quad (6.17)$$

$$\begin{aligned} S_s = & m \frac{\Phi_{mk}}{a} (\sin M \cos m\Delta - \cos M \sin m\Delta) \\ & - m \left(\frac{d\Phi_{mk}}{da} - \frac{\Phi_{mk}}{a} \right) \epsilon (\cos M \sin M \cos m\Delta - \cos^2 M \sin m\Delta) \\ & + 2m^2 \frac{\Phi_{mk}}{a} \epsilon (\sin M \cos M \cos m\Delta + \sin^2 M \sin m\Delta), \end{aligned} \quad (6.18)$$

where the relation $M = m(\varphi - \Omega_p t) + m\Delta$ has been used, and where Φ_{mk} has been evaluated at a . Inserting these results into the perturbation equations and averaging over φ yields:

$$\left(\frac{da}{dt} \right)_s = n_a a (m - 1) \epsilon \frac{a \Psi_{mk}}{GM_p} \sin m\Delta, \quad (6.19)$$

$$\left(\frac{d\epsilon}{dt} \right)_s = -n_a \frac{a \Psi_{mk}}{2GM_p} \sin m\Delta, \quad (6.20)$$

$$\left(\frac{d\varpi}{dt} \right)_s = \frac{n_a}{\epsilon} \frac{a \Psi_{mk}}{2GM_p} \cos m\Delta, \quad (6.21)$$

where one has defined

$$\Psi_{mk} \equiv a \frac{d\Phi_{mk}}{da} + 2m\Phi_{mk}. \quad (6.22)$$

The question of the effect of multiple resonant terms is complex and not addressed in these notes. The interested reader is referred to Borderies et al. (1983a) and Goldreich and Tremaine (1981).

6.3 Pressure tensor

The radial and tangential perturbing accelerations due to the ring pressure tensor are given in Eqs. (3.17) and (3.18). However, it is preferable for our purposes to derive the perturbing acceleration produced on a streamline of mass M by the material outside it.

The pressure tensor captures the effect of collisions of one streamline on its neighbors. The vertically integrated acceleration produced on any streamline in the continuum limit reads:

$$R_{vis} = -\frac{1}{a\sigma_0} \frac{\partial a P_{rr}}{\partial a} + \mathcal{O}(\epsilon), \quad (6.23)$$

$$S_{vis} = -\frac{1}{a^2\sigma_0} \frac{\partial a^2 P_{r\theta}}{\partial a} + \mathcal{O}(\epsilon), \quad (6.24)$$

The only subtlety here is that the streamline i boundaries lie at $(a_i + a_{i\pm 1})/2$; we have seen in section 5 that the pressure tensor depends on azimuth only through M' , which therefore differs from M'_i at these two boundaries. In the continuum limit, a similar problem arises, and the angular average needs an integration by part before it can be performed $\langle R \cos M \rangle = \langle 1/\sigma_0 \partial P_{rr} / \partial a \cos M \rangle = \langle 1/\sigma_0 [\partial P_{rr} \cos M / \partial a + (dm\Delta/da) P_{rr} \sin M] \rangle$.

Both the discretized and continuum approaches lead to the same result and the phase-averaged perturbation equations read

$$\left(\frac{da_i}{dt} \right)_{vis} = -\frac{4\pi}{an_a M_i} \Delta^\pm (a^2 a_{r\theta}), \quad (6.25)$$

$$\left(\frac{d\epsilon_i}{dt} \right)_{vis} = \frac{2\pi}{n_a M_i} \left[-\Delta^\pm (t_1 \cos \gamma + t_2 \sin \gamma) + (t_1^i \sin \gamma_i - t_2^i \cos \gamma_i) \Delta^\pm (m\Delta) \right], \quad (6.26)$$

$$\left(\frac{d\varpi_i}{dt} \right)_{vis} = \frac{2\pi}{n_a \epsilon_i M_i} \left[\Delta^\pm (t_1 \sin \gamma - t_2 \cos \gamma) + (t_1^i \cos \gamma_i + t_2^i \sin \gamma_i) \Delta^\pm (m\Delta) \right], \quad (6.27)$$

where M_i is the mass of streamline i , $\Delta X \equiv X^{i,i+1} - X^{i-1,i}$ and X^{ij} is evaluated at the boundary between streamlines i and j [i.e. in $(a_i + a_j)/2$, $|\Delta a|$ being the inter-streamline distance]; t_1, t_2 and $a_{r\theta}$ are the quantities introduced in Eqs. (5.28) through (5.31).

This results differs from Borderies et al. (1983a), Borderies et al. (1985) and Borderies et al. (1986) in several respects. First, σ_0 has been included here in the pressure tensor components. The rationale for this difference is that the full pressure tensor divergence defines the acceleration on a fluid particle and is therefore included in the difference $\Delta^\pm X$. This correction is unimportant in the WKB limit of Borderies et al. (1986) and in the nearly incompressible limit of Borderies et al. (1985). Also, Eqs (6.26) and (6.27) include a contribution —

the $\Delta^\pm(m\Delta)$ term — that is missing from the various BGT papers. This term provides in fact the dominant stress tensor contribution in the tight-winding approximation that is relevant for density waves; BGT were nevertheless able to recover the correct result from the other term by an (incorrect) non-local approximation to γ . Finally, factors a, a^2 have been pulled out of Eqs. (6.26) and (6.27), which are relevant only for perturbed flows, but not from Eq. (6.25), which applies to circular flows as well and where this dependence is important.

6.4 Mass, energy, and angular momentum budget of ring systems:

The question of energy dissipation and viscous angular momentum transport has been addressed in sec V. Here, we wish to derive more general expressions, in Eulerian variables (a, φ) . Furthermore, as we are mostly interested in radial transport, all the following expressions will be integrated over φ . For this purpose, we note $\langle X \rangle$ the azimuthal average of any quantity X . We have

$$\langle X \rangle = \frac{1}{2\pi} \int_0^{2\pi} d\varphi X = \frac{1}{2\pi} \int_0^{2\pi} dM X = \frac{1}{2\pi} \int_0^{2\pi} dM' X, \quad (6.28)$$

so that this definition is in agreement with the one used in section 5; note also that all the perturbation equations of the previous sections should more properly have been written in this bracket notation.

The three quantities we are interested in are the ring unperturbed surface density σ_0 , and the energy \mathcal{E} and angular momentum \mathcal{H} per unit unperturbed radial length a ,

$$\mathcal{E} = 2\pi a \sigma_0 E, \quad (6.29)$$

$$\mathcal{H} = 2\pi a \sigma_0 H. \quad (6.30)$$

By definition, these are azimuthally averaged quantities. In this section we depart from the semi-Lagrangian approach adopted so far to adopt a semi-Eulerian one instead. As such, we are interested in the time evolution in (a, φ) coordinates instead of using these quantities as Lagrangian labels. The main reason for this departure is that conserved quantities provide not only constraints on the dynamics, but also lead to a powerful amplitude equation for density waves. Note that, as any quantity $X = X(a, \varphi, t)$, one can always write

$$\frac{dX}{dt} = \frac{\partial X}{\partial t} + \frac{da}{dt} \frac{\partial X}{\partial a} + \frac{d\varphi}{dt} \frac{\partial X}{\partial \varphi}. \quad (6.33a)$$

The equation of conservation of mass is obtained from Eq. (3.16) either by change of variables or by more direct means and reads:

$$\frac{\partial \sigma_0}{\partial t} + \frac{1}{a} \frac{\partial}{\partial a} \left(a \sigma_0 \frac{da}{dt} \right) + \frac{1}{a} \frac{\partial}{\partial \varphi} \left(a \sigma_0 \frac{d\varphi}{dt} \right) = 0, \quad (6.31)$$

and yields, after azimuthal average,

$$\frac{\partial \sigma_0}{\partial t} + \frac{1}{a} \frac{\partial}{\partial a} \left(a \sigma_0 \left\langle \frac{da}{dt} \right\rangle \right) = 0. \quad (6.32)$$

Note that the designation of unperturbed surface density for σ_0 is somewhat improper because it evolves due to the radial drift that the perturbations (in particular the ring internal stress) induce.

The equations for the ring energy \mathcal{E} and angular momentum \mathcal{H} are most easily derived in integrated form. First, note that for any quantity X , using the mass conservation constraint Eq. (6.31), one has

$$a \sigma_0 \frac{dX}{dt} = \frac{\partial a \sigma_0 X}{\partial t} + \frac{\partial}{\partial a} \left(a \sigma_0 X \frac{da}{dt} \right) + \frac{\partial}{\partial \varphi} \left(a \sigma_0 X \frac{d\varphi}{dt} \right), \quad (6.33b)$$

so that after integration between two unperturbed radii³⁷ a_1 and a_2 and azimuthal average, one obtains (assuming X independent of φ and defined per unit mass such as E or H)

$$\begin{aligned} \int_{a_1}^{a_2} da \frac{\partial}{\partial t} (2\pi a \sigma_0 X) &= - \int_{a_1}^{a_2} da \frac{\partial}{\partial a} \left(2\pi a \sigma_0 X \left\langle \frac{da}{dt} \right\rangle \right) \\ &+ \int_{a_1}^{a_2} da 2\pi a \sigma_0 \left\langle \frac{dX}{dt} \right\rangle_{pert}. \end{aligned} \quad (6.34)$$

We can apply this result to the computation of the equations of evolution of \mathcal{E} and \mathcal{H} , by noting that³⁸

$$\frac{dE}{dt} = \frac{\Omega^2 a}{2} \frac{da}{dt}, \quad (6.35)$$

$$\frac{dH}{dt} = \frac{1}{2} \Omega a \frac{da}{dt} - \Omega a^2 \epsilon \frac{d\epsilon}{dt} = rS. \quad (6.36)$$

Let us consider first the perturbations induced by the satellite. Note that as the potential Eq. (6.16) is uniformly rotating at angular speed Ω_p , the change in specific energy and angular momentum are related by Jacobi's constant, and

$$\left\langle \frac{dE}{dt} \right\rangle_{sat} - \Omega_p \left\langle \frac{dH}{dt} \right\rangle_{sat} = 0. \quad (6.37)$$

From Eqs. (6.35) and (6.19), one has

$$\int_{a_1}^{a_2} da 2\pi a \sigma_0 \left\langle \frac{dE}{dt} \right\rangle_{sat} = \Omega_p \int_{a_1}^{a_2} da \pi m a \sigma_0 \epsilon \Psi_{mk} \sin m\Delta = \Omega_p \int_{a_1}^{a_2} da \mathcal{T}_s, \quad (6.38)$$

where $\mathcal{T}_s \equiv 2\pi a \sigma_0 \langle dH/dt \rangle_{sat} = \pi m a \sigma_0 \epsilon \sin m\Delta$ is the torque density due to the satellite.

³⁷This integration is very handy to tackle the change of variable $(r\theta)$ to (a, φ) for the pressure tensor contribution.

³⁸ $(\Omega_a/\kappa_a)^2 \epsilon^2 \simeq \epsilon^2$ consistently with earlier simplifications, but we keep the correct J_k terms to zeroth order in eccentricity.

Let us now consider the contribution of the ring self-gravity. The self-gravitational potential is also uniformly rotating with angular speed Ω_p , so that the changes in specific energy and angular momentum are again related by Jacobi's constant. It is useful to introduce the rate of transfer of specific energy (resp. specific angular momentum) L_E^{sg} (resp. L_H^{sg}) from all streamlines with radii $a_1 < a$ on all streamlines of radii $a_2 > a$ (which is the opposite of the rate of transfer from $a_2 > a$ on $a_1 < a$). By definition, and from Eq. (6.12) and (6.13), one has

$$L_E^{sg} = \Omega_p L_H^{sg} = -4\pi Gm\Omega_p \int_0^a da_1 \sigma_0(a_1) a_1 \epsilon_1 \int_a^{+\infty} da_2 \sigma_0(a_2) a_2 \times \frac{H(q_{12}^2) q_{12} \sin \gamma_{12}}{a_1 - a_2}. \quad (6.39)$$

The first equality follows from Eq. (6.12) by noting that $\Omega_p = (m-1)\Omega^{39}$ or simply by noting that the self-gravitational potential is stationary in the rotating frame so that Jacobi's integral applies.

With this definition, one easily checks that

$$\int_{a_1}^{a_2} da \, 2\pi a \sigma_0 \left\langle \frac{dE}{dt} \right\rangle_{sg} = -L_E^{sg}(a_2) + L_E^{sg}(a_1) = - \int_{a_1}^{a_2} \frac{\partial}{\partial a} L_E^{sg}, \quad (6.40)$$

$$\int_{a_1}^{a_2} da \, 2\pi a \sigma_0 \left\langle \frac{dH}{dt} \right\rangle_{sg} = -L_H^{sg}(a_2) + L_H^{sg}(a_1) = - \int_{a_1}^{a_2} \frac{\partial}{\partial a} L_H^{sg}, \quad (6.41)$$

so that L_E^{sg} and L_H^{sg} are energy and angular momentum luminosities. The preceding expressions are correct only if $|a_1 - a|, |a_2 - a| \ll a$, a condition which is satisfied in all cases of interest.

We can finally compute the contribution of the ring internal stress, which is somewhat more delicate to handle. First, we cannot use the discrete equations of section 6.3 as the equation for a keeps only the leading order term, whereas, as we shall see now, energy dissipation depends on the next-to-leading order terms. Instead, we revert to the continuous versions of components of the perturbing acceleration as given in Eqs. (3.17) and (3.18). Expressing the various derivatives in terms of $\partial/\partial a$ and $\partial/\partial\varphi$, and after some integrations by part, one obtains to leading orders in ϵ

$$\int_{a_1}^{a_2} da \, 2\pi a \sigma_0 \left\langle \frac{dE}{dt} \right\rangle_{vis} = \int_{a_1}^{a_2} da \left[-\frac{\partial L_E^{vis}}{\partial a} + \pi\Omega a(2qt_1 - 3a_{r\theta}) \right], \quad (6.42)$$

$$\int_{a_1}^{a_2} da \, 2\pi a \sigma_0 \left\langle \frac{dH}{dt} \right\rangle_{vis} = - \int_{a_1}^{a_2} da \frac{\partial L_H^{vis}}{\partial a}, \quad (6.43)$$

where L_E^{vis} and L_H^{vis} are defined by

³⁹For $m \neq 1$.

$$L_E^{vis} = 2\pi\Omega a^2 [a_{r\theta} + m\epsilon(2c_{r\theta} - s_{\theta\theta}) \cos \gamma + m\epsilon(2s_{r\theta} + c_{\theta\theta}) \sin \gamma + \epsilon(s_{rr} \cos \gamma - c_{rr} \sin \gamma)], \quad (6.44)$$

$$L_H^{vis} = 2\pi a^2 [a_{r\theta} + m\epsilon(2c_{r\theta} - s_{\theta\theta}) \cos \gamma + m\epsilon(2s_{r\theta} + c_{\theta\theta}) \sin \gamma - 2\epsilon(c_{r\theta} \cos \gamma + s_{r\theta} \sin \gamma)]. \quad (6.45)$$

The terms of order ϵ are negligible in front of $a_{r\theta}$ but note that their derivatives may be comparable to $2qt_1 - 3a_{r\theta}$ in Eq. (6.42). It is nevertheless legitimate to neglect them, as these two contributions are of a different qualitative nature: the former conserve energy and angular momentum, while the latter dissipate energy. Small energy and angular momentum redistribution terms do not affect the long term evolution, but small dissipation does. These terms are kept however as they are needed for part of the concluding discussion of section 7.2.3.

When these terms are neglected, L_H^{vis} reduces to the quantity introduced in Eq. (5.82) and $L_E^{vis} = \Omega L_H^{vis}$. Note that the second term on the right-hand side of Eq. (6.42) represents the rate of dissipation of macroscopic energy, and is equal to the rate of dissipation of energy in collisions as computed in Eq. (5.79).

We are now in position to write down the equations of evolution of energy and angular momentum in local form. Introducing

$$L_E^c = 2\pi a \sigma_0 E \left\langle \frac{da}{dt} \right\rangle, \quad (6.46)$$

$$L_H^c = 2\pi a \sigma_0 H \left\langle \frac{da}{dt} \right\rangle, \quad (6.47)$$

one can finally express them as

$$\frac{\partial \mathcal{E}}{\partial t} + \frac{\partial}{\partial a} (L_E^c + L_E^{sg} + L_E^{vis}) = \Omega_p \mathcal{T}_s + \pi \Omega a (2qt_1 - 3a_{r\theta}), \quad (6.48)$$

$$\frac{\partial \mathcal{H}}{\partial t} + \frac{\partial}{\partial a} (L_H^c + L_H^{sg} + L_H^{vis}) = \mathcal{T}_s. \quad (6.49)$$

These equations express the fact that the change in \mathcal{E} and \mathcal{H} is due to flux terms on one hand (the advective, self-gravity and viscous fluxes) and to source and sink terms (the satellite and the ring internal stress).

Note that Eq. (6.47) is valid even for more general expressions of the satellite torque than the one derived here. This equation allows us to derive an important feature of the confinement of rings by satellites. A complete discussion of the shepherding process is outside the scope of this lecture, so that we will only briefly recall some essential facts.

It is well-known, for example, that the outer edges of the A and B rings of Saturn correspond to resonances with satellites, and it has been argued that the angular momentum exchanges between the satellite and the ring material at the edge is responsible for the survival of the edge against viscous diffusion (Borderies et al., 1982). The same thing is very likely to be true for all the known narrow rings (Goldreich and Tremaine, 1979a; Borderies et al., 1989).

In the case of Saturn’s F ring and Uranus’ ϵ ring at least, the two “shepherd” satellites bracketing each ring have been observed by the *Voyager* probes.

The process works as follows. As already mentioned in section 2, the gravitational interaction between a ring and a satellite results in an outward flow of angular momentum: from the ring to the satellite if the satellite lies outside the ring (in which case $T_s < 0$) and from the satellite to the ring if it lies inside (in which case $T_s > 0$). We have seen also in section 5.3.2 that for not too strongly perturbed rings, the viscous stress induces an outward transport of angular momentum, from the inner edge to the outer edge of a narrow ringlet, so that the ringlet tends to spread. The spreading will be halted when the angular momentum fluxes induced by the satellites will balance the flux due to the viscous stress. Such an equilibrium is possible, because the satellite torques decrease in absolute value when the distance between the ring and the satellite increases: therefore, if the satellite torque is too small, the ring will spread until it reaches the right magnitude; if it is too large, the ring will contract until the satellite torque and the viscous torque have again adjusted. Of course, this equilibrium is not permanent: the inner satellite loses angular momentum, while the other gains some, and they are repelled by the ring. However, as they are usually much more massive than the rings, one can expect that the system will survive in quasi-equilibrium much longer than the ring alone would. Nevertheless, the evolution time-scales computed from these angular momentum exchanges are still in general uncomfortably short.

Let us now turn to the implication of Eq. (6.47) for this scenario. Once the quasi-equilibrium just described is obtained, $\partial\mathcal{H}/\partial t \simeq 0$ and $L_H^c \simeq 0$. Ignoring for simplicity the self-gravity term, the integration of this equation from, say, the inner edge a_i to some radius a inside the ring yields $L_H^{vis}(a) = \int_{a_i}^a T_s da$ (a similar result holds for the outer edge). Taking the limit $a \rightarrow a_i$, one obtains $L_H^{vis}(a_i) = 0$, a natural result considering that the torque has only a finite density (we have assumed that there is no very low optical depth material outside the ring). As unperturbed rings have a positive viscous luminosity, this condition can only be satisfied if the rate of perturbation of the edge is high enough so that the condition of reversal of the angular momentum flux is reached. One sees again that such an equilibrium can be obtained and is stable: if the satellite perturbation on the edge is too small, the ring spreads and the edge moves towards the satellite, whose perturbation increases as it gets closer, until the right value is obtained. Note that angular momentum reversal is a necessary feature of the shepherding process (the same conclusion is reached from a discussion of ring energetics; see Borderies et al. 1984).

7 Applications to ring dynamics

In this section, we wish to apply the apparatus of the previous sections to actual ring dynamical problems: the model of self-gravity for the rigid precession of elliptic rings, and the description of linear and nonlinear density waves excited at Lindblad resonances with external satellites. These applications are provided only as examples of use of the formalism; therefore only the major aspects of these questions will be addressed, in order to keep the emphasis on physical issues. Two of the major applications of the formalism, the discussion

of the evolution of ring and satellites eccentricities, and the detailed discussion of the shepherding mechanism are not described here, although they are of great importance for ring-satellite system evolution. The reader is referred to the specialized literature (see, e.g. Goldreich and Tremaine 1980, 1981, and Borderies et al. 1982, 1989) on these topics.

7.1 The self-gravity model for elliptic rings

Most of the Uranian rings (in particular, the α , β , γ , δ and ϵ) and some of the Saturnian ringlets (e.g. the Titan and Huygens ringlets), which are all very narrow features – from a few kilometers to a few tens of kilometers wide for radii of the order of 10^5 kilometers – are known to be eccentric, as discussed in sections⁴⁰ IV.3.1 and IV.3.3. These rings share a number of interesting features: their apses are almost aligned (a small apsidal shift has been detected in some rings, in particular the α and β rings of Uranus); they also exhibit a positive difference of eccentricity between the outer and inner edge (except, maybe, the $m = 0$ mode of the γ ring). The basic observational and dynamical properties of the Uranian rings have been reviewed by Elliot and Nicholson (1984).

These structures are submitted to various dynamical effects. The planet quadrupole moment tends to destroy the observed apse, but this tendency can be balanced by the self-gravity of the ring (Goldreich and Tremaine, 1979a,b; see below). The internal stress also acts on the apse alignment and on the ring mean eccentricity, and produces some radial spreading of the ring. This spreading can be overcome by the action of satellites (see section 6), which also influence the evolution of the mean eccentricity. In this section, a simplified discussion of the dynamics of narrow ringlets will be presented, mostly taken from the analysis by Borderies et al. (1983a). First, the changes in epicyclic semimajor axes will be ignored, under the assumption that an equilibrium between viscous spreading and the action of the satellites has been reached. Second, the ring will be represented with only two streamlines with equal masses $M_1 = M_2 = M_0/2$. Small quantities are supposed to be ordered by two small parameters, p_1 and p_2 such that $p_1 \ll p_2 \ll 1$. The two streamlines have semimajor axes a_1 and a_2 , with $a_1 < a_2$. Consistently with the approximations performed in the previous sections, one defines $a = (a_1 + a_2)/2$, and assumes $a_1 = a_2 = a$ in the perturbation terms, except in the difference $\Delta a_{21} = \delta a$. The difference of eccentricity between the outer and inner edge $\Delta \epsilon_{21} \equiv \delta \epsilon$ is taken to be $O(p_1)$, whereas the mean eccentricity $\epsilon \equiv (\epsilon_1 + \epsilon_2)/2$ is $O(p_2)$, so that $\delta \epsilon/\epsilon \ll 1$, as observed. We also define $m\Delta = m(\Delta_1 + \Delta_2)/2$ and $\delta(m\Delta) = m(\Delta_2 - \Delta_1)$. Furthermore, as $q \sim 1$, $\delta a/a$ is $O(p_1)$, as is $\epsilon \delta(m\Delta)$. Typically, the eccentricities range from a few times 10^{-4} to 10^{-2} , whereas the eccentricity differences $\delta \epsilon$ vary from a few times 10^{-5} to a few times 10^{-4} , so that the approximation $p_1 \ll 1$ and $p_2 \ll 1$ are very well satisfied. On the other hand, $\delta \epsilon/\epsilon$ ranges from 0.03 to 0.5, so that the approximation $p_1/p_2 \ll 1$ is cruder but not critical. With these orderings, to leading order in the various small quantities, one has

$$q_{ij} \cos \gamma_{ij} = a \frac{\delta \epsilon}{\delta a}, \quad (7.1)$$

⁴⁰Many of these rings are also inclined, but for simplicity we set the inclination to zero.

$$q_{ij} \sin \gamma_{ij} = a\epsilon_j \frac{\delta(m\Delta)}{\delta a}, \quad (7.2)$$

$$q_{12}^2 = q_{21}^2 = q^2 = \left(\frac{a\delta\epsilon}{\delta a}\right)^2 + \left(a\epsilon \frac{\delta(m\Delta)}{\delta a}\right)^2, \quad (7.3)$$

$$\gamma_{12} - \gamma_{21} = \delta(m\Delta) \sim O(p_1/p_2). \quad (7.4)$$

We are now in position to derive the equations of evolution of our simplified system. First, note that the equation for $m\Delta_i$ is related to the equation of evolution of ϖ_e by the streamline condition $M = m(\varphi - \Omega_p t) + m\Delta$, so that

$$\frac{d(m\Delta_i)}{dt} = (1 - m)\Omega_i + m\Omega_p - \frac{d\varpi_i}{dt}. \quad (7.5)$$

Note that Eq. (7.5) generalizes Eq. (4.59) to the case where Δ is time dependent. By definition, $m\Delta_i$ contains only periodic terms; the secular terms are accounted for by Ω_p . From Eqs. (4.21), (4.22), (6.13), (6.14), (6.26) and (6.27) applied to the evolution of the eccentricity and apsidal shift of the two streamlines, one can derive the equations of the four quantities ϵ , $m\Delta$, $\delta\epsilon$, and $\delta(m\Delta)$. They read, to leading order in the various small quantities:

$$\frac{d\delta\epsilon}{dt} = (\Omega_{sg} - \lambda_2)\epsilon\delta(m\Delta) + \lambda_1\delta\epsilon, \quad (7.6)$$

$$\frac{d\delta(m\Delta)}{dt} = \delta\Omega_{plan} - (\Omega_{sg} - \lambda_2)\frac{\delta\epsilon}{\epsilon} + \lambda_1\delta(m\Delta), \quad (7.7)$$

$$\frac{d\epsilon}{dt} = -\frac{\Omega_{sg} - \lambda_2}{4}\delta\epsilon\delta(m\Delta), \quad (7.8)$$

$$\frac{d(m\Delta)}{dt} = m\Omega_p - \Omega_{plan}, \quad (7.9)$$

where Ω_{sg} , λ_1 , λ_2 , Ω_{plan} and $\delta\Omega_{plan}$ are quantities homogeneous to frequencies and defined by

$$\Omega_{sg} = \frac{n}{\pi} \frac{M_0}{M_p} \left(\frac{a}{\delta a}\right)^2 H(q^2), \quad (7.10)$$

$$\lambda_1 = \frac{2t_1}{qn\sigma_0(\delta a)^2}, \quad (7.11)$$

$$\lambda_2 = -\frac{2t_2}{qn\sigma_0(\delta a)^2}, \quad (7.12)$$

$$\Omega_{plan} = (m - 1)n + \frac{3}{2}J_2n \left(\frac{R_p}{a}\right)^2 \left[1 + \frac{m - 1}{2}\right], \quad (7.13)$$

$$\delta\Omega_{plan} = \left(\frac{3}{2}(m - 1)n + \frac{21}{4}J_2n \left(\frac{R_p}{a}\right)^2 \left[1 + \frac{m - 1}{2}\right]\right) \frac{\delta a}{a}. \quad (7.14)$$

In these equations, R_p is the equatorial radius of the planet, $n = (GM_p/a^3)^{1/2}$ and the surface density is related to the ring mass by $2\pi a\delta a\sigma_0 = M_0$. Ω_{sg} is

a characteristic frequency imposed by the self-gravity of the ring; for typical values of the ring surface density ($\sigma_0 \sim 50 \text{ g/cm}^2$), Ω_{sg}^{-1} is of the order of a few years to a few tens of years (e.g. ~ 9 years for the α ring). λ_1^{-1} and λ_2^{-1} are characteristic time-scales imposed by the ring internal stress. They are usually much longer than Ω_{sg}^{-1} ; e.g. assuming $t_1, t_2 \sim \sigma_0 v^2$ with $v \sim 1 \text{ mm/s}$, $\lambda_1^{-1} \sim 90$ years for the α ring. This reflects the fact that the ring internal stress produces a very weak force, even compared to the ring self-gravity. Finally, Ω_{plan} and $\delta\Omega_{plan}$ are frequencies imposed by the planet. For simplicity, terms smaller than J_2 have been neglected. Note that even the J_2 term is completely negligible for $m \neq 1$, in which case $\Omega_{plan} \sim n$ and $\delta\Omega_{plan} \sim n\delta a/a$. For $m = 1$ (i.e. purely elliptic modes), the only remaining contribution is that due to J_2 : $\Omega_{plan} \sim J_2 n$ and $\delta\Omega_{plan} \sim J_2 n\delta a/a$, so that these two quantities are 10^2 or 10^3 times smaller for $m = 1$ than for $m \neq 1$. It has been implicitly assumed that the right-hand sides of Eqs. (7.6) through (7.9) are linear in the unknowns. This is not true, as Ω_{sg} , λ_1 and λ_2 depend on q . However, q is always different enough from unity that the dependence of these three frequencies on q can be ignored, and this assumption is made in the remainder of this subsection. Note also that the contribution of the satellites has not been included, as the equations derived in section 6.2 apply for a single isolated resonance, whereas the cumulative effect of all resonances should be considered.

We are now in position to describe some simple consequences of Eqs. (7.6) through (7.9). Note first that Eq. (7.9) uncouples from the other three, and implies that $dm\Delta/dt$ is a constant. This constant must be equal to zero, in accordance with the interpretation of Ω_p as the rotation velocity of the pattern defined by the streamlines. Therefore, Eq. (7.9) is in fact the relation imposing Ω_p :

$$\Omega_p = \Omega_{plan}/m. \quad (7.15)$$

This shows that a narrow ring described by an $m \neq 1$ mode precesses at a rate $\sim n$, i.e. $\sim J_2^{-1}$ faster than a purely elliptic ($m = 1$) ring. This feature is a direct consequence of the dominance of the planet on the motions, Eq. (4.51).

Note also that the time-scale of evolution of ϵ is $\sim (p_2/p_1)^2$ longer than the time-scale of evolution of $\delta\epsilon$ and $\epsilon\delta(m\Delta)$. Therefore, we can look into the evolution of these last two quantities while assuming that ϵ is constant in time, in first approximation, which effectively uncouples Eq (7.8) from Eqs. (7.6) and (7.7). These two equations show that a narrow ring has an equilibrium configuration (i.e., $d\delta\epsilon/dt = 0$ and $d\delta(m\Delta)/dt = 0$) for

$$\frac{\delta\epsilon_0}{\epsilon} = \frac{(\Omega_{sg} - \lambda_2)\delta\Omega_{plan}}{\lambda_1^2 + (\Omega_{sg} - \lambda_2)^2} \simeq \frac{\delta\Omega_{plan}}{\Omega_{sg}}, \quad (7.16)$$

$$\delta(m\Delta)_0 = -\frac{\lambda_1}{\Omega_{sg} - \lambda_2} \frac{\delta\epsilon_0}{\epsilon} \simeq -\frac{\lambda_1}{\Omega_{sg}} \frac{\delta\epsilon_0}{\epsilon}, \quad (7.17)$$

where $\Omega_{sg} \gg \lambda_1, \lambda_2$ has been used in the second equalities. Furthermore, the general solution of Eqs. (7.6) and (7.7) is given by

$$\delta(m\Delta) = \delta(m\Delta)_0 + A \exp(\lambda_1 t) \cos[(\Omega_{sg} - \lambda_2)t + \varphi_0], \quad (7.18)$$

$$\delta\epsilon = \delta\epsilon_0 - \epsilon A \exp(\lambda_1 t) \sin[(\Omega_{sg} - \lambda_2)t + \varphi_0], \quad (7.19)$$

where A is an arbitrary (but small) amplitude. The general solution consists of oscillations around equilibrium, which are damped if the viscous coefficient $\lambda_1 < 0$, as has usually been assumed in the literature. This is the case in the dilute approximation, but we have seen in chapter V that the opposite is true for dense systems, at least for small values of q . Let us assume for the time being that $\lambda_1 < 0$, so that the system is driven to its equilibrium point described by Eqs. (7.16) and (7.17). Note that Eqs. (7.18) and (7.19) show that t_2 is a pressure-like coefficient, while t_1 has a viscous-like action on the system.

The meaning of Eq. (7.16) is not especially obvious in the compact form in which it is displayed. Let us for definiteness consider the case of an $m = 1$ mode. This equation then reduces to

$$\delta\epsilon_0 = \frac{21\pi\epsilon}{4} J_2 \frac{M_p}{M_0} \left(\frac{R_p}{a}\right)^2 \left(\frac{\delta a}{a}\right)^3 \frac{1}{H(q^2)}. \quad (7.20)$$

For $m \neq 1$, one obtains

$$\delta\epsilon_0 = \frac{3\pi(m-1)\epsilon}{2} \frac{M_p}{M_0} \left(\frac{\delta a}{a}\right)^3 \frac{1}{H(q^2)}. \quad (7.21)$$

One sees that these equations relate parameters describing the overall shape of the ring, a , δa , ϵ , $\delta\epsilon$ to the mass of the ring M_0 , and indeed this relation has been used in the literature to estimate the mass of the α , β , δ and ϵ rings of Uranus (the data analysis has not yield values for $\delta\epsilon$ for the other rings, due to problems which are only partly understood). Furthermore, as $\lambda_1 \ll \Omega_{sg}$, $\epsilon\delta(m\Delta)_0 \ll \delta\epsilon$, so that $q \simeq a\delta\epsilon/\delta a$, and $\gamma \simeq 0$. Therefore, the width of the ring, which is given by $W = J\delta a$ as a function of azimuth, has the same azimuthal behavior as the ring radius $r = (r_1 + r_2)/2$, so that $W \propto r$, as observed. Note also that these two relations predict $\delta\epsilon_0 > 0$ for $m > 0$, as observed. Because of these successes, the self-gravity model was for a long time widely regarded as the correct explanation of the rigid precession of narrow elliptic rings.

In what concerns the evolution of the eccentricity, note that Eq. (7.8) implies that $d\epsilon/dt \simeq -\Omega_{sg}\delta\epsilon_0\delta(m\Delta)_0 \sim \lambda_1(\delta\epsilon_0)^2/\epsilon < 0$ if $\lambda_1 < 0$, so that Borderies et al. (1983a) were motivated to assume that the observed eccentricities were the result of a balance between viscous damping and the excitation by the ring “shepherd” satellites.

Let us conclude this subsection with a number of comments. First, if λ_1 is positive, the oscillations of $\delta\epsilon$ and $\delta(m\Delta)$ are amplified instead of damped, and the eccentricity grows, as can be seen from our estimate $d\epsilon/dt \sim \lambda_1(\delta\epsilon_0)^2/\epsilon$. This behavior is characteristic of what is commonly referred to as viscous overstabilities⁴¹, and this argument was used by Borderies et al. (1985) to argue that such instabilities could as well be responsible for the eccentricities of the narrow rings. However, the outcome of the evolution of the eccentricity depends critically on the existence of the oscillations of $\delta\epsilon$ and $\delta(m\Delta)$, and on the necessary

⁴¹Viscous instabilities are axisymmetric motions; viscous overstabilities involve an oscillatory response.

change of sign of λ_1 (see section 5), so that, in fact, an initially circular ring cannot reach eccentricities $\epsilon \gg \delta\epsilon$, at least in the framework of the two-streamline model for narrow rings (Longaretti and Rappaport, 1995); note that both effects were ignored in the analysis by Papaloizou and Lin 1988). It remains to be seen if the same conclusion holds for more general models of narrow rings.

But the most important problem encountered by the self-gravity model arose after the *Voyager II* encounter with Uranus, which revealed that the mass of the rings deduced from Eqs. (7.20) and (7.21) was roughly underestimated by a factor of ~ 10 . The problem is particularly acute for the α and β ring (Goldreich and Porco, 1987). The first piece of evidence comes from the radio data, the analysis of which gives estimates of the ring surface densities. The other piece of evidence is connected to the existence of an unexpectedly extended hydrogen atmosphere around Uranus; this atmosphere is the source of an extra torque acting on the ring, that the shepherd satellites have to balance (in addition to the viscous torque) in order for the narrow rings to survive, but it turns out that this requirement also can only be satisfied for ring surface densities about ten times larger than the ones derived from Eqs. (7.20) and (7.21) (for more details about this point, see Goldreich and Porco 1987).

On the other hand, the analysis of the radio data relies on standard radiative transfer theory, which, applied to the Uranian ring, is known to give inconsistent results, most probably because the mean separation between ring particles is not small compared to the radio wavelengths. Thus, the derivation of the ring surface densities can possibly be in error, although this does not seem to be a likely possibility. Similarly, the density of hydrogen in Uranus atmosphere at the ring location is extrapolated from the density at inner locations, but major errors in the extrapolation procedure seem rather unlikely. On the theoretical side, the dynamical agents which can enforce rigid precession are not very numerous: the precession rates due to the satellites and smooth pressure terms seem far too small, and the possibility put forward by Goldreich and Tremaine (1979a) that the rigid precession might alternatively be enforced by shock-like phenomena appears to be inconsistent with the small observed apsidal shifts. In conclusion, the issue of the rigid precession of the narrow rings is still open at the time of writing.

7.2 Density waves at Lindblad resonances with external satellites

The two *Voyager* spacecrafts have discovered tens of density (and bending) wavetrains in Saturn's rings, mainly the A and B rings. These wavetrains share a number of striking characteristics. First, they are all associated with resonances with satellites, suggesting that density waves are stable in Saturn's rings (see below). Note that the reverse is not true, i.e. a number of the Lindblad resonances in Saturn's rings are not associated with density waves: some are associated with gaps, some others don't exhibit any peculiar behavior at all. The reason of this disparity is only partly understood (see below). For simplicity, and because of their practical importance, we will only consider density waves excited at inner Lindblad resonances with Saturn's satellites. These waves propagate from the resonance outwards (whereas bending waves propagate inwards). The wavelengths, of the order of a few kilometers or tens of kilometers, are much

smaller than the mean radii of the waves (of the order of 10^5 kilometers). Because the wavelength is so short compared to the radii, the winding of the density variations schematically displayed on Figure 3 is very high (much higher than represented) so that these waves appear as quasi-circular features on the *Voyager* images. Generally, the waves propagate over a few (or a few tens) of cycles before they are damped by the ring internal stress. The radial wavelength varies like the inverse of the distance to the resonance, so that it becomes shorter as the wave propagates outwards. For example, the Mimas 5:3 density wave radial optical depth profile is displayed on Figure 10. The form of the surface density Eqs. (4.69) and (4.73) is able to reproduce correctly this optical depth profile at constant azimuth and time for an appropriate (and in fact uniquely determined) choice of the functions involved (Longaretti and Borderies, 1986). The propagation of this wave is obviously nonlinear, i.e. the density contrast is large compared to the background density. Assuming $\tau \propto \sigma$, Eq. (4.69) yields $\tau_p/\tau_t = 1 - q/1 + q$ where τ_p and τ_t are the optical depths at the peaks and troughs of the wave. From the data of Figure 10 one sees that $q \lesssim 1$; a linear wave propagation would require $q \ll 1$. Note that by definition, the wavenumber k is given by

$$k = m \frac{d\Delta}{da} + \frac{d\gamma}{da}. \quad (7.22)$$

The surface density varies radially as $\sigma = \sigma_0/[1 - q \cos(\int k da + cst)]$, so that $\int_{peak}^{peak} k da \simeq k\lambda = 2\pi$, where λ is the wavelength.

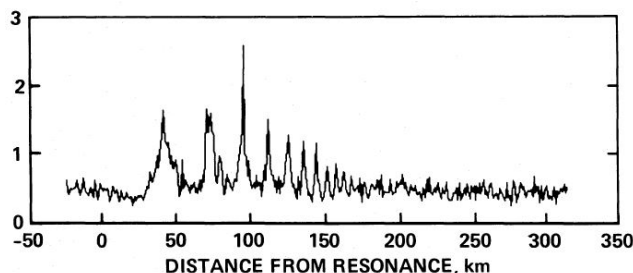


Figure 10: The radial variation of optical depth of the Mimas 5:3 density wave as a function of the distance to resonance (reproduced from Shu et al. 1985a).

The following discussion is self-contained, and no prior knowledge on the dynamics of density waves is required. However, some background on the usual Eulerian density wave linear theory at the introductory level of Shu (1984) is certainly helpful. The material of this section is mostly taken from the papers by Shu et al. (1985b,a); Borderies et al. (1985, 1986).

The analysis of density waves is performed in the framework of the WKBJ approximation (or tight-winding limit), which relies on the fact that the dominant contributions to the radial variations are due to the phase and not to the amplitude of the quantities under consideration. In this approximation, the dominant contribution to $J = \partial r / \partial a$ is due to the derivative of Δ and not to the derivative of ϵ , so that

$$ma\epsilon \frac{d\Delta}{da} \gg \frac{da\epsilon}{da}, \quad (7.23)$$

and, as a consequence,

$$\gamma \simeq \frac{\pi}{2}. \quad (7.24)$$

The wavenumber reduces to $k = md\Delta/da$, and is related to q and ϵ by⁴²

$$q|\sin \gamma| = q = |k|a\epsilon. \quad (7.25)$$

Note that for the wave of Figure 10, the wavelength is of the order of 10 km, so that $\epsilon \sim q/ka \sim 1/ka \sim 10^{-5}$ for $a \sim 10^5$ km, and the approximation $\epsilon \ll 1$ is remarkably good. It is also possible to check the validity of the WKBJ approximation from these data. The wave propagates over a radial distance $\Delta a_w \simeq 200$ km, so that $da\epsilon/da \sim -a\epsilon/\Delta a_w$. Therefore,

$$\left| \frac{da\epsilon/da}{ma\epsilon d\Delta/da} \right| \sim \frac{a\epsilon/\Delta a_w}{ka\epsilon} = \frac{\lambda}{2\pi\Delta a_w} \ll 1. \quad (7.26)$$

A general condition of validity of the WKBJ approximation will be derived below.

Our purpose is to describe how the wave is excited by the satellite and damped by the ring internal stress, and to estimate the exchanges of angular momentum between the wave and the satellite, which can be done in principle once a wave equation has been derived. However, let us derive first the wave dispersion relation, as quite a number of aspects of the wave propagation can be understood directly from it.

7.2.1 Dispersion relation

The dispersion relation is an equation relating the wave temporal frequency, here $\omega = m\Omega_p$ to its spatial frequency k . This relation is most directly obtained from the condition of existence of the wave, Eq. (4.59), which states that the resonance condition must be satisfied throughout the wave region. Eq. (4.59) can be recast as:

$$\left(\frac{d\varpi}{dt} \right)_{sg} + \left(\frac{d\varpi}{dt} \right)_{vis} + \left(\frac{d\varpi}{dt} \right)_{sat} = \kappa - m(\Omega - \Omega_p). \quad (7.27)$$

Let us evaluate the various terms on the left-hand side in the tight-winding limit. From Eq. (6.14), one has

$$\left(\frac{d\varpi}{dt} \right)_{sg} = \frac{2n_a a^2}{M_p \epsilon} \int_0^{+\infty} da' \frac{\sigma_0(a') H(q_{aa'}^2) q_{aa'} \cos \gamma_{aa'}}{a - a'}. \quad (7.28)$$

⁴²Note that q is positive by definition, but that k can be either positive or negative.

Furthermore, we expect that the largest contribution to the self-gravity integral comes from regions with $|a - a'| \ll a$, so that we may take $m\Delta(a') = m\Delta + k(a' - a)$; in this approximation Eq. (6.10) reads

$$q_{aa'} \exp(i\gamma_{aa'}) = ika\epsilon \exp(-iu) \frac{\sin u}{u}, \quad (7.29)$$

where we have defined

$$u = \frac{k(a - a')}{2}. \quad (7.30)$$

Inserting this result in Eq. (7.28) yields, treating σ_0 as a constant over the region of contribution of the integrand (with $n_a = (GM_p/a^3)^{1/2}$)

$$\left(\frac{d\varpi}{dt}\right)_{sg} = \frac{\pi G\sigma_0|k|}{n_a} C(q), \quad (7.31)$$

where

$$C(q) = \frac{4}{\pi} \int_0^\infty du \frac{\sin^2 u}{u^2} H\left(q^2 \frac{\sin^2 u}{u^2}\right). \quad (7.32)$$

Note that $C(q) \rightarrow 1$ as $q \rightarrow 0$, i.e. for linear waves. In general, $C(q)$ is a factor of order unity. Note also that most of the contribution to this integral comes from regions with $u \lesssim 1$, i.e. with $(|a - a'|/a \lesssim 1/|k|a \ll 1)$, as expected.

The contribution of the pressure term is computed from the results of section 6.3.; the dominant term in the tight-winding approximation comes from $\Delta^\pm(m\Delta)$ term with $\gamma_i \simeq \pi/2$, i.e.:

$$\left(\frac{d\varpi_i}{dt}\right)_{vis} = \frac{2\pi}{n_a\epsilon_i M_i} [t_2^i \Delta^\pm(m\Delta)], \quad (7.33)$$

where $t_i^{jk}(q, \langle\tau\rangle)$ is evaluated $q = q_{jk}$ [i.e. at $a = (a_j + a_k)/2$]. Taking the limit $\Delta a \rightarrow 0$ and using $q = a\epsilon k = a\epsilon(dm\Delta/da)$, one finally obtains

$$\left(\frac{d\varpi}{dt}\right)_{vis} = \frac{k^2 t_2}{n_a \sigma_0 q}. \quad (7.34)$$

Finally, let us argue that the contribution of the satellite can be neglected. From Eq. (6.21), and from the tight-winding condition $|k|a\epsilon = q \sim 1$, one has

$$\left|\frac{\dot{\varpi}_{sat}}{\dot{\varpi}_{sg}}\right| \lesssim \frac{|\Psi_{mk}|}{2\pi G\sigma_0 a}. \quad (7.35)$$

Typically in Saturn's rings, this quantity is ~ 0.1 to 0.5 , so that neglecting the satellite contribution is not quite correct, but not too bad.

Finally, the nonlinear dispersion relation reads

$$n_a[\kappa - m(\Omega - \Omega_p)] - \pi G\sigma_0|k|C(q) - \frac{k^2 t_2}{\sigma_0 q} = 0. \quad (7.36)$$

The dispersion relation expresses the fact that the ring self-gravity and internal stress adjust the fluid particles precession rate in order to maintain the resonance relation, $\kappa = m(\Omega - \Omega_p)$, throughout the wave region. Note that by allowing negative values of m , this dispersion relation is valid for both inner ($m > 0$) and outer ($m < 0$) Lindblad resonances.

Although q reaches values of order unity, it is always small enough that $C(q) \gtrsim 1$. It is therefore interesting to look into the linear limit of Eq. (7.36). For simplicity, we will assume that the ring behaves as a Newtonian fluid obeying an isothermal equation of state $p = c_0^2 \sigma$ where c_0 is the isothermal sound speed (of the order of the velocity dispersion). This approximation for the pressure tensor is rather crude, but we will see shortly that the viscous term can be neglected in the dispersion relation for the problem of interest here, so that the exact form of t_2 is not essential. In this approximation, t_2 can be computed from Eqs. (5.29) and (5.39), and reads

$$t_2 = -\sigma_0 c_0^2 \frac{1 - (1 - q^2)^{1/2}}{q(1 - q^2)^{1/2}}, \quad (7.37)$$

which reduces to $t_2 = -\sigma_0 c_0^2 q/2$ in the linear limit (note that $2k^2 t_2 / \Omega \sigma_0 q \sim k^2 c^2$, so that the following results are relevant even if the isothermal equation of state does not apply). In this approximation, the dispersion relation reads

$$2\Omega[\kappa - m(\Omega - \Omega_p)] - 2\pi G \sigma_0 |k| + k^2 c_0^2 = 0, \quad (7.38)$$

which is the standard density wave dispersion relation, except for the first term on the left-hand side which should read $\kappa^2 - m^2(\Omega - \Omega_p)^2$ (for a simple fluid mechanical derivation, see Shu 1984). This difference is due to the approximations we have made in the preceding sections, where $\kappa \simeq \Omega \simeq n_a \simeq m(\Omega - \Omega_p)$ was assumed for a nearly Keplerian disk in the vicinity of an inner Lindblad resonance with a satellite, except in terms involving the difference between κ and $m(\Omega - \Omega_p)$.

It is interesting to rederive Toomre's stability criterion from the exact linear dispersion relation. Stability is insured if the temporal frequency of the wave ω contains no imaginary part, i.e. if $(\omega - m\Omega)^2 > 0$, which implies $\kappa^2 - 2\pi G \sigma_0 |k| + k^2 c_0^2 > 0$. This expression has a minimum for $|k| = \pi G \sigma_0 / c_0^2$, and it is easy to check that this minimum is positive if

$$Q \equiv \frac{c\kappa}{\pi G \sigma_0} > 1. \quad (7.39)$$

A very similar criterion was originally derived by Toomre (1964) for the dynamics of spiral galaxies. Toomre's Q parameter expresses the fact that the ring (or stellar) velocity dispersion can stabilize the medium against the spontaneous generation of density waves. In rings, $Q \sim 1$ but the exact value is not very well known due to the uncertainty on the magnitude of the velocity dispersion. Shu 1984 has pointed out that the ring finite thickness and the existence of a finite size of particles can also have a stabilizing effect, and the associated criteria are closely related to Eq. (7.39). Indeed, as the ring thickness $H \sim c/\kappa$, Eq. (7.39)

can be recast as $H > \pi G \sigma_0 / \kappa^2$ (but this argument is *at most* dimensional: the ring can have a finite thickness even in the absence of velocity dispersion, due to the finite particle size); the criterion on the particle size is the same (note that the size of the largest particles of the distribution in Saturn's rings is comparable to the ring thickness). Presumably, the rings are stable due to all these effects, although we are still unable to decide on the basis of the available data if the stability criteria are satisfied.

An interesting consequence can be derived from the linear dispersion relation, Eq. (7.38). Solving for $|k|$, one obtains

$$|k| = \frac{\pi G \sigma_0}{c_0^2} \pm \left[\left(\frac{\pi G \sigma_0}{c_0^2} \right)^2 - \frac{2\Omega(\kappa - m(\Omega - \Omega_p))}{c_0^2} \right]^{1/2}. \quad (7.40)$$

The + sign corresponds to the short waves and the – sign to the long ones. Note that the loci of constant surface density (for example the wave crests) correspond to constant values of $m(\theta - \Omega_p t) + \int k da$, so that the isodensity curves $r(\theta)$ are solutions of the differential equation $k(dr/d\theta) + m = 0$. Consider inner Lindblad resonances for definiteness ($m > 0$); thus, for $k > 0$, $dr/d\theta < 0$ and the wave is trailing (it curves in the counter-rotation direction), while the opposite is true for $k < 0$ and the wave is leading. A similar conclusion holds at outer resonances ($k < 0$ corresponds to trailing waves there).

The short waves have a very high wavenumber at resonance and therefore oscillate quite rapidly, preventing an efficient coupling with the satellite potential, which varies smoothly with radius at the resonance. As a consequence, the satellite is not expected to excite short waves⁴³; on the contrary, as long waves have $|k| \rightarrow 0$ at the resonance, they are expected to couple much more efficiently with the satellite. On the basis of these arguments, the short waves are ignored in the remainder of this section. In the region of propagation, $|k| > 0$, which implies $\kappa - m(\Omega - \Omega_p) > 0$. In other words, denoting a_R is the resonance radius implicitly defined by the resonance relation $\kappa = m(\Omega - \Omega_p)$, the long trailing waves propagate outside the ILR (inner Lindblad resonance) and are evanescent inside, whereas the long trailing waves propagate inside the OLR (outer Lindblad resonance) and are evanescent outside⁴⁴. This is consistent with the directions of propagation derived from the wave group velocity. Toomre (1969) and Dewar (1972) have shown in the context of the linear density wave theory of spiral galaxies that the group velocity of the waves is given by⁴⁵ $c_g = \partial\omega/\partial k$, where $\omega = m\Omega_p$. Consequently, long leading waves are not expected to be excited at the Lindblad resonance by the satellite, as they would enter a region of

⁴³A more formal argument can be found in Goldreich and Tremaine (1979c), pp. 861 and 862.

⁴⁴Furthermore, long trailing waves propagating from Lindblad resonances are reflected on the corotation radius as a short leading waves (Goldreich and Tremaine 1978a, and Lin and Lau 1979). This process is not relevant to planetary rings, because the waves damp much before they reach the corotation radius.

⁴⁵The demonstration of this seemingly natural result would take us too far afield to be repeated here. The most elegant derivation is based on the use of a phase-averaged Lagrangian density of the wave, as in Dewar (1972), which shows at the same time that the conserved quantity associated with the invariance with rotation is (not surprisingly) the phase averaged angular momentum density, and that this quantity is transported radially at the group velocity of the wave. For a general introduction to the use of averaged Lagrangian densities in wave theory, see Whitham (1974), chapters 11 and 14.

evanescence (see also Goldreich and Tremaine 1979c and Shu 1984). Therefore, only long trailing waves are discussed in the remainder of these notes; $|m| \neq 1$ is also assumed for definiteness⁴⁶.

In the vicinity of the resonance, $\kappa - m(\Omega - \Omega_p) \simeq [3(m-1)\Omega_R/2](a - a_R)/a_R$, so that $(\pi G\sigma_0/c_0^2)^2 \gg 2\Omega[\kappa - m(\Omega - \Omega_p)]$ occurs for

$$\frac{|a - a_R|}{a_R} \ll \frac{\pi^2 G^2 \sigma_0^2}{3c_0^2 |m-1| \Omega_R^2} = \frac{1}{3Q^2 |m-1|} \sim 1, \quad (7.41)$$

a condition very largely satisfied. Therefore, keeping the leading order term in a Taylor expansion of Eq. (7.40) for long waves yields $2\pi G\sigma_0|k| = 2\Omega[\kappa - m(\Omega - \Omega_p)]$, i.e., the pressure term can be neglected for long waves near a Lindblad resonance. The same feature is obviously true of the nonlinear dispersion relation, as $C(q) \gtrsim 1$, so that Eq. (7.36) reduces to ($m \neq 1$)

$$|k|C(q) = \frac{3}{2\pi}(m-1) \left(\frac{M_p}{\sigma_0 a_R^2} \right) \left(\frac{a - a_R}{a_R} \right) \frac{1}{a_R}. \quad (7.42)$$

As the wavelength $\lambda \simeq 2\pi/|k|$, this relation predicts that $\lambda \propto 1/(a - a_R)$, as observed. As the coefficient of proportionality depends on σ_0 , the dispersion relation has been used in the analysis of density wave profiles to estimate the ring surface density.

Notice finally that $|k| \rightarrow 0$ as $a \rightarrow a_R$, so that the tight-winding condition $|ka| \gg 1$, which was used in the derivation of the dispersion relation, breaks down too close to the resonance. To estimate quantitatively the region of validity of the tight-winding condition, let us first compute the value λ_1 of the first wavelength from Eq. (7.42), and from the constraint $\int_{a_R}^{a_R + \lambda_1} |k| da = 2\pi$, taking $C(q) = 1$. One obtains

$$\frac{\lambda_1^2}{a_R^2} = \frac{8\pi^2}{3|m-1|} \left(\frac{\sigma_0 a_R^2}{M_p} \right). \quad (7.43)$$

It is customary to introduce a small parameter⁴⁷ δ , defined by

$$\delta \equiv \frac{2\pi\sigma_0 a_R^2}{3(m-1)M_p} \sim \frac{M_{ring}}{M_p}. \quad (7.44)$$

This parameter is typically $\sim 10^{-8}$. In terms of δ , one has $\lambda_1/a_R = (4\pi|\delta|)^{1/2} \sim 10^{-4}$, which implies $\lambda_1 \sim 10$ km, as observed. Note that for disks in general, the tight-winding condition, $|k|a \gg 1$, or equivalently, $\lambda_1/a \ll 1$, is valid as long as $(M_{disk}/M_*)^{1/2} \ll 1$, where M_* is the mass of the central object (star, black hole...), a condition which is not very well satisfied in spiral galaxies. Now, from the dispersion relation and from the expression of λ_1 , the constraint $|ka| \gg 1$ reads

$$4\pi \left(\frac{a_R}{\lambda_1} \right) \left(\frac{|a - a_R|}{\lambda_1} \right) \gg 1, \quad (7.45)$$

⁴⁶Extending the following results to $|m| = 1$ is straightforward but requires to maintain the $\mathcal{O}(J_2)$ difference between κ and Ω .

⁴⁷Usually, this small parameter is denoted by ϵ , but we have changed notation in order to prevent confusions with the epicyclic eccentricity.

or equivalently $|a - a_R|/\lambda_1 \gg 10^{-4}$, so that the tight-winding condition is in fact satisfied very close to the resonance, well inside the first wavelength. Neglecting the satellite contribution is not so good an approximation. We will see in the next subsection that in the linear limit, the satellite contribution is negligible only outside the first wavelength. This shows however that the satellite is not directly responsible for the existence of the wave throughout the propagation region: for most of its radial extent, the wave propagates essentially as a free wave due to the ring self-gravity.

7.2.2 Forced amplitude and wave damping

We are interested in this subsection in the description of stationary density waves, i.e. waves for which a, ϵ and Δ do not vary with time. Therefore, the wave is completely described by the knowledge of $\epsilon(a)$ and $\Delta(a)$. Following Shu et al. (1985b), we achieve this purpose by deriving an equation for the quantity⁴⁸.

$$Z = \epsilon \exp im\Delta. \quad (7.46)$$

With this definition, $q_{ij} \exp \gamma_{ij} = (a_i Z_i - a_j Z_j) \exp(-im\Delta_i)/(a_i - a_j)$, which suggests that the desired equation can be obtained from the computation of $(\epsilon \tilde{\omega} + i\dot{\epsilon}) \exp im\Delta$. This procedure yields⁴⁹

$$\frac{2}{\pi} \int_{-\infty}^{+\infty} dx' H(q_{xx'})^2 \frac{Z(x) - Z(x')}{(x - x')^2} + \frac{a_R k^2 (t_2 + it_1)}{\pi G \sigma_0^2 q} Z - \frac{Zx}{\delta} = -\frac{\Psi_{mk}}{2\pi G \sigma_0 a_R}, \quad (7.47)$$

where δ is the small parameter introduced in Eq. (7.44) and where $x \equiv (a - a_R)/a_R$ has been used instead of a as a distance parameter; $|x|$ measures the fractional distance to the resonance. The first term on the left-hand side represents the contribution of the ring self-gravity, the second is due to the ring internal stress, the last reflects the precession rate required by the existence of the wave pattern, and the term on the right-hand side is the satellite forcing (cf Eq. 6.22, with both signs of m allowed). This last term is a dimensionless quantity which ranges from ~ 0.1 to ~ 0.5 for the strongest resonances in Saturn's rings. Remember that it is of order $e_s^{|k|}$, where k is an integer (see section 4.3.2). All smoothly varying quantities have been pulled out of the self-gravity integral. Eq. (7.47) is the starting point of the analyses of Shu et al. (1985b) and Shu et al. (1985a). This equation has no analytic solution in the nonlinear case, but quite a number of its features can be understood in the linear limit, which we are therefore going to discuss next, following the solution developed by Shu et al. (1985b). In this limit, $q \rightarrow 0$ and one can take $H(q^2) = 1/2$. Furthermore, we will ignore the viscous terms for the time being. Neglecting t_2 is equivalent to neglecting the short-waves, a simplification which was justified in the previous subsection. Neglecting t_1 results in the suppression of the wave damping, but

⁴⁸This quantity is in fact the opposite of the complex conjugate of theirs, unscaled.

⁴⁹The contribution from the stress-tensor are given in the tight-winding approximation, for simplicity.

we will return to this question shortly. With these approximations, Eq. (7.47) reduces to

$$\frac{1}{\pi} \int_{-\infty}^{+\infty} dx' \frac{dZ/dx'}{x-x'} + \frac{Zx}{\delta} = \frac{\Psi_{mk}}{2\pi G\sigma_0 a_R}, \quad (7.48)$$

where the self-gravity integral has been integrated by parts. The remaining integral can be computed with the residue theorem⁵⁰, and one finally obtains

$$i \frac{dZ}{dx} + \frac{Zx}{\delta} = \frac{\Psi_{mk}}{2\pi G\sigma_0 a_R}, \quad (7.49)$$

which is the usual equation of linear density wave theory [see Shu 1984, Eq. (44)].

One can encompass both ILR and OLR solutions by introducing a new scaled radial coordinate $\xi = sx/|\delta|^{1/2}$ where $s = \text{sgn}(\delta)$. From the dispersion relation, we expect that the forced (i.e. particular) solution to this equation is a long wave, at least in the far wave region. Therefore, we wish to find the particular solution which is evanescent for $\xi \rightarrow -\infty$. As $\exp(is\xi^2/2)$ is an integrating factor, the desired solution is found to be⁵¹

$$Z = -is \frac{\Psi_{mk}}{2\pi G\sigma_0 a_R} \exp\left(is \frac{\xi^2}{2}\right) \int_{-\infty}^{\xi} dy \exp\left(-is \frac{y^2}{2}\right). \quad (7.50)$$

This solution is depicted in Figure B2 (see Appendix 8), but it has two interesting asymptotic expansions (Goldreich and Tremaine, 1979c; Shu, 1984) that capture most of its behavior. First, in the limit $\xi \ll -1$ (in the far evanescent region), replacing $\exp(-isy^2/2)$ by $(is/y)d\exp(-isy^2/2)/dy$ and integrating by part yields

$$Z \simeq \frac{\delta}{x} \frac{\Psi_{mk}}{2\pi G\sigma_0 a_R}. \quad (7.51)$$

On the other hand, for $\xi \gg 1$ (i.e. into the propagation region), using $\int_{-\infty}^{\xi} = \int_{-\infty}^{+\infty} - \int_{\xi}^{+\infty}$, and performing a similar integration by part, one obtains

⁵⁰Because the wave complex amplitude Z contains an exponential phase term, there is *no guarantee* that one can find a contour at infinity where the contribution vanishes, so that the resulting differential equation is not always valid (it would actually be remarkable that the self-gravity integral equation can be exactly replaced by a differential equation, even in the linear limit). In fact, for free waves, Eq. (7.49) is clearly wrong as it implies the absence of evanescence inside the resonance radius; however one can argue that the sign of k should be present as a factor for the first term (see Shu 1984, pp. 540 – 541, as well as the Appendix). In any case, it is shown in the Appendix that this equation is a rather accurate approximation for forced density waves throughout the disturbed region, and a very precise one as soon as $|x| \gtrsim (2|\delta|)^{1/2}/3$, i.e., nearly everywhere except in a rather limited band around the resonance radius. It is probably worth pointing out that the standard fluid treatment of linear density waves (e.g. Shu 1984), suffers from a similar mild limitation. In this fluid approach, the problem stems from the relation between the surface density and self-gravitational potential; the standard solution based on analytic continuation (Shu, 1970) and used in most linear analyses of density waves performed in the 70s and 80s, is only valid in the tight-winding approximation and does not apply in the evanescent region.

⁵¹This result also follows from an elementary variation of the constants technique.

$$Z \simeq \frac{\Psi_{mk}}{2\pi G\sigma_0 a_R} (2\pi|\delta|)^{1/2} \exp\left(i\frac{x^2}{2\delta} - is\frac{3\pi}{4}\right) + \frac{\delta}{x} \frac{\Psi_{mk}}{2\pi G\sigma_0 a_R}, \quad (7.52)$$

where $\int_{-\infty}^{+\infty} dx \exp(-ix^2/2\delta) = (2\pi|\delta|)^{1/2} \exp(-is\pi/4)$ has been used. The last term represents the non-wavy part of the response, and is negligible.

From this last result we can derive the expression of the eccentricity along the wave

$$\epsilon = \frac{|\Psi_{mk}|}{2\pi G\sigma_0 a_R} (2\pi|\delta|)^{1/2} \sim 10^{-4}, \quad (7.53)$$

which is seen to be independent of a ; the wavenumber $k = md\Delta/da$ reads

$$k = \frac{x}{a_R \delta} = \frac{3(m-1)M_p}{2\pi\sigma_0 a_R^3} \frac{a - a_R}{a_R}. \quad (7.54)$$

which, by comparison with Eq. (7.42), is seen to correspond to a long trailing wave, as expected. Finally, from $q = |k|a\epsilon$, one sees that $q \propto |x|$, so that the wave becomes nonlinear for

$$|x| = x_{nl} \equiv \frac{2\pi G\sigma_0 a_R}{|\Psi_{mk}|} \left(\frac{|\delta|}{2\pi}\right)^{1/2} \sim \frac{\lambda_1}{a_R}. \quad (7.55)$$

Therefore, density waves become nonlinear in the first wavelength or so, as observed. It is to be noted that although the linear theory predicts streamline crossing within a wavelength, the nonlinear contributions of the self-gravity integral prevent this to happen.

Let us now investigate the effects of the neglected viscous terms, and reintroduce them in Eq. (7.49). Using the fact that in the propagation region, $|dZ/dx| = |ika_R Z| \gg |\Psi_{mk}|/2\pi G\sigma_0 a_R$, this equation reads

$$-ka_R Z + \frac{Zx}{\delta} - \frac{a_R k^2}{\pi G\sigma_0^2 q} (t_2 + it_1) Z = 0. \quad (7.56)$$

As $t_i \sim \sigma_0 c^2 q$ for small q , the ratio of the first to the last term is of order $Q^2(m-1)x \ll 1$, where the velocity dispersion has been expressed in terms of Toomre's Q parameter. The viscous terms are indeed very small and balancing the two first terms gives back the dispersion relation for long trailing wave. However, if the contribution of t_2 is small and brings no qualitatively new information, the contribution of t_1 is qualitatively different because it is a pure imaginary number, indicating that k must contain an imaginary part: $k = k_r + ik_i$, where k_r is given Eq. (7.54) and

$$k_i a_R = -\frac{a_R k_r^2 t_1}{\pi G\sigma_0^2 q}. \quad (7.57)$$

Due to this new contribution, Z is now given by

$$Z = Z_{nv} \exp\left(-\int k_i a_R dy\right), \quad (7.58)$$

in the far wave zone, where Z_{nv} is the inviscid value of Z , Eq. (7.52). As a consequence, ϵ now reads

$$\epsilon = \epsilon_{nv} \exp\left(-\int_0^x k_i a_R dy\right), \quad (7.59)$$

where ϵ_{nv} is the inviscid value of ϵ , Eq. (7.53). This shows that the wave is damped if $t_1 < 0$, an assumption which is made in the remainder of these notes⁵². An estimate of the damping length scale x_{vis} can be obtained by setting $\int_0^x k_i a_R dy = 1$, which yields $Q^2 |m - 1| |x|_{vis}^3 / 2 |\delta| = 1$, i.e. $|x_{vis}| \simeq |\delta|^{1/3}$: this implies that density waves can propagate over about ten cycles, as observed. In their more quantitative analysis of wave damping, Shu et al. (1985a) have pointed out that the results displayed on Figure 6 play a central rôle. Indeed, as q increases with x , if the unperturbed optical depth τ_0 is smaller than some critical value, the coefficient of restitution $\epsilon_r \rightarrow 0$, and c diverges (remember that for all known materials ϵ_r is a decreasing function of c): as $t_1 \propto c^2$, this implies short damping length scales. On the other hand, if the unperturbed optical depth is larger than this critical value, ϵ_r depends much less on q , and the wave could propagate much farther. These authors have attributed to this effect the observed fact that density waves propagate much farther in the B ring than in the A ring of Saturn. However, they have also argued that in order to reproduce the observed short damping length scale of the A ring density waves, rather elastic materials were needed, which would rule out “dynamical ephemeral bodies” (DEBs) as a likely model candidate for ring particles. Unfortunately, DEBs are the most natural outcome of the ring collisional processes Weidenschilling et al. (1984); Longaretti (1989a). Either this particle model is incorrect, or other unmodelled processes are at work wave such as the scattering of the wave by large particles, as has been suggested at least by Shu et al. (1985a) and by Peter Goldreich (private communication). At the time of writing, this issue is still unresolved.

7.2.3 Satellite torque and angular momentum transport

The question of angular momentum exchanges between the rings and the satellites have been widely debated for the past ten years, for reasons that will now be exposed. First, note that for a steady-state wave propagating in an inviscid medium, Eq (6.49) reduces to

⁵²One sees also that the wave can be viscously unstable if the viscous coefficient is positive. However, one could expect, as for narrow rings, that oscillations of the eccentricity and phase shift would also be unstable, and possibly prevent the growth of the wave. Such oscillations are excluded by assumption in the present analysis. As the question is still open, we will not push it further in these notes. An analysis of the behavior of nonlinear density waves when the viscous coefficient is positive has been performed by Borderies et al. (1986), but these results are incomplete, as the possibility of oscillations of the eccentricity and phase of the wave has been excluded at the onset of their analysis.

$$L_H^{sg} = \int_0^a da \mathcal{T}_s. \quad (7.60)$$

Thus, for undamped density waves, all the angular momentum deposited by the satellite is carried away by the wave⁵³.

It is interesting to compute L_H^{sg} in the tight-winding approximation. From Eqs. (6.39) and (7.29), and assuming $k > 0$, one obtains

$$L_H^{sg} = -4\pi Gm\sigma_0^2 a_R^3 \epsilon^2 \int_{-\infty}^v dv_1 \int_{v-v_1}^{+\infty} du H\left(q^2 \frac{\sin^2 u}{u^2}\right) \frac{\sin 2u}{u^2}. \quad (7.61)$$

Interchanging the order of the integrals and performing the integration over v_1 yields

$$L_H^{sg} = -\pi^2 Gm\sigma_0^2 a_R^3 \epsilon^2 B(q), \quad (7.62)$$

where $B(q)$ is defined by

$$B(q) = \frac{4}{\pi} \int_0^{+\infty} du H\left(q^2 \frac{\sin^2 u}{u^2}\right) \frac{\sin 2u}{u}. \quad (7.63)$$

Note that $B(q) \rightarrow 1$ as $q \rightarrow 0$. This asymptotic form of the self-gravity angular momentum luminosity is similar to the approximation performed to obtain Eq. (7.49) from (7.48). Notice also that Eq. (6.39) predicts correctly L_H^{sg} to order ϵ^2 , although the basic streamline parametrization on which the whole analysis relies is valid only to order ϵ . Note finally that for $k < 0$ (leading wave) the luminosity Eq. (7.62) changes sign.

Let us now rederive the expression of the torque exerted on a wave excited at an inner Lindblad resonance in the limit of linear undamped waves (Goldreich and Tremaine, 1978c, 1979c). For definiteness we focus on an inner Lindblad resonance ($s = 1$); the torque has the same magnitude but opposite sign at an outer resonance.

From Eq. (6.38), (7.46) and (7.50), one finds

$$T_s = \int_0^{+\infty} da \mathcal{T}_s = -\frac{m\Psi_{mk}^2 a_R}{2G} \times \text{Im} \left[i \int_{-\infty}^{+\infty} dx \exp\left(i\frac{x^2}{2\delta}\right) \int_{-\infty}^x dy \exp\left(-i\frac{y^2}{2\delta}\right) \right], \quad (7.64)$$

where $\text{Im}(z)$ designates the imaginary part of a complex number z . Following Shu et al. (1985b), let us call N the complex number whose imaginary part is to be evaluated in Eq. (7.64) and compute the complex conjugate N^* . Interchanging the order of the integrals in N^* yields

⁵³This result is a direct consequence of the conservation of the wave action; see Dewar (1972).

$$N^* = -i \int_{-\infty}^{+\infty} dx \exp\left(i\frac{x^2}{2\delta}\right) \int_x^{+\infty} dy \exp\left(-i\frac{y^2}{2\delta}\right), \quad (7.65)$$

so that

$$\text{Im}N = \frac{N - N^*}{2i} = \frac{1}{2} \int_{-\infty}^{+\infty} dx \int_{-\infty}^{+\infty} dy \exp\left(i\frac{x^2 - y^2}{2\delta}\right) = \pi\delta, \quad (7.66)$$

Plugging this result into Eq. (7.64) gives back the standard expression of the linear torque⁵⁴

$$T_s = -\frac{\pi^2 m \Psi_{mk}^2 \sigma_0}{\mathcal{D}}, \quad (7.66)$$

where

$$\mathcal{D} \equiv \left(a \frac{d}{da} [\kappa^2 - m^2(\Omega - \Omega_p)^2] \right)_{a_R} = \frac{3(m-1)GM_p}{a_R^3}. \quad (7.67)$$

The same expression is obtained from Eqs. (7.53) and (7.62), as expected from Eq. (7.60). It is also instructive to see how the torque accumulates with radius; to this effect, the cumulative integrand $N(x)$ the imaginary quantity in Eq. (7.64) is illustrated on Figure B2 (see Appendix 8).

Actual waves are affected by nonlinear effects and by viscous damping. The effect of the ring viscosity (or more correctly, internal stress) are not expected to be very important, as the damping occurs in the far wave region, whereas a numerical evaluation of $\int_{-\infty}^x \mathcal{T}_s da$ as a function of x shows that most of the torque is deposited within a few wavelengths of the resonance⁵⁵. Shu et al. (1985a) argue that nonlinear effects don't reduce the torque much below its linear value, but their conclusion is dependent on the details of their model equation; however, a similar conclusion was reached by Longaretti and Borderies (1986) from a nonlinear kinematic analysis of the Mimas 5:3 density wave⁵⁶. Therefore, Eq. (7.66) should give a correct estimate of the angular momentum exchange between rings and satellite at Lindblad resonances.

As the wave is damped, the angular momentum flux due to the ring self-gravity falls below the value implied by Eq. (7.60). The variation of L_H^{sg} with a can be related to the viscous coefficient t_1 in the following way, slightly adapted

⁵⁴Because the linear equation is not exact, as discussed in an earlier footnote, one may at first glance question the validity and relevance of this result. However, it is well-known that the linear torque is independent of the details of the physics of disks; the same linear torque obtains in disks without self-gravity but pressure and/or damping instead (Meyer-Vernet and Sicardy 1987 have produced what is probably the most generic justification of this result). As a consequence, the integrated linear torque is correct, but of course the details of the torque density are not in the near-resonance region are not, where most of the torque is deposited.

⁵⁵This conclusion is robust although the details of the torque deposition implied by Eq. (7.49) are not).

⁵⁶This analysis suffers also from some limitations, but this conclusion is most probably robust. It is fair to say though, that the nonlinear torque magnitude is still somewhat uncertain to this date

from Borderies et al. (1985). From Eq. (6.47), we can eliminate da/dt in Eq. (6.32) in favor of L_H^c . This yields

$$2\pi\Omega a^3 \frac{\partial\sigma_0}{\partial t} + \frac{\partial L_H^c}{\partial a} - \frac{L_H^c}{2a} = 0. \quad (7.68)$$

Furthermore, from $L_E \equiv L_E^c + L_E^{sg} + L_E^{vis}$ (with a similar definition for L_H^{sg}), and from $L_E^{sg} = \Omega_p L_H^{sg}$ and Eqs. (6.44) through (6.47), one obtains

$$L_E = \Omega L_H + (\Omega_p - \Omega)L_H^{sg} - \frac{3}{2}\Omega L_H^c + 2\pi a^2 \Omega \epsilon [t_1 \cos \gamma + t_2 \sin \gamma]. \quad (7.69)$$

Computing $\partial L_H^{sg}/\partial a$ from there, and using Eqs. (6.48) and (6.49) finally yields

$$\frac{\partial}{\partial a} (L_H^{sg} - 2\pi a^2 \epsilon m [t_2 \sin \gamma + t_1 \cos \gamma]) = -2\pi m a q t_1 + \mathcal{T}_s, \quad (7.70)$$

which is the fundamental equation describing wave damping⁵⁷. In the tight-winding limit ($\gamma = \pi/2$), t_1 disappears from the left-hand side. The contribution of the remaining t_2 term is usually small in planetary rings, but Shu et al. (1985a) have pointed out that it might generate a phenomenon referred to as a ‘‘Q barrier’’ in the linear theory of density waves in spiral galaxies (see, e.g., Toomre 1969): as the wave propagates away from the resonance, the increase in macroscopic energy dissipation due to the presence of the wave (with respect to unperturbed regions) results in an increase of the velocity dispersion. If the increase is important enough, the two roots of the dispersion relation (short and long waves) will merge, and the long wave becomes evanescent, until the velocity dispersion has dropped again. Therefore, the long wave could be partly ‘‘reflected’’ as a short wave on the newly formed evanescent region, and partly transmitted as the observed long wave. In order to avoid this interesting, but rather complex possibility, Shu et al. (1985a) have neglected the contribution of t_2 , an approximation made at the onset by Borderies et al. (1986). Whether Q barriers actually occur in Saturn’s rings is still an open question.

In any case, Eq. (7.70) relates the radial variation of the amplitude of the motion, $\partial\epsilon/\partial a$ to the viscous coefficient t_1 . One sees again that the wave is damped if $t_1 < 0$, and that viscous overstabilities can take place in the opposite case (but see the comment on footnote 43).

⁵⁷From the linear theory of density waves, it is known that the wave amplitude is fixed either from a second order WKB analysis (in the wave propagation region) or from the equation for the wave action, i.e., from the equation of angular luminosity conservation (see, e.g., Dewar 1972). The same consideration follows in the nonlinear regime, and in the wave propagation region, where the tight-winding condition applies, the satellite contribution to the amplitude in Eq. (7.47) is negligible; similarly, in the same approximation, the self-gravity contribution to de/dt cancels, and one needs an alternative way to constrain the wave amplitude. This is provided by the wave-damping equation, supplemented by the nonlinear dispersion relation and the conservation of the total (viscous and self-gravitational) angular momentum luminosity once the torque is totally deposited, which provide enough constraints to determine the wavenumber k , the nonlinearity parameter q and the surface density σ_0 (see Borderies et al. 1986 for details; the only uncertainty in this analysis, as pointed out earlier, is the magnitude of the nonlinear torque, although it should emerge self-consistently if one starts from the exact equations and avoids the tight-winding approximation).

Let us come back now to the discussion of the effects of the satellite torque on the evolution of the ring. Let us first assume for the sake of the argument that the wave is in steady state. Due to the ring viscosity, and according to Eq. (6.49), Eq. (7.60) now reads $L_H^{sg} + L_H^{vis} \simeq T_s + L_{vis}^-$ in the propagation region, where L_{vis}^- is the unperturbed angular momentum flux inside the wave region. Denoting the unperturbed flux outside the wave region by L_{vis}^+ , the steady state condition implies $L_{vis}^+ = L_{vis}^- + T_s$. First, notice that L_{vis}^- and L_{vis}^+ are positive and T_s is negative. If the satellite torque is larger than the unperturbed angular momentum flux, $L_H > 0$ outside the wave region and $L_H < 0$ inside, resulting in a steady loss of angular momentum, an inward mass drift and the formation of a gap in the end. Goldreich and Tremaine (1978c) have argued that this process was responsible for the formation of the Cassini division by Mimas. Once a gap is open, the torque can be reduced from its full value (the resonance region is not completely occupied with ring material, so that the torque integral is truncated), and another equilibrium or quasi-equilibrium can be reached in which the satellite confines the inner edge of the gap (see section 6). On the other hand, if $L_{vis}^- + T_s > 0$, an enhancement of the surface density in the ring region might result, a feature apparent in the observed wave profiles. Borderies et al. (1986) provide the following explanation for this effect. If a strong enough density wave is launched in a medium of constant background surface density, q will quickly reach values such that $a_{r\theta} < 0$ in the wave zone, so that $L_H < 0$ and an inward drift again takes place. As the surface density increases, the angular momentum flux needed to evacuate the torque can be obtained for lower values of q , which decreases until it becomes $\lesssim q_2$, the critical value for viscous angular momentum flux reversal (see section 5). Then L_H is positive again, and a quasi steady-state can be maintained. These authors have also used this argument to show that strong waves have their amplitudes limited to $q \lesssim q_2 < 1$.

As satellite torques are negative, satellite orbits expand in time. Calculations based on the cumulative effects of all torques excited in the rings show that the related time-scales of satellite recession are remarkably short, e.g. $\sim 10^7$ years for the shepherd satellites of the F ring (Goldreich and Tremaine, 1982; Borderies et al., 1984). In the same time, a substantial inward drift of ring material should have taken place (Lissauer et al., 1984), and the analysis of the situation in 1984 was that either the rings were young or that some essential piece of physics was overlooked, e.g. that nonlinear saturation might reduce the torque magnitude below its linear value. This consideration actually motivated the development of a nonlinear theory of density waves; however, nonlinear effects do not seem to reduce significantly the satellite torques. Conversely, the idea that the rings are young is now somewhat more popular; Dones (1991), e.g., has given some support to a recent cometary origin for the rings, which appears to be the most likely late mechanism of formation of ring systems. However, the issue is not yet completely settled.

8 Conclusion

A general formalism for the analysis of the dynamics of major ring systems (in the sense defined in the introduction) has been presented here. This formalism draws on two complementary approaches, one which deals with the macroscopic

ring motions, and one related to the microphysical collisional processes⁵⁸. It should not be forgotten that the formalism relies on a fluid approach, which is strictly valid only for phenomena whose characteristic length-scale is larger than the typical particles' mean size and mean separation. Also, the dynamics is treated in the one-fluid approximation.

Obviously the collisional behavior is much less understood than the global dynamics, limiting our interpretation of the finest dynamical effects, although some important general features of the ring internal stress have been uncovered in the past few years. Note that it might be difficult to improve systematically on this point, at least in the framework of the Boltzmann collision term, which relies on the assumption of “molecular chaos”, and neglects velocity and position correlations of the particles. The condition of validity of this assumption has been extensively discussed in Plasma Physics on the basis of the so-called BBGKY hierarchy, and a criterion has been derived, which states that correlations are negligible whenever the mean kinetic energy of individual particles is much larger than their mean energy of mutual interaction. In ring systems, the velocity dispersion is comparable to the mean two-body gravitational potential, so that this criterion is not satisfied, although it is not strongly violated. It seems important however not to disregard heuristic approaches at the profit of purely formal developments, as many breakthroughs have already been performed in this way. Also, it is likely that direct N-body numerical simulations will bring useful information on this front in the future.

On the side of the global dynamics, there are still some major unresolved problems. The most critical is probably the question of the rigid precession of narrow elliptic rings. As argued in section 7.1, the results of the recent encounter of Voyager II with the Uranian system have cast some doubts on the validity of the self-gravity model put forward by Goldreich and Tremaine (1979a). It has also appeared that the standard radiative transfer theory is not appropriate for the analysis of the radio data on the Uranian rings, due to the high density and particle close packing that is prevalent in these systems.

The analyses of the damping of density waves on one hand, and of the collisional evolution of the ring particle size distribution on the other, suggest two contradictory models of ring particle structure and collisional properties. This issue might be alleviated if as yet unmodelled damping mechanisms are found, e.g. the scattering of the wave by large particles (see section 7.2.2); alternatively, the DEBs modeled might be disproved in the end. Also, the absence of perturbation at some resonances is not yet understood; similarly, a detailed criterion for gap opening remains to be established.

The Uranian rings are apparently correctly described as elliptic modes. However, the mechanism of selection of the observed modes is not yet understood (why, e.g., does the α ring have an $m = 1$ mode and the delta ring an $m = 2$?). Also, the kinematic analysis of the γ ring still exhibits unexplained kinematic residuals (see French et al. 1988).

For a long time, no convincing mechanism of confinement of the inner edges of Saturn's rings (like the A and B rings, for example) had been proposed. However, it has recently been argued that such edges could be maintained by ballistic transport processes (see Durisen et al. 1992). Further studies are needed

⁵⁸In ring dynamics, “microphysical” has a rather strange meaning, as the individual ring particles are macroscopic in size.

to confirm or disregard this proposal.

The question of the confinement of the Neptunian ring arcs is still open, although some interesting progress has been made recently (see Porco 1991).

Finally, let us point out that some interesting questions concerning the dynamics of charged particles are still open, as, e.g., questions related to the formation, propagation (if any) and disparition of spokes.

All these issues, as well as a number of others, are the object of active ongoing research.

Acknowledgements

The material presented here represents mostly the work of a collaboration between N. Borderies, P. Goldreich and S. Tremaine over the past ten years or so. I am indebted to N. Borderies and P. Goldreich of many discussions on all aspects of the content of these notes, and I wish to thank them for these fruitful exchanges.

Appendix

On the validity of the complex plane integration of the self-gravity integral

The objective of the present Appendix is to discuss in some detail the identity

$$\frac{2}{\pi} \int_{-\infty}^{+\infty} dx' \frac{Z(x) - Z(x')}{(x - x')^2} = -i \frac{dZ}{dx}, \quad (1)$$

that has been used in the derivation of Eq. (7.49) by Shu et al. (1985b) on the basis of complex contour integration theory.

A Free density waves

It is certain that this relation is not correct independently of the functional form of Z . Indeed, the solution of Eq. (7.49) for free waves (right-hand side set to zero) reads

$$Z_f = \exp \pm ix^2/2\delta. \quad (2)$$

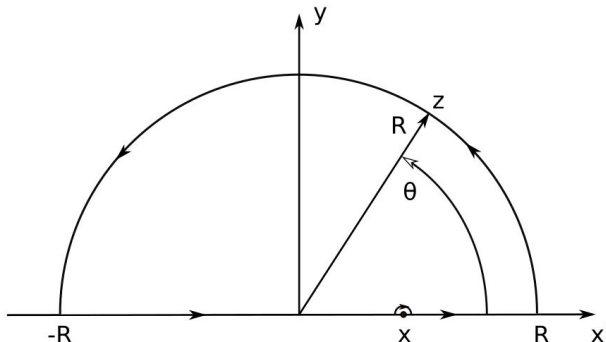


Figure A1: Contour of complex integration for free waves. As usual, the choice of direction around the pole in $x' = x$ (upper or lower small half-circle) does not influence the end result.

For this functional form, the analytic continuation of Z in the complex plane $z = x + iy$ never gives a vanishing integral on any contour joining the real line at $\pm\infty$. Consider the $\exp +ix^2/\delta$ solution with $\delta > 0$ for example. On the upper half-circle (see Figure A1), $z = Re^{i\theta}$ and $\exp +ix^2/\delta = \exp(iR^2 \cos 2\theta) \exp(-R^2 \sin 2\theta)$, so that the exponential diverges for $R \rightarrow \infty$ and $\theta \in [\pi/2, \pi]$; the same conclusion follows for a lower half-circle for $\theta \in [-\pi/2, 0]$. Therefore the contribution of the closing contour is diverging for $R \rightarrow +\infty$, whereas Eq. (1) assumes it vanishes. At least for this form of Z , Eq. (1) is plainly wrong.

This conclusion is not surprising. The quadratic phase of Eq. (2) implies that the tight-winding approximation is valid for both positive and negative x (Z_f is symmetric), except for an extremely narrow range around $x = 0$. But $-idZ/dx = kZ$ with $k = x/\delta$ everywhere whereas in the tight-winding limit, the left-hand side of Eq. (1) is $|k|Z$ [see the derivation of Eq. (7.31)] implying the presence of an evanescent zone inside the resonance radius, in contradiction with Eq. (2).

In fact, if one assumes *a priori* that the wave is evanescent outside the ILR and OLR radii and propagating with wavenumber k inside, one can recover this result from contour integration, as the sign of the wave number fixes which semi-circle (upper or lower half-plane) must be chosen to complete the contour (see Shu 1984, Eqs. 78 through 81). This argument assumes the form of the solution, but does not help us to quantify the error associated with this assumption. This question is addressed in the remainder of this Appendix.

B Forced density wave

One might ask if Eq. (1) is valid or at least approximately valid for the form (7.50) of Z , which would give an *a posteriori* justification for the use of this relation in the case of forced density waves. This problem is examined here and the associated error is analyzed in the process.

For definiteness, the analysis focuses on inner Lindblad resonances, but outer resonances can be treated in the same way.

B.1 Conclusions in a nutshell

For readers who want to skip the details of the soon-to-be-performed contour integration, let me just jump to the conclusion derived in the remainder of this section:

1. Eq. (7.49), albeit not exact throughout the wave region for forced linear density waves, nevertheless captures the correct asymptotic behavior in the evanescent and propagation zone. In fact, the error becomes negligible for $|x| \gtrsim \sqrt{2\delta}/3$ (from Figure B5), i.e., almost everywhere except in a rather limited band around the resonance radius⁵⁹ (δ is defined in Eq. 7.44). Moreover, within this narrow band, Eq. (7.50) produces only a mild logarithmic divergence of the self-gravity integral, indicating that a minor alteration of this function in this range would result in a nearly exact solution.
2. Because the magnitude of the torque (one the most important aspects of the linear theory of density wave) does not depend on the details of the physics (see, e.g., Meyer-Vernet and Sicardy 1987), this model equation gives the correct integrated torque no matter what. Furthermore, the normalized torque accumulation as a function of $x/\sqrt{2\delta}$ is shown on Figure B2 for Z given by Eq. (7.50); this indicates that most of the torque accumulates in the domain of accuracy of Eq. (1), so that the detail of this accumulation is also rather accurate.

⁵⁹For comparison, the first wavelength is $\lambda = 2\sqrt{\pi\delta}$, i.e. nearly a factor of 10 larger than the preceding limit.

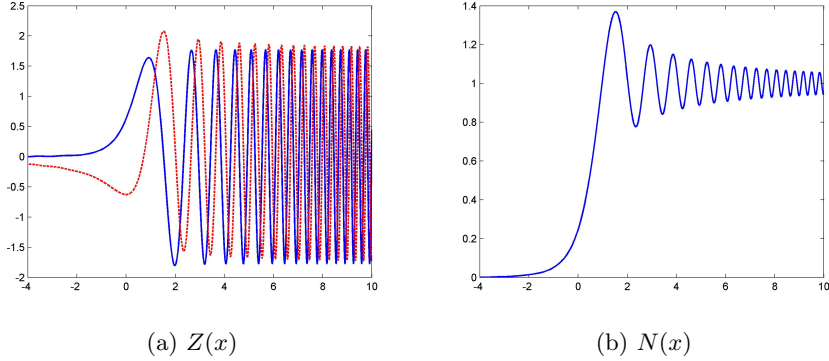


Figure B2: The real (solid line, $\propto \epsilon \sin m\Delta$) and imaginary (dotted line, $\propto \epsilon \cos m\Delta$) part of $Z(u)/(2\delta)^{1/2}$ [Eq. (3)] as a function of the normalized distance $u = x/\sqrt{2\delta}$ are shown on the left. On the right, the normalized cumulative torque as a function of $x/\sqrt{2\delta}$, i.e., the cumulative integral defined as $Im(N)$ in Eqs. (7.64) and (7.65), normalized by $\pi\delta$.

As a consequence, Eq. (7.49) appears to be a remarkably good model equation for linear density waves throughout the wave region. This conclusion may seem hardly unexpected, but is worth pointing out nonetheless, as the problem addressed in this Appendix is easily overlooked and in any case not mentioned in Shu et al. (1985b) where Eq. (1) is stated without further justification. And indeed, because Eq. (7.49) recovers a known form of linear density wave theory, the problem was either overlooked or deemed unimportant.

B.2 Setting up the problem

To tackle this problem, let us first rescale x, x' by $1/(2\delta)^{1/2}$ and ignore the normalization factor of Z which simplifies Eq. (7.50) in the complex plane to

$$Z(u) = (2\delta)^{1/2} \exp(+iu^2) \int_{-\infty}^u du' \exp(-iu'^2), \quad (3)$$

where the $-\infty$ limit of the complex integral is on the x axis and $(u, u') = (z/(2\delta)^{1/2}, z'/(2\delta)^{1/2})$. Note that the rescaling x, x', z, z' by $1/(2\delta)^{1/2}$ does not change the normalization of integrals of the form $\int_C dz' [Z(x) - Z(z')]/(x - z')^2$ on any contour C due to the invariance of $dzdz'/(x - z')^2$. Because of this rescaling invariance, we keep the notation z, z', x, x' for the rescaled quantities, and forget about the normalization factor in Eq. (3), except when needed to state relevant scalings in actual physical variables.

It is convenient to first focus on the complex integral in Eq. (3).

Because $\int_{-\infty}^z dz' \exp(-iz'^2)$ is analytic, the integral can be evaluated on any path and one can write

$$\int_{-\infty}^z dz' \exp(-iz'^2) = \int_{-\infty}^0 dx' \exp(-ix'^2) + e^{i\theta} \int_0^R dr \exp(-ir^2 e^{2i\theta}). \quad (4)$$

The first integral has a principal value expression:

$$\int_{-\infty}^0 dx' \exp(\pm i x'^2) = \int_0^{+\infty} dx' \exp(\pm i x'^2) = \frac{\pi^{1/2}}{2} e^{\pm i\pi/4}, \quad (5)$$

and so does the second one in the limit $R \rightarrow \infty$ and for $\sin 2\theta < 0$:

$$\int_0^{+\infty} dr \exp(-ir^2 e^{2i\theta}) = \pm \frac{\pi^{1/2}}{2} e^{-i\theta}. \quad (6)$$

The sign on this last relation depends on the choice of the branch of the square root function, which is implicitly involved in the result⁶⁰: the square root of $e^{2i\theta}$ is $\pm e^{i\theta}$. It is customary to chose the + sign but it is not possible to make this choice consistently throughout the integration domain. Let us discuss this for $\theta \in]\pi/2, \pi[$ to illustrate the point:

1. For $\theta \rightarrow \pi/2^+$, the integral should converge to $\int_0^{-\infty} dx' \exp(-ix'^2)$ so that the minus sign should be chosen, consistently with Eq. (5).
2. Conversely, for $\theta \rightarrow \pi^-$, the integral should converge to $\int_0^{+\infty} dx' \exp(-ix'^2)$ and consistency now implies to choose the plus sign instead.

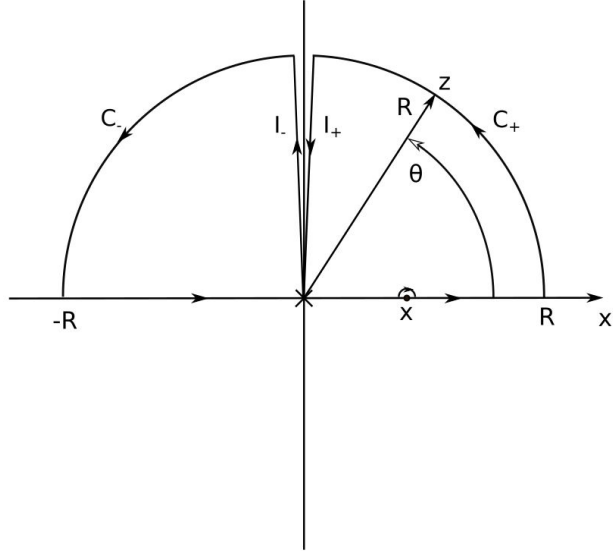


Figure B3: Contour of complex integration for forced wave. The whole y axis except $z = 0$ is a cut in the complex plane where the second integral in the expression of Z Eq. (4) changes sign. I_+ and I_- are located at vanishing angular distance from the y axis.

The same remarks apply to $\theta \in]-\pi/2, 0[$. Note that because the integrals in Eq. (5) are evaluated on the real axis, their sign is unambiguous. As a consequence, a cut has to be made in complex plane to allow for this change of

⁶⁰This can be formally seen through a change of variable in the integral from z to $(\exp 2i\theta)^{1/2} z$.

sign convention in the integral. This cut can be freely chosen, but it turns out that the most convenient place is along the y axis. Note that the cut must be made both along positive and negative y values (2θ increases by 2π each time θ increases by π). At first sight, this seems to imply that the two half-planes separated by the y axis become disconnected, but in fact a contour can go from one half-plane to the other through $z = 0$, where the integral in Eq. (4) is zero and its sign can be left unspecified.

As a consequence of this discussion, the contour sketched on Figure B3 is chosen to evaluate the left-hand side of Eq. (1) (this evaluation can also be performed by choosing a similar contour in the lower half-plane). More specifically, and defining the contour C as $C = C_+ + C_- + I_+ + I_-$, the objective is to provide relevant bounds to the modulus of the integral

$$\mathcal{I}_R(x) = \int_C dz' \frac{Z(x) - Z(z')}{(x - z')^2}. \quad (7)$$

In conclusion of this preliminary, by defining the square root of $\exp 2i\theta$ as $\exp i\theta$ for $\theta \in] - \pi, \pi]$, one can rewrite Eq. (4) as

$$\int_{-\infty}^z dz' \exp(-iz'^2) = \frac{\pi^{1/2}}{2} e^{i\pi/4} + \varepsilon e^{i\theta} \int_0^R dr \exp(-ir^2 e^{2i\theta}), \quad (8)$$

with $\varepsilon = +1$ for $\theta \in [0, \pi/2^-]$ and $\varepsilon = -1$ for $\theta \in [\pi/2^+, \pi]$.

B.3 Evaluation on C_+ and C_-

For any given x , the $Z(x)/(z' - x)^2$ term obviously has vanishing contribution as $R \rightarrow +\infty$ on C_+ and C_- and is ignored. Similarly, $(z - x)^2 \simeq z^2$ in the same limit. One is therefore interested in estimating the asymptotic behavior of $\int_{C_+, C_-} dz Z(z)/z^2$.

Note first the following relevant relation, already used in Eq. (7.51) and (7.52), which follows from an integration by part:

$$\int dr e^{pr^2} = \left[\frac{e^{pr^2}}{2pr} \right] + \int dr \frac{e^{pr^2}}{2pr^2}. \quad (9)$$

This relation is valid independently of the convergence of the integral on any interval where the integral is finite. Note also that the last term is of the order of e^{pr^2}/r^3 for $r \gg 1$ (as can be seen from a further integration by part). This result is valid for any complex number p .

Let us start with C_- . In this range of θ , the integral in Eq. (8) converges at $R = \infty$ and repeating the reasoning used for Eq. (7.51) with the help of Eq. (9) leads to (setting $p = -ie^{2i\theta}$ and remembering that $\varepsilon = -1$)

$$e^{i\theta} \int_{-\infty}^z dz' \exp(-iz'^2) = i \frac{e^{-iz^2}}{2z} + \mathcal{O}\left(\frac{e^{-iz^2}}{z^3}\right) \quad (10)$$

and $Z = i/2z$ for $R \gg 1$ (consistently with the analytic continuation of Eq. [7.51]).

As a consequence, $\left| \int_{C_-} dz Z(z)/z^2 \right| \rightarrow 0$ as $R \rightarrow +\infty$.

The contribution of C_+ requires a little more care due to the divergence of the integral in Eq. (8) as e^{-iz^2} now diverges at large R , but can nevertheless be

handled in a similar way. Let us first chose an arbitrary radius R_0 such that $1 \ll R_0 \ll R$ to rewrite Eq. (8) as

$$\begin{aligned}
\int_{-\infty}^z dz' \exp(-iz'^2) &= \frac{\pi^{1/2}}{2} e^{i\pi/4} + e^{i\theta} \int_0^{R_0} dr \exp(-ir^2 e^{2i\theta}) \\
&\quad + e^{i\theta} \int_{R_0}^R dr \exp(-ir^2 e^{2i\theta}) \\
&= \frac{\pi^{1/2}}{2} e^{i\pi/4} + C_0 \\
&\quad - i \frac{e^{-iz_0^2}}{2z_0} + i \frac{e^{-iz^2}}{2z} + \mathcal{O}\left(\frac{e^{-iz^2}}{z^3}\right), \quad (11)
\end{aligned}$$

where C_0 stands for the integral from 0 to R_0 and $z_0 = R_0 e^{i\theta}$. From this expression, it follows again that $Z = i/2z$ to leading order (the other terms are exponentially suppressed by the e^{iz^2} factor in this range of θ). This again leads to $\left| \int_{C_+} dz Z(z)/z^2 \right| \rightarrow 0$ as $R \rightarrow +\infty$.

B.4 Evaluation on I_+ and I_-

These are the only remaining contributions that may invalidate Eq. (1). Defining $\mathcal{I}_R^\pm(x)$ as the contributions of I_\pm to $\mathcal{I}_R(x)$, one has:

$$\begin{aligned}
\mathcal{I}_R^+(x) &= i \int_R^0 dy \frac{Z(x) - Z(iy)}{(x - iy)^2} \\
&= -i \int_0^R dy \frac{Z(x)}{(x - iy)^2} + i \frac{\pi^{1/2}}{2} e^{i\pi/4} \int_0^R dy \frac{e^{iy^2}}{(x - iy)^2} + \\
&\quad i \int_0^R dy \frac{e^{iy^2}}{(x - iy)^2} \int_0^y dy' e^{-iy'^2} \quad (12)
\end{aligned}$$

Similarly:

$$\begin{aligned}
\mathcal{I}_R^-(x) &= i \int_0^R dy \frac{Z(x) - Z(iy)}{(x - iy)^2} \\
&= i \int_0^R dy \frac{Z(x)}{(x - iy)^2} - i \frac{\pi^{1/2}}{2} e^{i\pi/4} \int_0^R dy \frac{e^{iy^2}}{(x - iy)^2} + \\
&\quad + i \int_0^R dy \frac{e^{iy^2}}{(x - iy)^2} \int_0^y dy' e^{-iy'^2}, \quad (13)
\end{aligned}$$

so that

$$\mathcal{J}_R(x) \equiv \mathcal{I}_R^+(x) + \mathcal{I}_R^-(x) = 2i \int_0^R dy \frac{e^{iy^2}}{(x - iy)^2} \int_0^y dy' e^{-iy'^2}. \quad (14)$$

It is not possible to evaluate this integral with the theorem of residues, as we would be facing the very same problem we are trying to solve. However something has been gained with respect to the initial integral in Eq. (1), as the pole

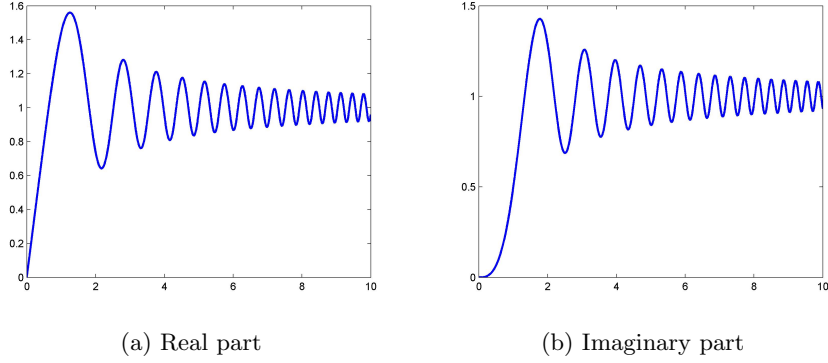


Figure B4: Real and imaginary part of $\int_0^y dy' e^{-iy'^2}$ as a function of y , normalized to their common asymptotic value $\sqrt{2\pi}/4$.

is no longer on the axis (except for the single point $x = 0$) so that this integral can be bounded. Let us first derive an upper bound to the modulus:

$$|\mathcal{J}_{+\infty}(x)| \leq 2 \int_0^{+\infty} \frac{dy}{x^2 + y^2} \left| \int_0^y dy' e^{-iy'^2} \right|. \quad (15)$$

Figure B4 shows the behavior of the real and imaginary part of $\int_0^y dy' e^{-iy'^2}$ as a function of y . This shows that both the real and imaginary part of $\int_0^y dy' e^{-iy'^2}$ are bounded by $1.6 \times (2\pi)^{1/2}/4 \simeq 3\sqrt{2\pi}/8$ (i.e., about $3/2$ their limiting values at $R \rightarrow +\infty$), so that

$$\left| \int_0^y dy' e^{-iy'^2} \right| \lesssim \frac{3\sqrt{\pi}}{4} \sim 1. \quad (16)$$

From this, one gets

$$|\mathcal{J}_{+\infty}(x)| \leq \frac{3\sqrt{\pi}}{4} \int_0^{+\infty} \frac{dy}{x^2 + y^2} = \frac{3\pi^{3/2}}{8|x|} \simeq \frac{2}{|x|} \quad (17)$$

This shows that the contributions of $I_+ + I_-$ to $\mathcal{I}_{+\infty}(x)$ are negligible in Eq. (7.49) when $|x| \gtrsim 1$.

Conversely, for $|x| \ll 1$, one can see that $\mathcal{J}_{+\infty}(x)$ diverges logarithmically with x . Indeed, in this limit, the largest contribution to $\mathcal{J}_{+\infty}(x)$ comes from $|y| \lesssim |x|$. Defining c such that $1 \gg c \gg |x|$, one has

$$|\mathcal{J}_R(x)| \simeq 2 \left| \int_0^c \frac{y dy}{x^2 + y^2} \right| \simeq |\ln c^2 - \ln x^2| = -2 \ln \left| \frac{x}{c} \right|. \quad (18)$$

It must be noted that one can always find a value of c such that Eq. (18) is exact for $|x| \rightarrow 0$. Figure B5 shows that $c = 1/4$ with a high precision.

More generally these two scalings ($|x| \gg 1$ and $|x| \ll 1$) can be tightened with the help of a numerical quadrature of the integrals in Eq. (14), the results of which are shown on Figure B5.

This somewhat tedious analysis of the domain of validity of Eq. (1) for forced density waves has reached its end. The conclusions stated in section B.1 follow

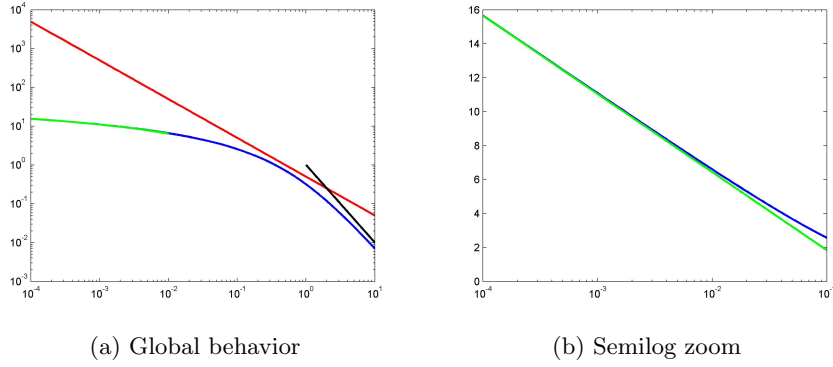


Figure B5: The left graph shows the behavior of $|\mathcal{J}_{+\infty}(x)|$ as a function of x in log scale (only $x > 0$ is shown as the integral depends only on $|x|$). The red line corresponds to $1/2x$, which gives a tighter strict upper bound to this quantity. The black line corresponds to x^{-2} , which captures more closely the $x \gg 1$ asymptotic behavior. The green line corresponds to $-2 \ln 4x$. The right graph zoom shows that $-2 \ln 4x$ is nearly exactly superposed onto the graph of $|\mathcal{J}_{+\infty}(x)|$, confirming the logarithmic divergence as $x \rightarrow 0$.

in a straightforward manner, once reverting to the original scaling of x and Z and comparing the magnitude of the neglected contribution of C to the satellite forcing term.

References

- S. Araki and S. Tremaine. The dynamics of dense particle disks. *Icarus*, 65:83–109, 1986.
- N. Borderies and P. Y. Longaretti. Description and behavior of streamlines in planetary rings. *Icarus*, 72:593–603, 1987.
- N. Borderies, P. Goldreich, and S. Tremaine. Sharp edges of planetary rings. *Nature*, 299:209–211, 1982.
- N. Borderies, P. Goldreich, and S. Tremaine. The dynamics of elliptical rings. *Astron. J.*, 88:1560–1568, 1983a.
- N. Borderies, P. Goldreich, and S. Tremaine. Perturbed particle disks. *Icarus*, 55:124–132, 1983b.
- N. Borderies, P. Goldreich, and S. Tremaine. The variations in eccentricity and apse precession rate of a narrow ring perturbed by a close satellite. *Icarus*, 53:84–89, 1983c.
- N. Borderies, P. Goldreich, and S. Tremaine. Unsolved problems in planetary ring dynamics. In R. Greenberg and A. Brahic, editors, *Planetary Rings*, pages 713–734. University of Arizona Press, 1984.
- N. Borderies, P. Goldreich, and S. Tremaine. A granular flow model for dense planetary rings. *Icarus*, 63:406–420, 1985.
- N. Borderies, P. Goldreich, and S. Tremaine. Nonlinear density waves in planetary rings. *Icarus*, 68:522–533, 1986.
- N. Borderies, P. Goldreich, and S. Tremaine. The formation of sharp edges in planetary rings by nearby satellites. *Icarus*, 80:344–360, 1989.
- A. Brahic. Systems of colliding bodies in a gravitational field. I - Numerical simulation of the standard model. *Astron. Astrophys.*, 54:895–907, 1977.
- J. N. Cuzzi, R. H. Durisen, J. A. Burns, and P. Hamill. The vertical structure and thickness of Saturn’s rings. *Icarus*, 38:54–68, 1979.
- R. L. Dewar. A Lagrangian Derivation of the Action-Conservation Theorem for Density Waves. *Astrophys. J.*, 174:301–307, 1972.
- L. Dones. A recent cometary origin for Saturn’s rings? *Icarus*, 92:194–203, 1991.
- R. H. Durisen. Transport effects due to particle erosion mechanisms. In R. Greenberg and A. Brahic, editors, *Planetary Rings*, pages 416–446. University of Arizona Press, 1984.
- R. H. Durisen, P. W. Bode, J. N. Cuzzi, S. E. Cederbloom, and B. W. Murphy. Ballistic transport in planetary ring systems due to particle erosion mechanisms. II - Theoretical models for Saturn’s A- and B-ring inner edges. *Icarus*, 100:364–393, 1992.

- J. L. Elliot and P. D. Nicholson. The rings of Uranus. In R. Greenberg and A. Brahic, editors, *Planetary Rings*, pages 25–72. University of Arizona Press, 1984.
- R. G. French, J. L. Elliot, and S. E. Levine. Structure of the Uranian rings. II - Ring orbits and widths. *Icarus*, 67:134–163, 1986.
- R. G. French, J. L. Elliot, L. M. French, J. A. Kangas, K. J. Meech, M. E. Ressler, M. W. Buie, J. A. Frogel, J. B. Holberg, J. J. Fuensalida, and M. Joy. Uranian ring orbits from earth-based and Voyager occultation observations. *Icarus*, 73: 349–378, 1988.
- P. Goldreich and C. C. Porco. Shepherding of the Uranian Rings. II. Dynamics. *Astron. J.*, 93:730–737, 1987.
- P. Goldreich and S. Tremaine. The excitation and evolution of density waves. *Astrophys. J.*, 222:850–858, 1978a.
- P. Goldreich and S. Tremaine. Towards a theory for the Uranian rings. *Nature*, 277:97–99, 1979a.
- P. Goldreich and S. Tremaine. Precession of the epsilon ring of Uranus. *Astron. J.*, 84:1638–1641, 1979b.
- P. Goldreich and S. Tremaine. The excitation of density waves at the Lindblad and corotation resonances by an external potential. *Astrophys. J.*, 233:857–871, November 1979c.
- P. Goldreich and S. Tremaine. Disk-satellite interactions. *Astrophys. J.*, 241: 425–441, 1980.
- P. Goldreich and S. Tremaine. The origin of the eccentricities of the rings of Uranus. *Astrophys. J.*, 243:1062–1075, 1981.
- P. Goldreich and S. Tremaine. The dynamics of planetary rings. *Ann. Rev. Astron. Astrophys.*, 20:249–283, 1982.
- P. Goldreich and S. D. Tremaine. The velocity dispersion in Saturn’s rings. *Icarus*, 34:227–239, 1978b.
- P. Goldreich and S. D. Tremaine. The formation of the Cassini division in Saturn’s rings. *Icarus*, 34:240–253, 1978c.
- I. S. Gradshteyn and I. M. Ryzhik. *Table of integrals, series and products*. New York, Academic Press, 5th corr. and enl. ed., 1980.
- P. K. Haff. Grain flow as a fluid-mechanical phenomenon. *J. Fluid Mech.*, 134: 401–430, 1983.
- L. D. Landau and E. M. Lifshitz. *Physical kinetics*. Pergamon Press, 1987.
- C. C. Lin and Y. Y. Lau. Density wave theory of spiral structure of galaxies. *Stud. in App. Math.*, 60:97–163, 1979.
- J. J. Lissauer, S. J. Peale, and J. N. Cuzzi. Ring torque on Janus and the melting of Enceladus. *Icarus*, 58:159–168, 1984.

- P.-Y. Longaretti. Saturn's main ring particle size distribution — An analytic approach. *Icarus*, 81:51–73, 1989a.
- P.-Y. Longaretti. Uranian ring dynamics — An analysis of multimode motions. *Icarus*, 82:281–287, 1989b.
- P.-Y. Longaretti. Planetary ring dynamics: from Boltzmann's equation to celestial mechanics. In D. Benest and C. Froeschle, editors, *Interrelations Between Physics and Dynamics for Minor Bodies in the Solar System*. Editions Frontières. Available on arXiv: astro-ph/1606.00759, 1992.
- P.-Y. Longaretti and N. Borderies. Nonlinear study of the Mimas 5:3 density wave. *Icarus*, 67:211–223, 1986.
- P.-Y. Longaretti and N. Borderies. Streamline formalism and ring orbit determination. *Icarus*, 94:165–170, 1991.
- P.-Y. Longaretti and N. Rappaport. Viscous overstabilities in dense narrow planetary rings. *Icarus*, 116:376–396, 1995.
- D. Lynden-Bell and J. E. Pringle. The evolution of viscous discs and the origin of the nebular variables. *Monthly Not. Roy. Astron. Soc.*, 168:603–637, 1974.
- N. Meyer-Vernet and B. Sicardy. On the physics of resonant disk-satellite interaction. *Icarus*, 69:157–175, 1987.
- C. D. Murray and S. F. Dermott. *Solar system dynamics*. Cambridge University Press, 1999.
- J. C. B. Papaloizou and D. N. C. Lin. On the pulsational overstability in narrowly confined viscous rings. *Astrophys. J.*, 331:838–860, 1988.
- C. C. Porco. An explanation for Neptune's ring arcs. *Science*, 253:995–1001, 1991.
- F. Reif. *Fundamentals of statistical and thermal physics*. Waveland Press, 1965.
- H. Salo and J. Lukkari. Numerical simulations of collisions in systems of non-identical particles. *Earth, Moon and Planets*, 30:229–243, 1984.
- F. H. Shu. On the Density-Wave Theory of Galactic Spirals. II. The Propagation of the Density of Wave Action. *Astrophys. J.*, 160:99, 1970.
- F. H. Shu. Waves in planetary rings. In R. Greenberg and A. Brahic, editors, *Planetary Rings*, pages 513–561. University of Arizona Press, 1984.
- F. H. Shu and G. R. Stewart. The collisional dynamics of particulate disks. *Icarus*, 62:360–383, 1985.
- F. H. Shu, L. Dones, J. J. Lissauer, C. Yuan, and J. N. Cuzzi. Nonlinear spiral density waves - Viscous damping. *Astrophys. J.*, 299:542–573, 1985a.
- F. H. Shu, C. Yuan, and J. J. Lissauer. Nonlinear spiral density waves - An inviscid theory. *Astrophys. J.*, 291:356–376, 1985b.

- I. G. Shukhman. Collisional dynamics of particles in Saturn's rings. *Sov. Ast.*, 28:574–585, 1984.
- G. R. Stewart, D. N. C. Lin, and P. Bodenheimer. Collision-induced transport processes in planetary rings. In R. Greenberg and A. Brahic, editors, *Planetary Rings*, pages 447–512. University of Arizona Press, 1984.
- A. Toomre. On the gravitational stability of a disk of stars. *Astrophys. J.*, 139:1217–1238, 1964.
- A. Toomre. Group Velocity of Spiral Waves in Galactic Disks. *Astrophys. J.*, 158:899–913, 1969.
- S. J. Weidenschilling, C. R. Chapman, D. R. Davis, and R. Greenberg. Ring particles — Collisional interactions and physical nature. In R. Greenberg and A. Brahic, editors, *Planetary Rings*, pages 367–415. University of Arizona Press, 1984.
- G. B. Whitham. *Linear and nonlinear waves*. J. Wiley, New York, 1974.
- J. Wisdom and S. Tremaine. Local simulations of planetary rings. *Astron. J.*, 95:925–940, 1988.

